University of Alberta

Mapping and characterization of a caffeine-sensitive mutant in *Drosophila melanogaster*

by

Brian James Lee

A thesis submitted to the Faculty of Graduate Studies and Research in partial fulfillment of the requirements for the degree of Master of Science

in

Molecular Biology and Genetics

Department of Biological Sciences

Edmonton, Alberta

Fall 2006

Library and Archives Canada

Published Heritage Branch

395 Wellington Street
Ottawa ON K1A 0N4
Canada

Bibliothèque et Archives Canada

Direction du Patrimoine de l'édition

395, rue Wellington
Ottawa ON K1A 0N4
Canada

Your file Votre référence
ISBN: 978-0-494-22304-8
Our file Notre référence
ISBN: 978-0-494-22304-8

NOTICE:
The author has granted a non-exclusive license allowing Library and Archives Canada to reproduce, publish, archive, preserve, conserve, communicate to the public by telecommunication or on the Internet, loan, distribute and sell theses worldwide, for commercial or non-commercial purposes, in microform, paper, electronic and/or any other formats.

The author retains copyright ownership and moral rights in this thesis. Neither the thesis nor substantial extracts from it may be printed or otherwise reproduced without the author's permission.

AVIS:
L'auteur a accordé une licence non exclusive permettant à la Bibliothèque et Archives Canada de reproduire, publier, archiver, sauvegarder, conserver, transmettre au public par télécommunication ou par l'Internet, prêter, distribuer et vendre des thèses partout dans le monde, à des fins commerciales ou autres, sur support microforme, papier, électronique et/ou autres formats.

L'auteur conserve la propriété du droit d'auteur et des droits moraux qui protège cette thèse. Ni la thèse ni des extraits substantiels de celle-ci ne doivent être imprimés ou autrement reproduits sans son autorisation.

In compliance with the Canadian Privacy Act some supporting forms may have been removed from this thesis.

While these forms may be included in the document page count, their removal does not represent any loss of content from the thesis.

Conformément à la loi canadienne sur la protection de la vie privée, quelques formulaires secondaires ont été enlevés de cette thèse.

Bien que ces formulaires aient inclus dans la pagination, il n'y aura aucun contenu manquant.

Canada

Abstract

The caffeine-sensitive *Drosophila melanogaster* mutant *huc*95DE was previously isolated in a screen for hydroxyurea and/or caffeine sensitivity and mapped to 95D11-E7, delineating *huc*95DE to 23 possible genes. I have mapped *huc*95DE to 95E1-E7-E8, narrowing the number of candidates to 9, resulting in a renaming to *huc*95^{E}. When reared on caffeine, *huc*95^{E} exhibit small, disorganized eyes with fewer ommatidia that appear irregular and fused when homozygously expressed in the eye. *huc*95^{E} hemizygotes exhibit pupal lethality at caffeine concentrations as low as 0.25 mM, but can survive in normal media suggesting that *huc*95^{E} is not required for viability. In the presence of caffeine, *huc*95^{E} hemizygotic third instar larvae exhibit degenerating imaginal discs and hemizygotic pupae contain no visible adult structures. Staining of these discs with acridine-orange and caspase-3 demonstrates high levels of apoptosis, providing and explanation for these developmental defects.

Table of Contents

Chapter 1: Introduction 1
Section 1-2: Caffeine and adenosine 2
Section 1-3: Adenosine and cAMP signalling 4
Section 1-4: Caffeine and calcium signalling 9
Section 1-5: Excess calcium levels can signal apoptosis 12
Section 1-6: Caffeine can inhibit signalling by phosphoinositide 3-kinase 16
Section 1-7: Caffeine and cell cycle control 20
Section 1-8: *huc*95DE was isolated in a screen for novel cell cycle checkpoint mutants 22
Section 1-9: Literature Cited 33

Chapter 2: The Mapping and Identification of *huc*95^{E} 40
Section 2-1: Introduction 40
Section 2-2: Materials and Methods 42
Section 2-2a: Fly stocks and crosses 42
Section 2-2b: PCR and sequencing 43
Section 2-2c: Embryo DNA Preparation and PCR 45
Section 2-2d: RT-PCR and RNA isolation 45
Section 2-2e: Synthesis and mapping of transgenic rescue lines 46
Section 2-3: Results 48
Section 2-3a: Mapping of *huc95*^{DE} through Recombination 48
Section 2-3b: Mapping of *huc95*^{DE} through P-element mobilization and flanking deletion synthesis 50
Section 2-3c: Deficiency Mapping and Complementation Analysis 53
Section 2-3d: Sequencing of candidate genes 58
Section 2-3e: Transgenic rescue experiments 69
Section 2-4: Discussion 70
Section 2-5: Literature cited 75
Tables and Figures 80

Chapter 3: The Characterization of the *Drosophila huc*95^{E} Mutants 97
Section 3-1: Introduction 97
Section 3-2: Materials and Methods 100
Section 3-2a: Caffeine titration 100
Section 3-2b: Ionizing Irradiation Sensitivity Assay 100
Section 3-2c: Imaginal Disc Antibody staining 101
Section 3-3: Results 101
Section 3-3a: The viability of huc95^{E} hemizygotes is compromised at concentrations as low as 0.25 mM of caffeine 101
Section 3-3b: Ionizing radiation does not substantially affect the viability of *huc95*^{E} hemizygotes 102
Section 3-2c: *huc95*^{E} hemizygote third instar larvae display increased apoptosis in eye imaginal discs when reared in media containing 2 mM caffeine 103

Section 3-4: Discussion 106
Section 3-5: Literature cited 116
Tables and Figures 120

Chapter 4: Conclusion 128
Section 4-2: Literature cited 132

Appendix 133

List of Tables

Table 2-1: Predicted genes in the region of 95DE of the third chromosome. 80

Table 2-2: Putative transcripts that map to the *Df(3R)W6* region 81

Table 2-3: Relevant fly stocks used in the mapping of *huc*95^{E} 82

List of Figures

Figure 1-1: Comparison of the structures of caffeine, adenosine, and cyclic AMP 2

Figure 1-2: Mechanism of adenosine receptor stimulation and the consequent activation of cAMP production 5

Figure 1-3: The cAMP pathway 7

Figure 1-4: The generation and removal of cyclic AMP 8

Figure 1-5: Calcium signalling mediated by phospholipase C 10

Figure 1-6: Mechanism of calcium-induced apoptosis 15

Figure 1-7: General mechanism of checkpoint control 21

Figure 1-8: Method for generating homozygous ommatidial mitotic clones using the *EGUF-GMR-hid* system 25

Figure 1-9: Development of the *Drosophila* eye imaginal disc 26

Figure 1-10: A genetic screen of chromosome 2L to identify mutants that are sensitive to hydrozyurea and caffeine during eye development 28

Figure 1-11: Scanning electron micrographs of adult eyes from individuals of the genotype *EGUF*/+; FRT82B *GMR-hid*3R *CL*3R grown in the absence and presence of caffeine 30

Figure 1-12: Eye imaginal discs from individuals of the genotypes *EGUF/+; FRT82B huc*95^{DE}*/ TM3 Ser* and *EGUF/+; FRT82B huc*95^{DE}*/ FRT 82BGMR-hid3R CL3R* grown in the presence of caffeine and labeled with the nucleoside analog BrdU 32

Figure 2-1: Strategy to map *huc*95^{E} through recombination 83

Figure 2-2: Resultant recombination map of *huc*95^{DE} mapping strategy 84

Figure 2-3: P-element strategy for mapping *huc*95^{DE} 85

Figure 2-4:Alternative crossing scheme for P-element strategy to map *huc*95^{DE} 86

Figure 2-5: Isolation of homozygous *Df*(3R)*W6* DNA for delineation of the region uncovered by *Df*(3R)*W6* 87

Figure 2-6: Determination of the extent of *Df*(3R)*W6* 88

Figure 2-7: Localization of the *huc*95DE mutation to the cytological region of 95E1-E7-E8 89

Figure 2-8: Possible model for a p38 mitogen activated protein kinase as a candidate for *huc*95^{E} 90

Figure 2-9: *p38c* and *mRpS24* are expressed in *huc*95^{E} hemizygotes 91

Figure 2-10: Splicing defect in *myo*95E in *huc*95^{E} hemizygotes 92

Figure 2-11: Analysis of alternative splicing in *myo*95E that bypass splicing of exon 9 93

Figure 2-12: Creation of *myo*95E genomic rescue construct 94

Figure 2-13: *myo*95E transgenic rescue test for *huc*95^{E} hemizygote caffeine sensitivity 95

Figure 2-14: hemizygotes expressing the rescue construct exhibit splicing of intron 8 in *myo*95E 96

Figure 3-1: Caffeine sensitivity of *huc*95^{E} hemizygotes 120

Figure 3-2: Effects of ionizing radiation on *huc*95^{E} hemizygote viability 121

Figure 3-3: Eye discs dissected from *EGUF/+; FRT 82B huc95^{DE}/ FRT82B GMR-hid3R CL3R* larvae that were stained to visualize apoptosis by acridine orange staining 122

Figure 3-4: Degeneration of *huc*95^{E} hemizygote imaginal discs in the presence of caffeine 123

Figure 3-5: Apoptosis and cellular proliferation in eye-antennal discs from *huc*95^{E} hemizygotes in the presence and absence of caffeine 124

Figure 3-6: Apoptosis and cellular proliferation in wing discs from *huc*95^{E} hemizygotes in the presence and absence of caffeine 125

Figure 3-7: Possible model for the caffeine-induced apoptosis in *huc*95^{E} hemizygotes 126

Figure 3-8: Mechanism of autophagy 127

List of Symbols and Abbreviations

	Male		Virgin female
AAA	ATPase Associated with Various Cellular Activities	**AC**	Adenylyl Cyclase
AIF	Apoptosis-Inducing Factor	**AMP**	Adenosine Monophosphate
Apaf-1	Apoptosis Protease Activation Factor-1	**ATM**	Ataxia Telangiectasia-Mutated
ATP	Adenosine triphosphate	**ATR**	ATM and Rad3-related
BrdU	Bromodeoxyuridine	***ca***	Claret
Ca^{2+}	Calcium Ions	**cAMP**	Cyclic AMP
CDK1	Cyclin Dependent Kinase-1	**C Nap-1**	Centrosomal Nek2-Associated Protein-1
CyO	Second chromosomal balancer	**DAG**	Diacylglycerol
Df	Deficiency	***e***	Ebony
EGUF	*Eyeless* promoter-*GAL4*; *UAS Flp-recombinase*	***Elav***	Embryonic Lethal Abnormal Visual
EMS	Ethyl Methanosulphonate	**ER**	Endoplasmic Reticulum
FMW	First Mitotic Wave	**GFP**	Green Fluorescent Protein
GMR-hid	*Glass Multiple Reporter* promoter-*Head Involution Defective*	**GPCR**	G-Protein Coupled Receptor
G Protein	GTP/GDP binding Protein	**GTP/GDP**	Guanosine Triphosphate /Diphosphate
Gy	Gray	**HU**	Hydroxyurea
Hu	Humoral	***huc***	Hydroxyurea and/or Caffeine Sensitive
IAP	Inhibitor of Apoptosis Protein	**IQ**	Isoleucine-Glutamine motifs
IP_3	Inositol 1,4,5 Trisphosphate	**IP_3R**	IP_3 Receptor

LC3	Microtubule Associated Protein-1 Light Chain 3	**mM**	Millimolar
Nek	NIMA Related Kinase	**NIMA**	Never In Mitosis in *Aspergillus nidulans*
p70S6K	p70 Ribosomal S6 Kinase	**PAS**	Preautophagosome
PH-3	Phosphohistone-3	**PI3K**	Phosphoinositide 3 kinase
PKA	Protein Kinase A	**PKB**	Protein Kinase B
PKC	Protein Kinase C	**RyR**	Ryanodine Receptor
Sb	Stubble	***Ser***	Serrate
SMAC	Second Mitochondrial Activator of Cell Death	**SMW**	second mitotic wave
Tb	Tubby	***TM6***	Third chromosome balancer
TM3	Third chromosome balancer	***TP***	Transposition
UAS	Upstream Activating Sequence	***Ubx***	Ultrabithorax
w	White		

Chapter 1: Introduction

Caffeine is the most widely used psychoactive drug in the world today, with total consumption levels on average of 76 mg/person/day, reaching 210-238 mg/person/day in the United States and Canada, and up to 400 mg/person/day in the United Kingdom and Scandinavian countries (Gilbert, 1984; Barone and Roberts, 1996; Mandel, 2002). Much of this usage (which transcends age and cultural boundaries) occurs because caffeine acts as a neurological stimulant to suppress mental and physical fatigue and improve attention and arousal, without substantial or clearly documented negative side effects at typical consumption levels. Caffeine also exhibits a wide variety of other pharmacological effects, including sensitizing cells to irradiation and genotoxic drugs (presumably by overriding cell cycle checkpoint responses), promoting apoptosis, and altering cellular calcium levels through its effects on calcium channels (Lau and Pardee, 1982; Schlegel and Pardee, 1986; He *et al.*, 2003; Zucchi and Ronca-Testoni, 1997; Rousseau *et al.*, 1988). These additional effects have made caffeine a useful tool in research for studying cellular proliferation, cell death, and molecular mechanisms involving calcium signalling including muscle contraction or calcium channel excitation. Despite its wide consumption and use as a reagent in research, the mechanism underlying these diverse actions of caffeine have not been fully elucidated. Therefore, it is important (both from a practical research standpoint as well as medically and clinically) to understand the mechanisms underlying the pharmacological activities of caffeine. My project represents an effort to characterize gene functions that protect cells from caffeine toxicity in *Drosophila*.

Section 1-2: Caffeine and adenosine

Many of caffeine's effects are thought to stem from structural similarities to the nucleoside adenosine and other structurally related derivatives (such as 2-deoxyadenosine, adenine, and the signalling molecule, cyclic adenosine monophosphate (cAMP) - see Figure 1-1) that are involved in a multitude of signalling pathways regulating various cellular and physiological processes (Nishijima *et al.*, 2003).

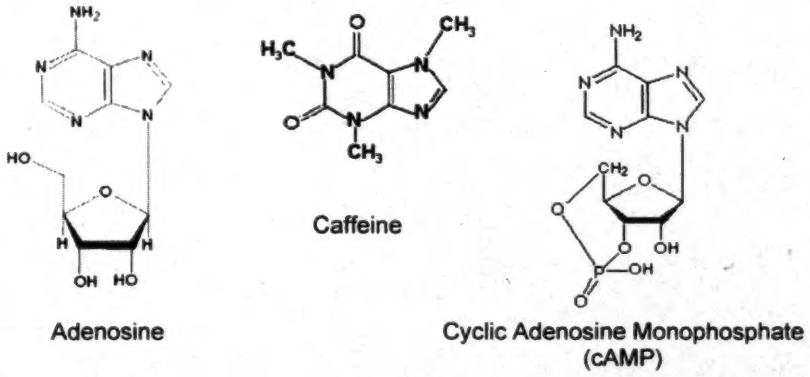

Figure 1-1. Comparison of the structures of caffeine, adenosine and cyclic AMP

Concerning adenosine, it is a common metabolite made by all cells and is often formed as a by-product of energy utilization through the catabolism of adenosine triphosphate (ATP). Levels of adenosine play a central role in the energy metabolism of a cell by acting as a key indicator of energy utilization, initiating certain processes when imbalances between energy consumption and energy supply occur (Dunwiddie and Fredholm, 1988). Consequently, altering levels of adenosine can modulate many diverse cellular processes including cell proliferation and cell death, and can physiologically modulate changes in the cardiovascular system, central nervous system, gastrointestinal tract and immune system, as well as mast cell degranulation, pain modulation, and

asthma (Schulte and Fredholm, 2003). Because of these effects, adenosine levels must be constantly regulated to prevent untimely events or processes from occurring (Jacobson *et al.*, 1999; Merighi *et al.*, 2003). As a result, constant levels of adenosine are maintained by the phosphorylation or deamination to AMP or inosine respectively, by the enzymes adenosine deaminase or adenosine kinase.

Because of its similarity to adenosine, caffeine is thought to exert its effects by interacting with adenosine receptors or other interacting partner proteins and either mimicking or antagonizing adenosine. In fact, it was the study of the antagonistic effects of caffeine that first indicated the existence of adenosine receptors (De Gubareff and Sleator Jr., 1965). Adenosine receptors are subdivided into four different receptor subtypes (classified as A_1, A_{2A}, A_{2B}, and A_3, respectively), originally classified according to their abilities to either inhibit (as is the case of A_1 receptors) or stimulate (as is the case of A_2 receptors) levels of the ubiquitous secondary messenger, cyclic AMP (cAMP) (van Calker *et al.*, 1978; van Calker *et al.*, 1979; Londos *et al.*, 1980; Fredholm, 1982). Stimulatory A_2 receptors were further subdivided according to their abilities to stimulate cAMP production within brain slices at low (A_{2A}) and high (A_{2B}) adenosine concentrations, which was further supported through ligand-binding assays and molecular biological analysis revealing differential affinities to adenosine derivatives (Daly *et al.*, 1983; Bruns *et al.*, 1986; Fredholm *et al.*, 2001). A_3 receptors (which generally result in a decrease in cAMP levels) were discovered on the basis of sequence similarity during the molecular cloning of a rat testis cDNA library and were classified because of their insensitivity to the antagonistic actions of methylxanthines, a trait which was responsible for this class remaining unknown until 1992 (Zhou *et al.*, 1992; Palmer *et al.*, 1995). All

adenosine receptors belong to a class of transmembrane receptors that are associated with guanosine triphosphate/diphosphate (GTP/GDP)-binding proteins (G-proteins) called G-protein coupled receptors (GPCRs). G-proteins consist of a heterotrimeric complex of three subunits (labelled α, β, and γ, respectively) that contain a binding pocket for GTP or GDP within the first (α) subunit (Gilman, 1987) as shown in Figure 1-2A. Each class of adenosine receptor associated with particular types of different G-proteins that are thought to impart selective activities for each receptor, possibly serving as a link to various other cell signalling pathways (Schulte and Fredholm, 2003). For instance, A_1 and A_3 receptors have been found to interact with $G_{i1/2/3}$, and G_O proteins (causing decreased levels of cAMP), whereas A_{2A} and A_{2B} receptors have been found to associate with G_S, G_{OLF}, and $G_{15/16}$ receptors, and G_S, $G_{Q/11}$ proteins, respectively (resulting in increased levels of cAMP) (Schulte and Fredholm, 2003). A_3 receptors have also been found associated with $G_{Q/11}$ as well, suggesting that these receptors could serve dual functions of either stimulating or inhibiting cAMP production, depending upon which complex is formed. As a result, the interaction of adenosine receptors with various different G-proteins further adds to the complexity of the regulation and signalling of these receptors and consequently, the possible effects that adenosine analogs such as caffeine may exert.

Section 1-3: Adenosine and cAMP signalling

Much of adenosine's ability to elicit effects on a multitude of systems involves the formation of the ubiquitous secondary messenger cAMP. cAMP is produced in response to the availability of nutrients, or the presence of hormones, ions or other

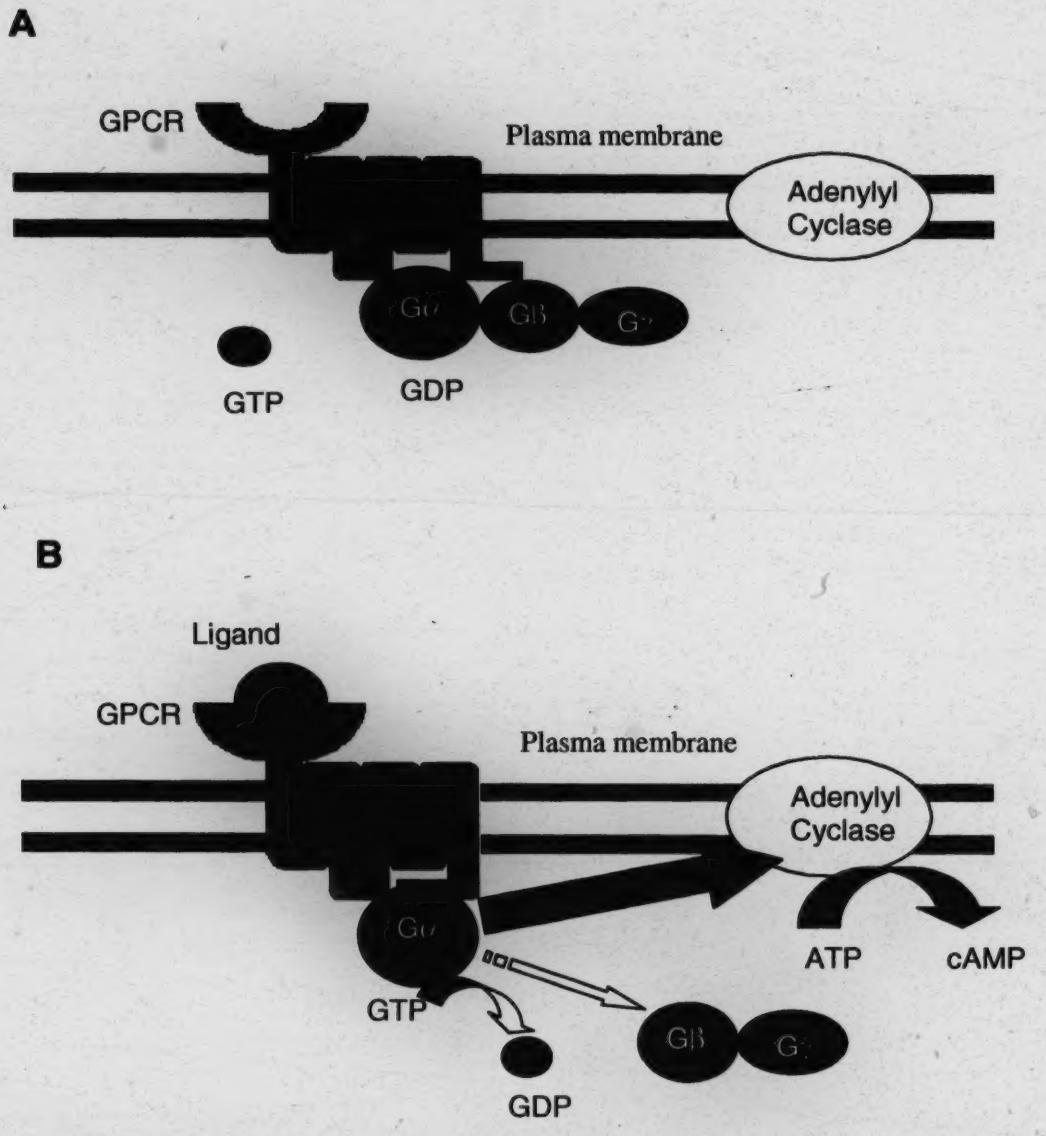

Figure 1-2. Mechanism of adenosine receptor stimulation and the consequent activation of cAMP production. In its unstimulated state (**A**), the transmembrane G-protein coupled receptor (GPCR) contains GDP in a binding pocket of the first α subunit in a heterotrimeric complex associated with the receptor. When stimulated by a ligand (**B**), GDP is replaced by GTP, which signals dissociation of the $\beta\gamma$ subunits and consequent activation of adenylyl cyclase by activated Gα, which converts ATP to cAMP.

signalling molecules (Daniel *et al.*, 1998). cAMP transduces signals from activated GPCRs by activating protein kinase A (PKA), which then initiates the response by phosphorylating its substrates (Daniel *et al.*, 1998). Upon stimulation of GPCRs by a specific ligand, an allosteric change within the α subunit of the G-protein in the receptor causes the G-protein to become active by the replacement of GDP for activating GTP (Figure 1-2B). This causes the α subunit to become activated, dissociating from the β and γ subunits (still held together as a dimer) and activating the enzyme adenylyl cyclase (AC) (Daniel *et al.*, 1998). AC catalyzes the formation of cAMP from ATP, which then interacts with the effector molecule PKA: the apical kinase in the cAMP-signalling cascade. PKA exists as a tetrameric holoenzyme composed of two catalytic subunits and a homodimer of regulatory subunits. Upon activation by cAMP at the regulatory domain, the catalytic subunits dissociate from the holoenzyme and phosphorylate serine (S) or threonine (T) residues in a specific RRX(S/T) motif (whereby R represents arginine and X represents any amino acid residue), regulating a variety of intracellular proteins, enzymes, ion channels, and gene expression through direct interaction with such transcription factors as cAMP response element binding proteins (CREB), cAMP response element modulator (CREM), activating transcription factor-1 (ATF-1), NF-κB, and nuclear receptors (Figure 1-3) (Daniel *et al.*, 1998). As a result, many different systems and processes can be regulated through cAMP signalling, which in turn, can be activated by stimulation of adenosine receptors (Della Fazia *et al.*, 1997). Levels of cAMP signalling are controlled by the activity of phosphodiesterases, (which serve to break down intracellular cAMP, reducing signal by reducing the secondary messenger), phosphatases (which reduce signalling by counteracting the kinase activity of PKA), and

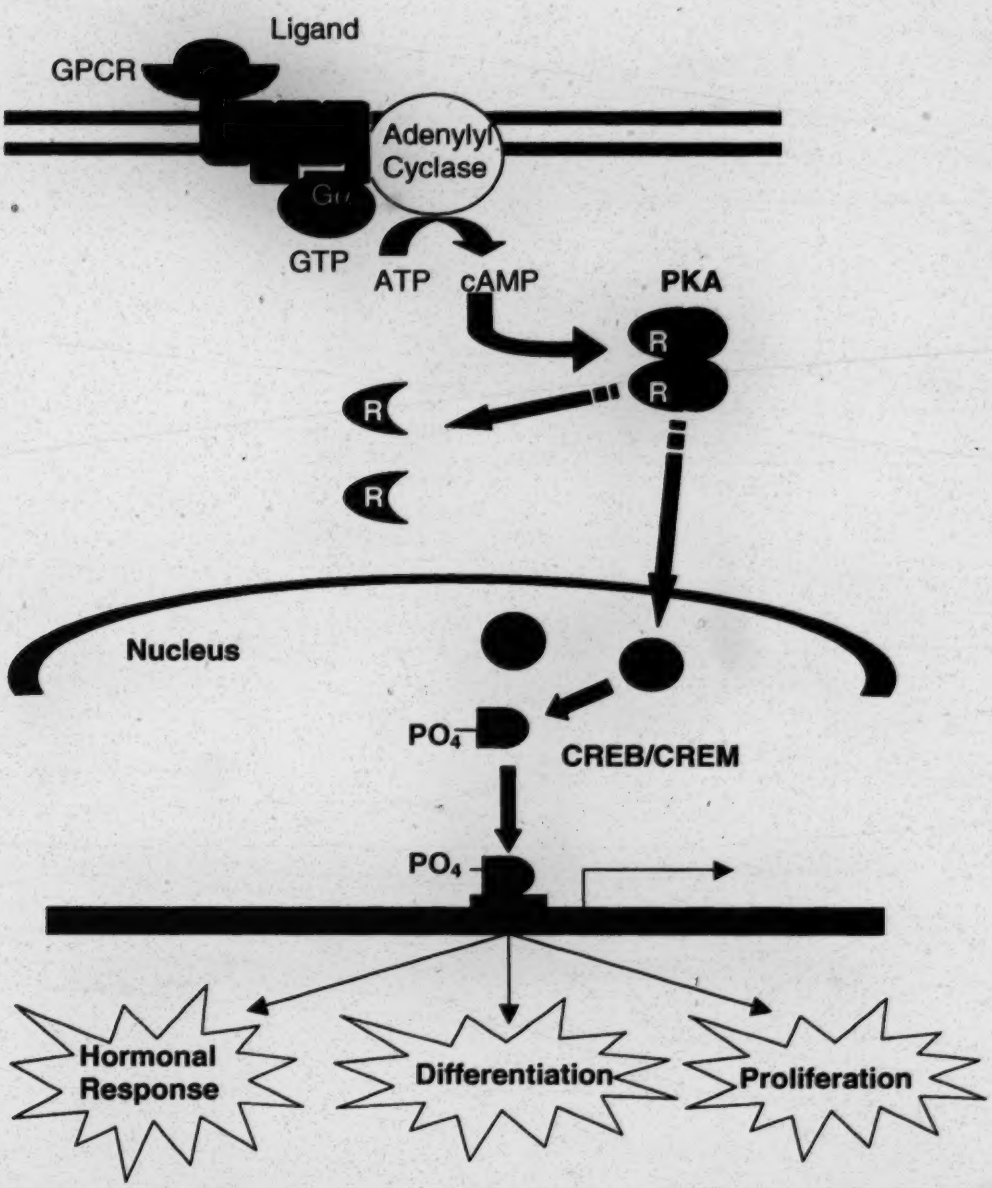

Figure 1-3. The cAMP pathway. Upon formation of cAMP from ATP by adenylyl cyclase, this secondary messenger molecule can interact with the effector molecule PKA at regulatory (R) domains to free the catalytic subunits (C) which translocate into the nucleus and serve to phosphorylate transcription factors and enzymes such as cAMP response element binding proteins (CREB) and cAMP response element modulators (CREM). These factors can then interact with cAMP response elements (CRE) to bring about regulation in various cellular processes. (Adapted from Della Fazia *et al.*, 1997)

PKA inhibitors (which prevent the phosphorylation of important substrates through inhibition of PKA itself) (Daniel *et al.*, 1998). Caffeine can interfere with cAMP signalling and affect cellular processes regulated by this pathway by its agonistic or antagonistic actions towards different adenosine receptors, or by its actions (at concentrations in the mM range) as a phosphodiesterase inhibitor, preventing breakdown of cAMP (Figure 1-4) (Vernikos-Danellis and Harris III, 1968). As a result, the mechanisms of action of caffeine are not yet clearly defined, since various steps can be affected.

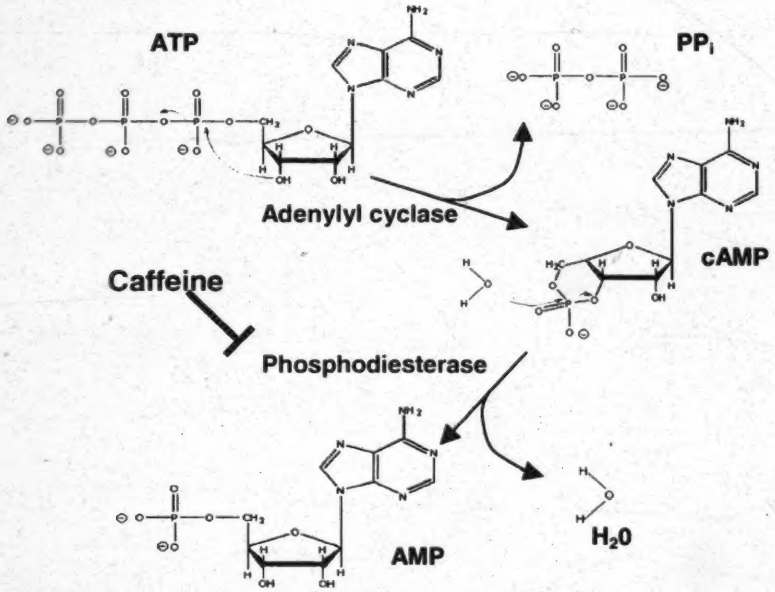

Figure 1-4. The generation and removal of cAMP. The signalling molecule cAMP is synthesized by the enzyme adenylyl cyclase from ATP upon activation from GPCRs. To regulate intracellular levels, cAMP is hydrolyzed by cAMP phosphodiesterase to form AMP. This process is inhibited by caffeine and may result in some of the effects mediated by this drug.

Section 1-4: Caffeine and calcium signalling

Caffeine affects calcium levels by influencing the regulation of ion channels and adenylyl cyclase signalling pathways through inhibition of adenosine receptors. Normally, the amount of free intracellular calcium ions (Ca^{2+}) is tightly regulated such that the concentration of extracellular Ca^{2+} is about four orders of magnitude higher (approximately 1.2 mM) than that within the cell (approximately 100 nM in resting cells) (Hanson *et al.*, 2004; Saris and Carafoli, 2005; Waring, 2005). This is accomplished by controlling the entry or efflux of Ca^{2+}, and the active sequestration and storage of intracellular Ca^{2+} within intracellular compartments (such as the endoplasmic reticulum (ER) or mitochondria) through various channels and transporters. Increased levels of cytosolic Ca^{2+} are made available through the controlled release from ER pools, where they can interact with molecules that require Ca^{2+} binding for regulation in various biochemical and signal transduction pathways, or act by themselves to signal other events in the cell. This regulation allows Ca^{2+} to act as a general signalling molecule for many different cellular, physiological and developmental events, since the release or entry of only a small amount of Ca^{2+} can significantly alter the concentration gradient between intra and extracellular Ca^{2+}. Many extracellular signals such as hormones, neurotransmitters, and growth factors, as well as membrane depolarization or mechanical and environmental stress, initiate their respective cellular responses by a regulated release of Ca^{2+} within the cell. With regard to adenosine receptors, certain G-proteins of the G_Q subtype can activate phospholipase C, an enzyme involved in the hydrolysis of phospholipids on the inner layer of the plasma membrane (Yakel *et al.*, 1993; Gao *et al.*, 1999; Linden *et al.*, 1999). When phospholipase C is activated, it hydrolyzes

phosphatidylinositol 4,5-bisphosphate (PIP_2), producing the secondary messengers diacylglycerol (DAG) and inositol 1,4,5-trisphosphate (IP_3) (see Figure 1-5). DAG remains in the inner layer of the plasma membrane and recruits protein kinase C (PKC), a calcium dependent protein kinase responsible for phosphorylating various proteins to bring about the associated changes in the cell, while IP_3 diffuses and binds to IP_3

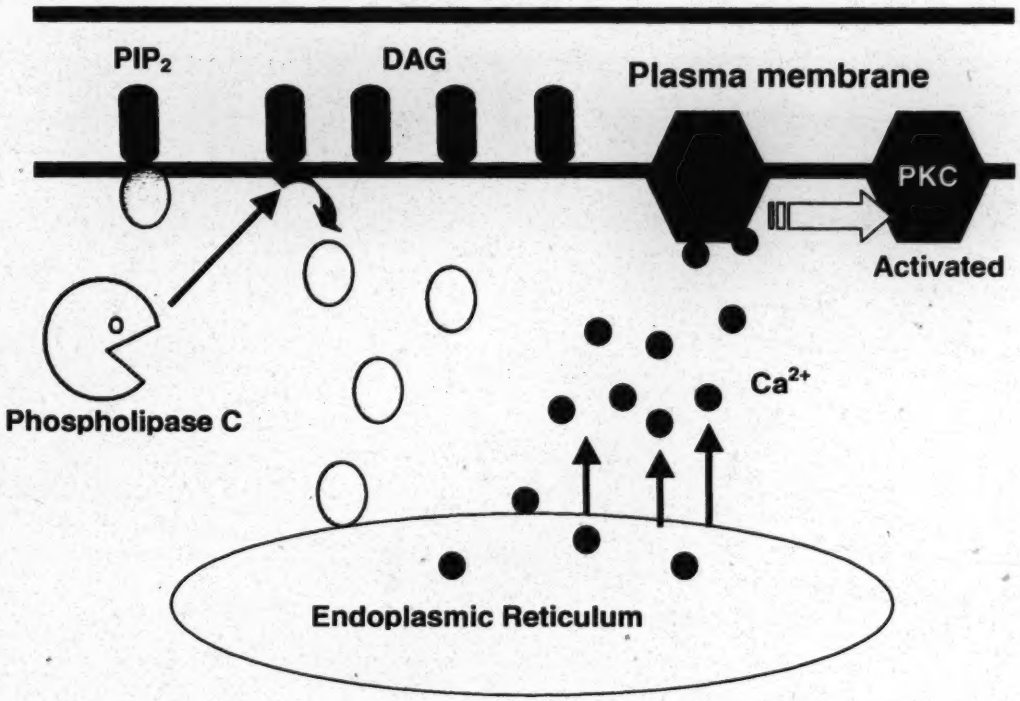

Figure 1-5. Calcium signalling mediated by phospholipase C. The intracellular concentration of calcium (Ca^{2+}) is tightly controlled such that its release from Ca^{2+} stores such as the endoplasmic reticulum (ER) can be used to signal various processes through activation of a Ca^{2+} dependent general protein kinase PKC. Phospholipase C (which may be activated through adenosine signalling) hydrolyzes phosphatidylinositol 4,5-bisphosphate (PIP_2) to produce the secondary messengers inositol 1,4,5 trisphosphate (IP_3) and diacylglycerol (DAG). DAG recruits PKC, while IP_3 signals the release of Ca^{2+} from the ER for PKC activation.

receptors (IP_3R) in the ER (the main storage and release organelle of intracellular Ca^{2+}), causing a release of Ca^{2+} within the cytosol. IP_3R are large (~1200 kDa) tetrameric protein whose subunits form a Ca^{2+} channel (through interaction of integral membrane-spanning carboxy-terminal domains) with an exposed cytoplasmic amino-terminal domain responsible for binding IP_3 (Hanson *et al.*, 2004). Activation of IP_3R however, is controlled not only by binding of IP_3, but also by the binding of free Ca^{2+} (in amounts of up to 500 nM) to an exposed cytoplasmic amino acid stretch between the carboxy and amino-terminal domains (Hanson *et al.*, 2004). The binding of Ca^{2+} at this concentration acts synergistically with IP_3 to induce the opening of the channel and release of Ca^{2+}. At concentrations higher than 500 nM however, IP_3R opening is inhibited, serving as a control mechanism to prevent pathological Ca^{2+} increases in the cytosol. Because of the similarity of caffeine and adenosine, interaction of caffeine at these receptors could affect downstream regulation of Ca^{2+} release in certain situations. In addition to this, another class of Ca^{2+} receptors with sequence and structural similarities to IP_3R are also present within the ER, called ryanodine receptors (RyR). RyR were named because of their sensitivity to the plant alkaloid ryanodine, and have also been implicated in the regulation of cytosolic Ca^{2+} (Mignery *et al.*, 1989). RyR are also large (approximately 2.3 Mda) tetrameric proteins, but differ from IP_3R in their biophysical and pharmacological properties. For example, the activity of RyR is increased by treatment with negatively charged polyanionic molecules (such as pentosan polysulphate, polyvinyl sulphate and heparin), whereas the activity of IP_3R is decreased (Bezprozvanny *et al.*, 1993; Palade *et al.*, 1989). Furthermore, treatment with protamine (a positively charged molecule) could reversibly inhibit the activity of RyR (Koulen and Erlich, 2000). These studies suggest

that the high negative charge of these polyanions served to increase the local negative charge of RyR, attracting more Ca^{2+} to the receptor thereby activating it, and that the positive charge of protamine indirectly blocks the channel by creating a cation-repelling environment at the pore complex at sites of Ca^{2+} regulation. It has also been reported that RyRs are sensitive to treatment with caffeine, evoking Ca^{2+} release (consequently, caffeine is often used in studies involving these receptors) (Rousseau *et al.*, 1988; McPherson *et al.*, 1991). As a result, increases in the levels of Ca^{2+} in the cytosol (possibly by the action of caffeine on RyR) could serve to also affect other channels, thereby further increasing the cytosolic concentration.

Section 1-5: Excess calcium levels can signal apoptosis

One important means of regulating cytosolic calcium levels and coordinately regulating respiration is by controlling the intake of Ca^{2+} into the mitochondria (the site for aerobic respiration and generation of ATP). Elevations of calcium levels within the cytosol of metabolically active cells can signal increases in the activity of citric acid cycle enzymes within the mitochondrial matrix, resulting in an increase in the rate of ATP production (Hanson *et al.*, 2004; Saris and Carafoli, 2005). In addition to providing the necessary energy requirements to carry out basic cellular metabolism, this increased rate of ATP production can also be used to re-establish the Ca^{2+} gradient through the activation of Ca^{2+} ATPases (ATP-dependent Ca^{2+} pumps that actively sequester Ca^{2+} back into storage organelles, or expel Ca^{2+} from the cell, and are crucial for keeping the concentration of intracellular Ca^{2+} at approximately 100 nM). If the concentration of Ca^{2+} becomes too high within the mitochondrial matrix however, the mitochondria could swell, rupture, or undergo permeability changes, which may release pro-apoptotic proteins into the

cytoplasm. These pro-apoptotic proteins include cytochrome C, second mitochondrial activator of cell death (SMAC/Diablo), and apoptosis-inducing factor (AIF) (Hanson *et al.*, 2004). Cytochrome C is a 13 kDa nuclear encoded protein that serves as an electron carrier within the electron transport chain and is important for the establishment of the electropotential gradient in the generation of ATP through oxidative phosphorylation. Release of cytochrome C into the cytoplasm acts as a general signal for the initiation of apoptotic events however, by interacting with pro-apoptotic proteins to form the apoptosis promoting structure called the apoptosome, described below (Wang *et al.*, 2005). SMAC/Diablo commits the cell to programmed cell death by interacting with, and suppressing the actions of inhibitors of apoptosis proteins (IAP) which negatively regulate apoptosis by binding key apoptotic proteins such as caspase 9 (Wang *et al.*, 2005; Du *et al.*, 2000). AIF is a nuclear encoded flavoprotein that resides in the mitochondrial intermembrane space, and is responsible for the condensation and fragmentation of nuclear DNA upon its release into the cytoplasm, an event that is associated with apoptosis (Susin *et al.*, 1999; Wang *et al.*, 2005). The process of apoptosis is mediated by the activation of caspases (aspartate-directed cysteine proteases that cleave specific substrates at cysteine residues) from inactive zymogens (proenzymes). These activated caspases then serve as initiators and effectors of programmed cell death (see Figure 1-6). Caspases are expressed as single chain proenzymes containing an NH_2-terminal domain, a large (20 kDa) catalytic subunit and a smaller (10 kDa) subunit (Wang *et al.*, 2005). Caspases can be classified into two categories. Initiator caspases such as caspase 2, 8, 9, and 10, are characterized by long N-terminal prodomains that contain conserved protein-protein interaction motifs.

Effector caspases such as caspase 3, 6, and 7, possess either smaller, or no prodomains at all. Upon proteolytic activation, initiator caspases recruit and activate effector caspases, which cleave their target proteins to bring about the orderly demise of the cell. This process is initiated when the released cytochrome C and other components such as dATP, apoptosis protease activation factor-1 (Apaf-1), and pro-caspase 9 assemble into a high molecular weight heptameric wheel-like complex called the apoptosome, consisting of seven Apaf-1/caspase 9 dimers that transiently associate with cytochrome C (Wang *et al.*, 2005). The formation of the apoptosome allows for the efficient activation of initiator caspase 9 as the association of cytochrome C to pro-caspase 9 allows Apaf-1 to interact with pro-caspase 9 at a caspase-associated recruitment domain (CARD) in the N terminus, resulting in its activation. Once activated, caspase 9 cleaves effector caspases 3, 6, and 7, which, upon activation, will cleave at aspartate-cysteine residues on intracellular substrates such as the DNA repair enzyme poly(ADP-ribose) polymerase (PARP) (which when cleaved, translocates AIF from the mitochondria to the nucleus), caspase-activated DNase (CAD), nuclear lamins, gelsolin (an actin-capping protein important in maintaining cell shape and structure in the transition of gel to sol states of cytoplasm), and fodrin (a protein important in maintaining cell shape, stabilizing membrane structures, and linking the cytoskeleton to plasma membranes or intracellular vesicles). All of these processes serve to destabilize nuclear and cytoplasmic integrity in a characteristic sequence of apoptotic events.

The cycling of Ca^{2+} between the ER and mitochondria is a key event in the signalling of apoptosis with the process of depleting ER stores emerging as an important trigger. Ca^{2+} continuously cycles between the mitochondria and ER, allowing

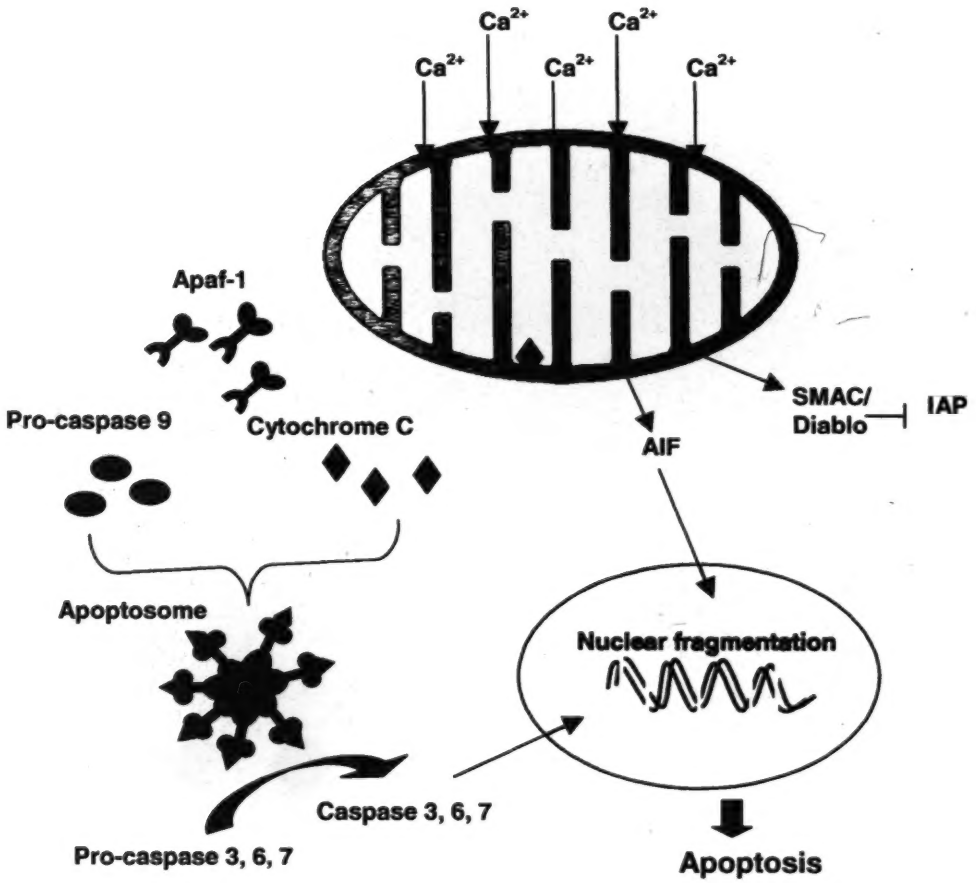

Figure 1-6. Mechanism of calcium-induced apoptosis. Mitochondrial rupture mediated by excessive Ca^{2+} influx can result in the release of cytochrome C, apoptosis-inducing factor (AIF), and Diablo (*aka* second mitochondrial activator of cell death (SMAC)) into the cytoplasm to initiate apoptosis. Cytochrome C interacts with apoptosis protease activation factor 1 (Apaf-1) and pro-caspase 9 to form the apoptosome, which activates caspase 9 to induce cleavage of effector caspases 3, 6, and 7, which directly bring about the events of apoptosis. AIF translocates into the nucleus (which is mediated by the activity of the activated caspases) to bring about DNA fragmentation while Diablo commits the cell to programmed cell death by inhibiting inhibitors of apoptosis proteins (IAP) that normally prevent apoptosis from occurring.

mitochondria to regulate Ca^{2+} signalling and levels within the ER (Demaurex and Distelhorst, 2003). Depletion of Ca^{2+} from the ER pool, and the consequent increase of Ca^{2+} in mitochondria, signals apoptosis and can provide some insight into how caffeine might induce apoptosis. For instance, Chinese hamster ovary cells transfected with the RyR and treated with 10 μM of ryanodine (which is just enough to lock the RyR in an open state) and 10 mM caffeine, undergo apoptosis caused by the rapid caffeine-induced depletion of Ca^{2+} from the ER (Pan *et al.*, 2000). Addition of caffeine has been linked to apoptosis in a variety of cell types, although the dosage required for this effect differs amongst different cell types and the role that caffeine plays in these apoptotic events might be more complex than interaction at RyRs (Fernandez *et al.*, 2003; Jafari and Rabbani, 2000; He *et al.*, 2003). For instance, evidence in JB6C141 cells suggests that caffeine-induced apoptosis is mediated by the tumor suppressor p53, which activates the proapoptotic protein Bax to release cytochrome C (He *et al.*, 2003). This ultimately results in the activation of caspase 3 (the major effector caspase responsible for apoptosis) to mediate apoptotic events.

Section 1-6: Caffeine can inhibit signalling by phosphoinositide 3-kinase

Caffeine can affect the signalling molecule phosphoinositide (PI) 3-Kinase (PI3K), which has been implicated in such processes as cellular proliferation, apoptosis, differentiation, and metabolic regulation (Foukas *et al.*, 2002; Katso, *et al.*, 2001; Osaki *et al.*, 2004; Franke *et al.*, 2003). PI3Ks phosphorylate the D3'-OH position of the inositol ring of phosphoinositides to create secondary lipid messengers which interact with other signalling molecules downstream to exert their effect. They can be further subdivided into four classes (classes I_A, I_B, II, and III, respectively) based upon lipid

substrate specificity, structure, and mode of regulation (Vanhaesebroeck *et al.*, 1997; Fruman *et al.*, 1998). Class I enzymes are the most well studied class of PI3Ks and consist of a 110 kDa catalytic subunit (of either α, β, δ, or γ) associated with a regulatory adaptor subunit (p85α, p85β, p55α, p55γ, p50α, p87, or p101) linking the enzyme to signalling molecules upstream (Fruman *et al.*, 1998). Upon activation, class I enzymes phosphorylate phosphatidylinositol 4,5-bisphosphate (PtdIns-4,5-P_2) to produce the secondary lipid messenger PtdIns-3,4,5-P_3. These lipid messengers interact with other signalling molecules such as protein kinase B (PKB/Akt) and **p70** ribosomal **S6** **k**inase (p70S6K) at **p**leckstrin **h**omology (PH) domains to mediate their effects. This class is further subdivided into classes I_A and I_B, with I_A consisting of PI3Ks (containing either p110α, β, or δ) that interacts with the regulatory subunits p85, p55, and p50 (via two **s**rc **2** **h**omology (SH2) domains) and specifically transduce signals of phosphorylated tyrosines from activated receptor tyrosine kinases (RTKs), and I_B consisting of p110γ-containing PI3Ks that interact with the regulatory subunits p101 and p87 and are activated through interactions with the βγ subunit of heterotrimeric G proteins from GPCRs (Fruman *et al.*, 1998; Wymann and Marone, 2005). The least amount of information is known about class II enzymes, although it is believed that they may be involved in modulating and regulating clathrin distribution and assembly through formation of PtdIns-3-P, and have been found to bind PtdIns-3,4-P_2 *in vitro* (Wheeler and Domin, 2006). Class III enzymes exclusively produce PtdIns-3-P, which regulates vesicle trafficking by interacting with proteins containing FYVE finger domain (Fruman *et al.*, 1998). Class I_A PI3Ks also possess protein kinase activity (in addition to the lipid kinase activity that all PI3Ks possess) and have been reported to phosphorylate many

exogenous substrates such as insulin receptor substrate 1, phosphodiesterase 3B, and autoregulatory phosphorylation of Ser608 of a p85α adaptor subunit, which serves to inhibit lipid kinase activity of the p110 catalytic subunit (Lam *et al.*, 1994; Rondinone *et al.*, 2000; Beeton *et al.*, 2000).

PI3K can be activated by cytokines and growth factors that recruit PI3K to the membrane for interaction with its phosphoinositide substrate (Cantrell, 2001; Krasilnikov, 2000). Upon formation of phosphorylated phosphoinositides, these secondary lipid messengers signal the activation of AGC (protein kinase A, G, and C) kinases such as PKB and p70S6K, which mediate responses by the regulating downstream enzymes and regulatory proteins (Brazil and Hemmings, 2001; Lizcano *et al.*, 2003). PKB has been linked to inhibition of apoptosis and differentiation corresponding with an increase in cell proliferation resulting in cancer (Franke *et al.*, 2003). Regulation of this signalling pathway is accomplished by dephosphorylation of secondary lipid messengers by **SH**2 domain-containing **i**nositol 5'-**p**hosphatase (SHIP) - 1/2 and PTEN (**p**hosphatase and tensin homologue deleted on chromosome **ten**) phosphatases, which dephosphorylate inositides and phosphoinositides at their 5' and 3' position, respectively (Cantrell, 2001).

PI3K signal transduction is also an important component of the insulin-signalling pathway (Shepherd, 2005). The hormone insulin rapidly stimulates class I_A PI3K signalling to promote glycogen synthesis, inhibition of lipolysis, stimulation of protein biosynthetic pathways, and the translocation of the GLUT4 glucose transporter (a receptor required to allow the entry of extracellular glucose) to the plasma membrane (Shepherd, 2005; Bose *et al.*, 2002). In addition to regulating glucose metabolism and

utilization, insulin signalling is also a major regulator of cell growth and development in *Drosophila* and is highly conserved from *Drosophila* to humans (Lizcano *et al.*, 2003; Bikopoulos *et al.*, 2004). *Drosophila* contains one insulin receptor (DinR) and seven insulin-like peptides, as well as homologues of mammalian insulin receptor substrates, PI3K, PTEN, PKB/Akt, and p70SK6. Because of these similarities, *Drosophila* is a useful model in the study of this pathway and its role in the coordination of cellular growth, proliferation and cell survival, with development (Bikopoulos *et al.*, 2004). Expression of ***D**rosophila* **i**nsulin-**l**ike **p**eptide **2** (DILP2) results in an increase in body mass and growth in the developing eye when exclusively overexpressed in this tissue, whereas inhibition of insulin signalling corresponds to a decrease in the overall size of the fly and a reduction in the growth of imaginal discs (Edgar, 1999; Brogiolo *et al.*, 2001). These results reflect the ability of insulin signalling to inhibit the apoptosis, thereby allowing continued growth of cells and tissues by preventing cell death (Bertrand *et al.*, 1998; Lee-Kwon *et al.*, 1998; Yenush *et al.*, 1998).

It was recently determined that caffeine could inhibit the lipid kinase activity of class I PI3Ks *in vitro* at an IC_{50} of 75 μM for p110δ, 400 μM for p110α and p110β, and 1 mM for p110γ. Caffeine can also block the ability of insulin to stimulate PKB with IC_{50} values similar to those required for inhibition of PI3K activity and insulin-stimulated glucose transport in these cells (Foukas *et al.*, 2002). This suggests that caffeine could mediate its effects by directly inhibiting PI3K and its resultant downstream signalling, an effect that could also be related to caffeine's ability to induce apoptosis as inhibition of PI3K signalling could prevent PKB from inhibiting apoptosis.

Section 1-7: Caffeine and cell cycle control

Another interesting effect of caffeine is its ability to sensitize cells to radiation and various other DNA damaging or checkpoint-inducing agents. Checkpoints are regulatory mechanisms that temporarily halt the cell cycle to allow for the completion of critical events such as DNA replication, repair, or chromosomal segregation (Weinert and Hartwell, 1989). Checkpoints are crucial for ensuring that the cell undergoes an orderly, unidirectional progression through the cell cycle, ensuring that subsequent steps are completed prior to cellular division. Failure to do so results in loss of genomic fidelity (as unrepaired mutations are carried on to the next generation) and compromises genomic integrity and chromosomal stability as DNA damage caused by incomplete replication and double stranded breaks, ultimately leads to loss of chromosomal information. Observations made in a variety of cell lines treated with ionizing radiation or DNA damaging drugs revealed that checkpoint-induced delays that normally occur upon exposure to these agents, are disrupted by caffeine (Rauth, 1967; Lau and Pardee, 1982; Schlegel and Pardee, 1986). The presumed mechanism of caffeine's ability to override checkpoint responses comes from evidence suggesting that caffeine inhibits the protein kinase activity of **A**taxia **T**elangiectasia-**M**utated (ATM) and **ATM** and **R**ad3 related (ATR) kinases (Blasina *et al.*, 1999; Sarkaria *et al.*, 1999; Zhou *et al.*, 2000). These kinases have been shown through genetic and biochemical evidence to be major regulators of DNA damage-induced cell cycle checkpoint and repair pathways that become activated upon detection of DNA damage or incomplete replication (Abraham, 2001). Once activated, these kinases phosphorylate downstream checkpoint effector kinases Chk1 (on S345 and S317 by ATR) and Chk2 (on T68 by ATM), which in turn

phosphorylate Cdc25 on S216, as well as the inhibitory kinases Wee1 and Myt1 (Figure 1-7) (Abraham, 2001). Cdc25 is the phosphatase responsible for removing the inhibitory phosphate residues on tyrosine (Y) 15 (mediated by both Wee1 and Myt1) and T14 (mediated by Myt1) of the master regulator of mitosis Cyclin Dependent Kinase 1 (CDK1). CDK1, a complex of Cdc2 and Cyclin B, is directly responsible for starting the initial progression into mitosis by phosphorylating critical substrates, such as histones to cause condensation of chromatin in early prophase. Phosphorylation of Cdc25 at S216 prevents activation of CDK1 because it results in an allosteric movement of Cdc25 that reveals a binding site for 14-3-3 proteins and results in sequestration of Cdc25 in the cytoplasm, keeping it away from nuclear CDK1. In contrast, phosphorylation of Myt1 and Wee1 kinases by Chk1 activates these kinases to mediate inhibitory phosphorylation of CDK1. Thus, the mechanism of caffeine's ability to radiosensitize or chemosensitize cells treated with genotoxic agents is believed to be through the inhibition of ATM and ATR kinases, such that checkpoints which would normally be activated through exposure to these agents, are abrogated.

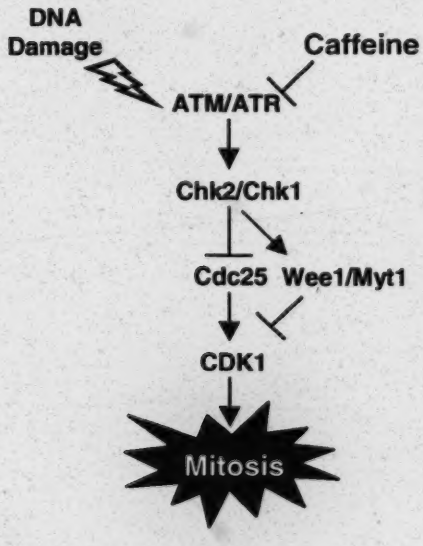

Figure 1-7. General mechanism of checkpoint control. Upon detection of DNA damage, the master regulatory kinases Ataxia Telangiectasia-mutated (ATM) and ATM and Rad3 related (ATR) kinases activate downstream kinases Chk1 and Chk2, which initiate a G_2 checkpoint by inhibiting Cdc25 and the consequent activation of CDK1, which commits the drive towards mitosis. Chk1 and Chk2 are also involved in activation of inhibitory kinases Wee1 and Myt1, which maintain the checkpoint through inhibitory phosphorylation of CDK1. Caffeine inhibits the actions of ATM and ATR, resulting in the abrogation of the checkpoint and consequent premature entry into mitosis.

Section 1-8: *huc*95DE was isolated in a screen for novel cell cycle checkpoint mutants

Since caffeine has the ability to override checkpoint responses by the inhibition of ATM and ATR, it has become a useful tool in the study of cell cycle checkpoint and DNA damage response pathways (Tenzer and Pruschy, 2003; Blasina *et al.*, 1999; Sarkaria *et al.*, 1999). This ability also made caffeine an attractive chemical to use for the possible discovery of novel cell cycle mutants, particularly if some of these mutants remained hidden due to functional redundancies within the cell cycle regulatory machinery (Silva, 2002). Control of the cell cycle is of critical importance because if left unregulated, it could lead to cancer or cell death due to genomic and chromosomal instability. Consequently, redundant mechanisms exist that can compensate for defects in components of the pathway (Abrahams, 2001). Previously, a screen was designed to discover possible novel cell cycle checkpoint mutants that may have not been detected in other screens due to possible redundancy in cell cycle checkpoint and repair systems (Silva, 2002). A precedent for this idea was suggested by the discovery of the *mus*304 gene. This gene, which was isolated from a collection of **mu**tagen **s**ensitive *Drosophila* mutants, encodes a novel DNA checkpoint gene, suggesting that perhaps other regulators of the cell cycle may also be currently undetected, particularly if their functions were masked by redundant checkpoint regulation mechanisms (Henderson, 1999; Brodsky, 2000; Silva, 2002). A strategy was devised whereby the progeny of EMS-mutagenized *Drosophila* were assayed for the ability to develop normal eyes when they were raised in the presence of hydroxyurea (a drug that inhibits ribonucleoside reductase: an enzyme involved in the synthesis of deoxyribonucleotides) and caffeine. The rationale of the strategy was that an S-phase checkpoint would be induced by hydroxyurea (by affecting

the cell's ability to replenish the depleting deoxyribonucleotide pools during DNA replication), but inhibition of the master cell cycle and DNA damage/repair pathway regulators ATM and ATR by caffeine might partially override this checkpoint response, forcing cells to undergo inappropriate mitosis unless another pathway independent of ATM and ATR could be activated to maintain the checkpoint. As a result, mutations affecting genes involved in such a redundant pathway that would normally be masked by the effects of DNA repair pathways could be uncovered. Mutations affecting genes involved in such a checkpoint response would be expected to render mutants more sensitive to these drugs, resulting in developmental defects.

Since the original premise of the screen was to discover novel cell cycle mutants, it was necessary to have a method that would allow for both the detection of such mutants and permit these mutants to be viable and fertile. Because components that regulate cell cycle checkpoint responses would target the same mitotic machinery required for all cell divisions, mutations affecting these components could often be expected to result in non-conditional lethality or sterility. To address this problem, a method that allows for creation of an adult eye composed entirely of homozygous mutant ommatidial cells in an otherwise heterozygous fly was used (Stowers and Schwarz, 1999). This method takes advantage of the GAL4-UAS system and FLP-FRT system adopted from yeast and involves driving GAL4 expression from an *eyeless* promoter (ensuring that GAL4 expression is limited to the developing eye), which would then bind to Upstream Activator Sequences fused to a FLP recombinase transgene (Golic and Lindquist, 1989; Brand and Perrimon, 1993; Stowers and Schwarz, 1999). FLP recombinase then induces site-specific mitotic recombination at FRT sites on the chromosomes within the cells of

the developing eye, resulting in twin clones of homozygous cells. Selection against one class of homozygous ommatidial cells is then accomplished by expression of a transgene carrying ***h**ead **i**nvolution **d**efective* (a gene that produces a pro-apoptotic protein) under control of a late-expressed eye-specific promoter ***G**lass **M**ultiple **R**eporter* (*GMR-hid*). As a result, the development of any cell inheriting *GMR-hid* is terminated, leaving only cells that are homozygous for the mutagenized chromosome (see Figure 1-8). The *Drosophila* compound eye is an ideal organ for such a screen, as it is not required for viability of the organism and is an easily viewed structure, allowing many different mutant phenotypes affecting size, texture, and organization to be distinguished. The eye also has a well-established (albeit complex) system of development, making it an excellent organ to study how pattern formation is regulated by the control and timing of cell proliferation and differentiation. The adult eye is composed of approximately 700 repeating facets or ommatidia, each of which is generated from 19 precursor cells that develop within the eye-antennal imaginal disc (Wolff and Ready, 1993). Each ommatidium, responsible for focusing and transmitting light from a small portion of the visual field to the optic regions of the brain, consists of a precise concentric arrangement of 8 photoreceptor cells surrounded by accessory cone and pigment cells. From embryogenesis until the end of the second larval instar, cells in the eye-antennal disc proliferate in an unpatterned manner. During the last larval instar, ommatidial specification and retinal differentiation becomes evident through the appearance of a dorsal-ventral invagination called the morphogenetic furrow that migrates posteriorly to anteriorly along the apical surface of the eye-antennal disc (Figure 1-9). Cellular proliferation in the anterior part of the eye imaginal disc still remains mitotically

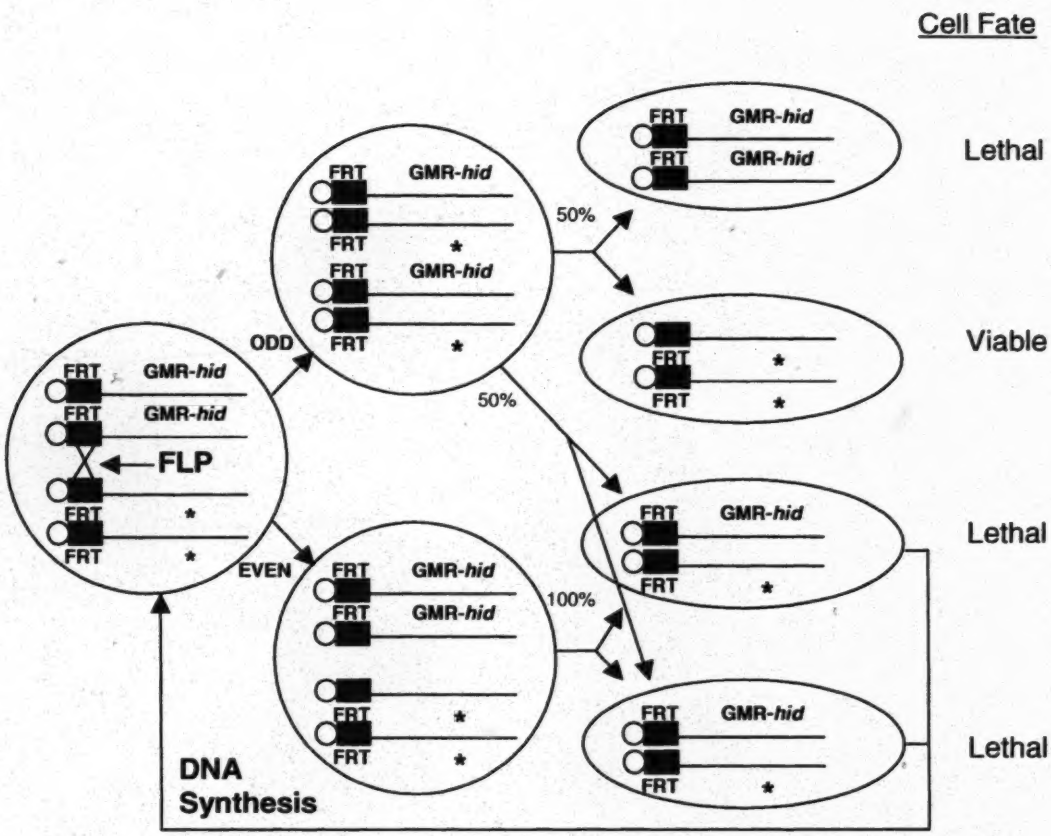

Figure 1-8. Method for generating homozygous ommatidial mitotic clones using the EGUF-GMR-*hid* system. GAL4 expression is driven from the *eyeless* promoter, restricting expression of GAL4 to ommatidial cells, where it interacts with upstream activating sequence (UAS) to drive expression of a Flp recombinase. Flp recombinase mediates homologous recombination at FRT sites and expression of the dominant death gene *hid*, driven by the Glass Multiple Reporter (GMR) promoter to restrict expression of this gene within the developing eye, ensures that only cells inheriting homozygous combinations of the chromosome of interest (designated by the chromosome arm with an asterisk) survive to undergo the next round of replication. After several generations, the result would be a *Drosophila* eye composed entirely of homozygous clones for this chromosome. Results from both an odd and even number of recombination events are depicted, along with the predicted percent chance of these cells producing homozygous or heterozygous progeny cells (from Stowers and Schwarz, 1999).

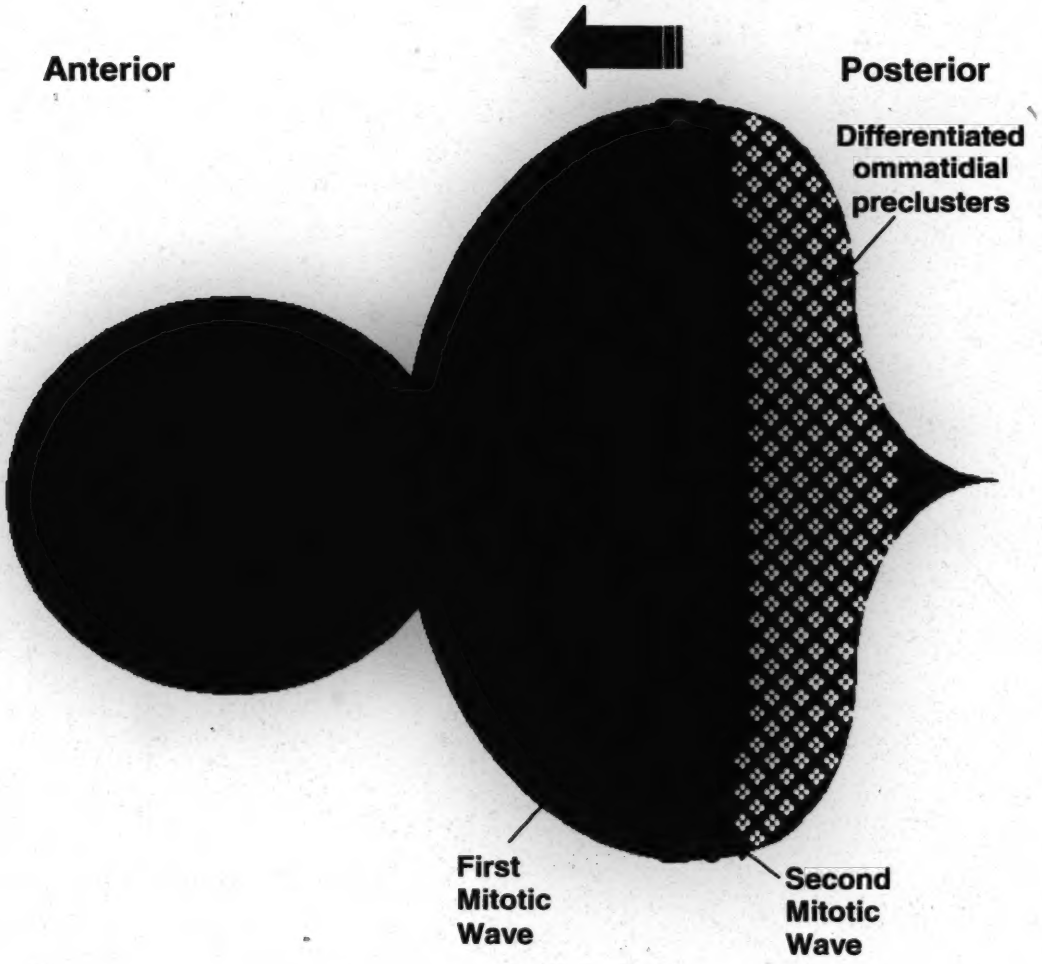

Figure 1-9. Development of the *Drosophila* eye imaginal disc. During the first and second larval instars, cells within the developing eye are mainly proliferative and governed by individual cell cycles (blue dots indicative of cells in S-phase and red dots indicative of cells undergoing mitosis). During the last larval instar, the morphogenetic furrow (MF – green bar) designating retinal differentiation and specification migrates in a posterior to anterior direction, synchronizing and arresting cells in G_1 that are caught in its wake. Within the furrow, ommatidial precursors are specified and organized into preclusters for differentiation into ommatidia, while cells that are not organized undergo a single round of mitosis forming a second mitotic wave prior to differentiating (note: proliferative cells ahead of the furrow are often referred to as the first mitotic wave even though these cells have no obvious synchrony or pattern).

unpatterned and uncoordinated. Directly ahead of the furrow however, cells proceed through S-phase then undergo a semi-synchronized mitosis referred to as the first mitotic wave (FMW) (Wolff and Ready, 1993). Upon exit from mitosis, these cells become arrested in G_1 as they enter the furrow. Within the furrow, the G_1 arrested ommatidial precursors become specified and organized into five-cell pre-clusters that will eventually differentiate into an adult ommatidium (Wolff and Ready, 1993; Baker, 2001). Behind the morphogenetic furrow, the cells of the pre-clusters undergo neuronal differentiation and never divide again while the remaining unspecified cells surrounding the G_1-arrested ommatidial pre-cluster cells synchronously undergo a round of S-phase and mitosis referred to as the second mitotic wave (SMW). These cells will then be recruited to make up the remaining 14 precursor cells required for a complete ommatidium. The SMW is necessary to generate enough precursor cells to complete each ommatidium. Supernumerary cells generated at this stage are destroyed later in the pupa by apoptosis, ensuring that a precise number of cells are maintained for development of the adult eye (Wolff and Ready, 1993; Baker, 2001). Because the eye is characterized by specific requirements and a temporal pattern of cell cycle regulation, it is an amenable system for identifying mutations causing defects in cell cycle regulation.

Using the method described earlier, referred to herein as the EGUF-GMR*hid* method for *eyeless*-GAL4; UAS-FLP, 3 of the 5 large chromosome arms in *Drosophila* (2L, 2R, and 3R, respectively) were screened (see Figure 1-10 for an example of the screening procedure for 2L). From the initial cross, F_1 males that displayed a rough-eye phenotype in the presence of 3 mM hydroxyurea (HU) and 2 mM caffeine were re-tested on normal media to identify conditional mutants, which were then confirmed and mapped

further. From this screen, a total of 9 mutations (herein referred to as *huc* mutants for ***h**ydroxy**u**rea **c**affeine-dependent* mutants) were isolated, with 8 mutations mapping to the left arm of the second chromosome (that were subsequently separated into 5 complementation groups), and 1 mutation mapping to the right arm of the third chromosome. This 3R single mutant was mapped by deficiency mapping and complementation analysis to cytological region 95D-E (and was thus referred to as *huc*95^{DE}). The *huc*95^{DE} mutant displayed a severely reduced and disorganized eye with irregular and fused ommatidia when larvae were grown on media containing HU and

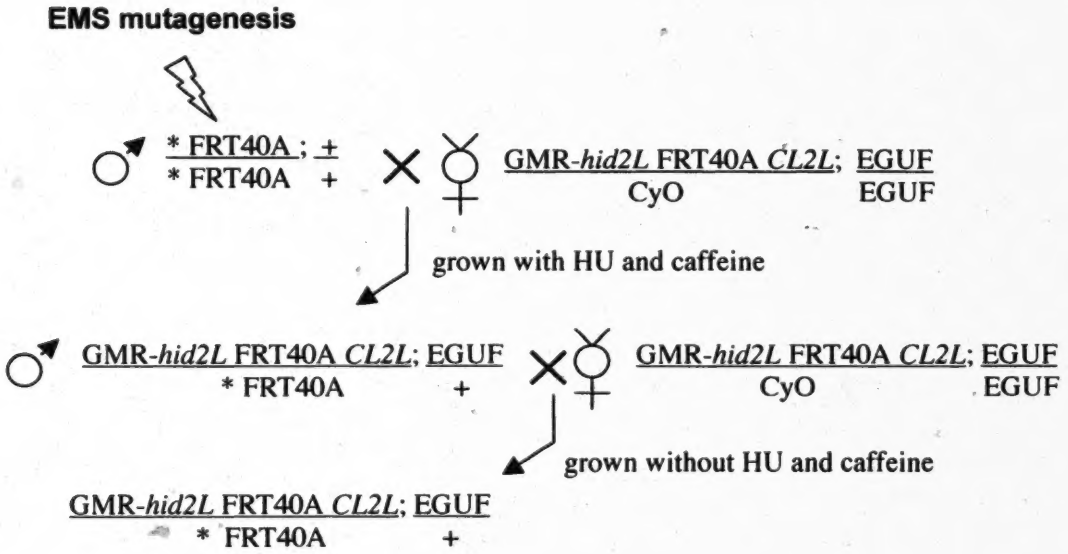

Figure 1-10. A genetic screen of chromosome 2L to identify mutants sensitive to hydroxyurea and caffeine during eye development. Eye-specific recombination between centromerically located FRT sites, in combination with eye-specific expression of the apoptotic inducing gene *hid*, results in eyes that are essentially a clone of a single genotype; the genotype of the remainder of the organism is heterozygous. F_1 larvae are grown in the presence of HU and caffeine. Males exhibiting an eye phenotype are selected and crossed again to EGUF females and progeny are grown in the absence of HU and caffeine. Male progeny from this cross that exhibit a wild-type or near wild-type phenotype were isolated for further analysis. Similar methods were applied in screening chromosomes 2R and 3R, using arm-specific FRT stocks (from Silva, 2002).

caffeine. This phenotype was more severe than any of the other mutants mapped on the second chromosome (see Figure 1-11). It was later discovered that treatment of *huc*95DE with caffeine alone produced this severe eye phenotype, whereas treatment with hydroxyurea alone produced eyes that were similar to wildtype, suggesting that *huc*95DE are primarily sensitive to caffeine. When *huc*95DE hemizygous larvae are viable were reared on standard molasses media. *huc*95DE hemizygotes however, displayed caffeine-dependent lethality when grown in media containing caffeine concentrations as low as 0.5 mM, suggesting that the gene associated with this mutation was not essential, but was conditionally required for viability in the presence of caffeine.

To determine if these defects occurred as a result of cell cycle abnormalities during early stages of ommatidial differentiation, imaginal eye discs were dissected from *EGUF/+; FRT82B huc*95DE*/FRT82B GMR-hid*3R third instar larvae and analyzed using antibodies to a neuronal RNA-binding protein called **e**mbryonic **l**ethal, **a**bnormal **v**isual (ELAV), which stains all differentiated neuronal cells (Silva, 2002; Yao *et al.*, 1993). Imaginal discs from trans-heterozygous mutant larvae grown in the presence of caffeine were smaller and more fragile than heterozygous controls and ELAV staining revealed that differentiation of the ommatidial preclusters still occurs with no change in size of the individual pre-clusters of trans-heterozygous mutant eye discs (although the pattern appeared to be slightly disrupted) (Figure 1-12). This suggests that the decreased size of the eye imaginal discs is due to fewer cells being present as opposed to smaller cells within the disc. The eye imaginal discs were also treated with Bromodeoxyuridine (BrdU), a base analogue of thymidine that is incorporated during DNA synthesis, identifying cells undergoing S phase. Third instar larval eye imaginal discs from trans-

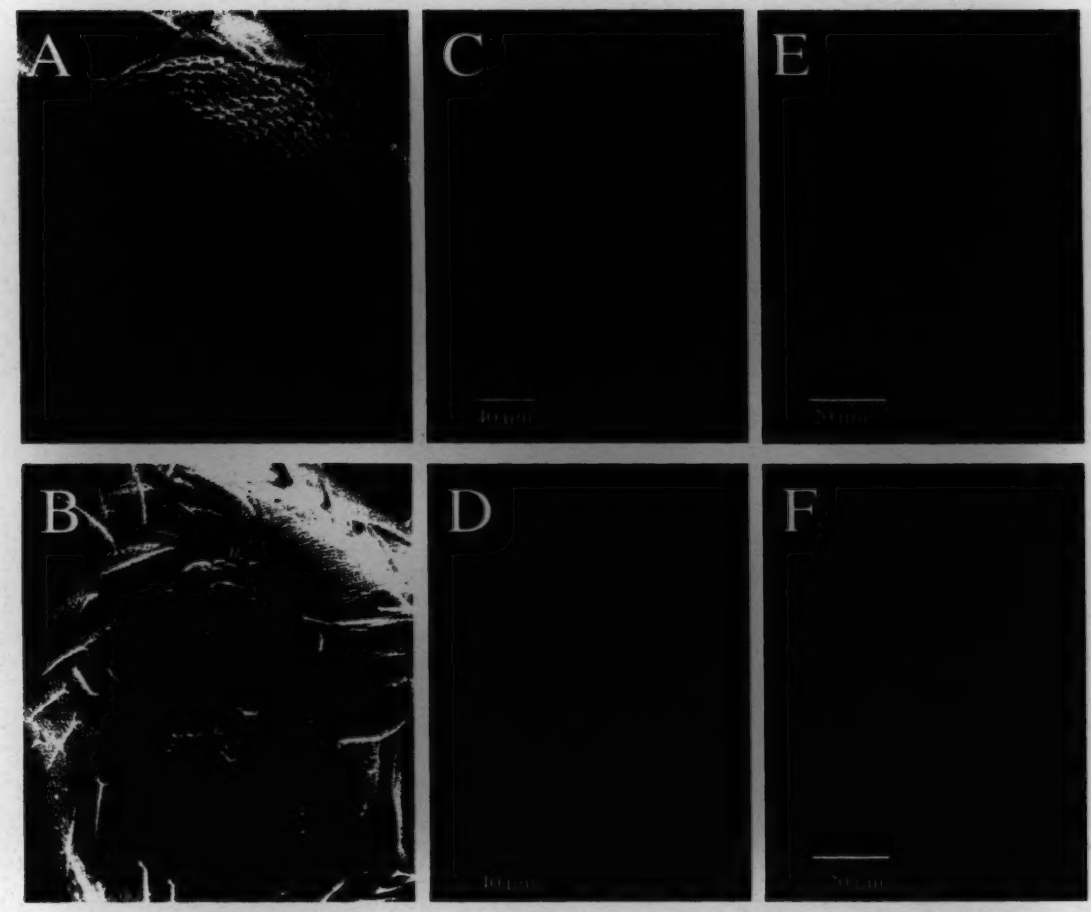

Figure 1-11. Scanning electron micrographs of adult eyes from individuals of the genotype *EGUF/+; FRT82B huc95E-D/ FRT82B GMR-hid3R CL3R* grown in the absence (A) and presence (B) of caffeine. The phenotype depicted here is indistinguishable from the phenotype that is observed when individuals are grown in the presence of both HU and caffeine. Eye imaginal discs from individuals of the genotypes *EGUF/+; FRT82B huc95E-D/ TM3 Ser* (C and E) and *EGUF/+; FRT82B huc95E-D/ FRT82B GMR-hid3R CL3R* (D and F) grown in the presence of caffeine. In the presence of caffeine, eyes are severely reduced in size and ommatidia are fused and greatly reduced in number (compare A and B). Staining with elav antibody reveals neuronal differentiation still occurs. Discs are smaller at third instar compared to heterozygous controls (compare C and D) but individual cells are not reduced in size (compare E and F) (from Silva, 2002).

heterozygous *huc*95DE mutants and heterozygous controls treated with caffeine and HU fewer cells stained with BrdU in the presence of these drugs were found to be comparable to controls (see Figure 1-12) (Silva, 2002). In addition, the pattern of staining ahead and behind of the morphogenetic furrow seemed to be disrupted and more diffuse in the presence of caffeine, suggesting that this mutant may have cell proliferation defects during ommatidial development, or exhibit aberrant proliferation due to an increase in apoptotic responses.

Mapping of *huc*95DE by E. Silva identified 25 potential candidates within this region, which was reduced to 22 as a result of complementation tests with mutants of three genes: *Syntaxin 1A* (*Syx1A*), *Adenomatous polypopsis coli 2* (*Apc2*), and *Tuberous sclerosis complex 1 (Tsc1)*. Because of the severity of the *huc*95DE phenotype, and the fact that this mutant showed defects that could be due to effects on cell cycle regulation, the gene associated with this mutant became an attractive candidate to pursue. As a result, my project was developed to identify the gene associated with the *huc*95DE mutation, determine the nature of the mutation, and carry out further phenotypic analysis to elucidate the specific defects caused by the mutation.

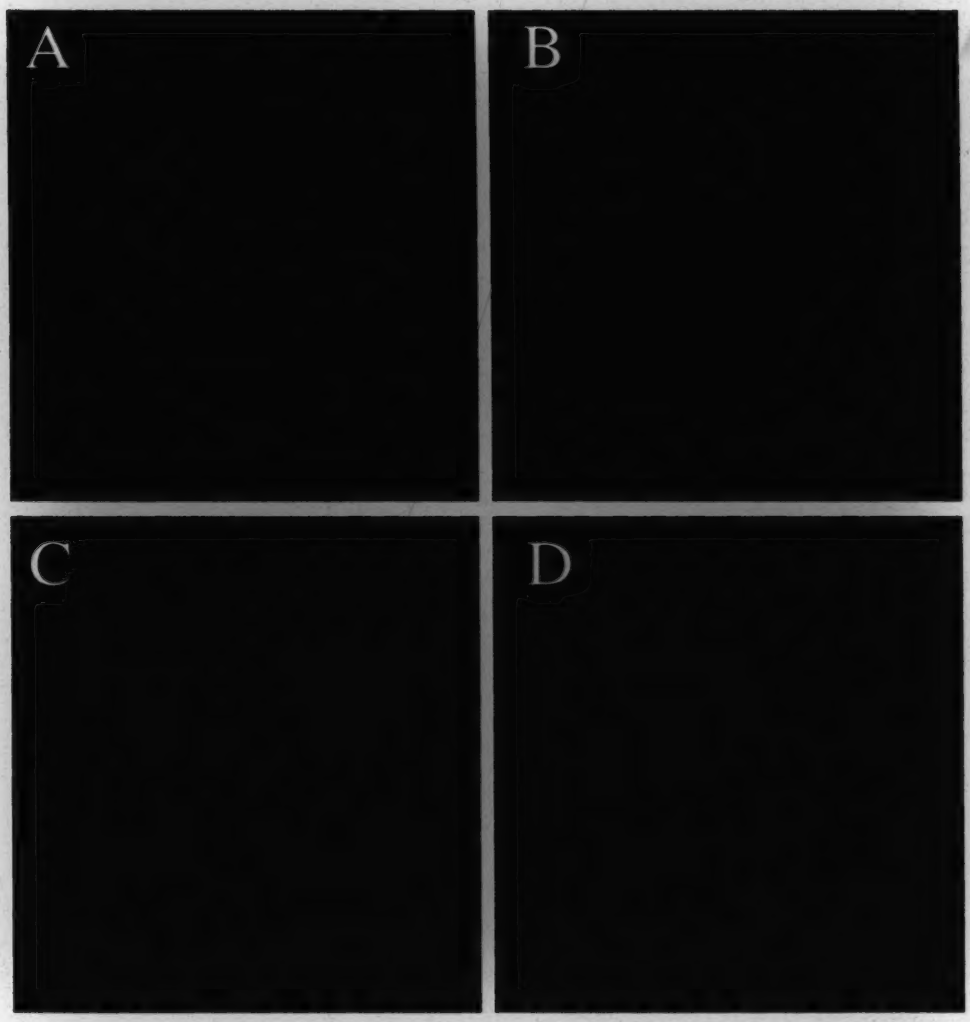

Figure 1-12. Eye imaginal discs from individuals of the genotypes *EGUF/+; FRT82B huc95E-D/ TM3 Ser* (A and C) and *EGUF/+; FRT82B huc95E-D/ FRT82B GMR-hid3R CL3R* (B and D) grown in the presence of caffeine and labeled with the nucleoside analog BrdU (from Silva, 2002).

Section 1-9: Literature Cited

Abraham, R. T. 2001. Cell cycle checkpoint signaling through the ATM and ATR kinases. *Genes & Dev* **15**:2177-2196.

Baker, N. E. 2001. Cell proliferation, survival, and death in the *Drosophila* eye. *Semin Cell Dev Biol* **12**: 499-507.

Barone, J. J. and H. R. Roberts. 1996. Caffeine consumption. *Food Chem Toxicol* **34**:119-129.

Beeton, C. A., E. M. Chance, L. C. Foukas and P. R. Shepherd. 2000. Comparison of the kinetic properties of the lipid– and protein-kinase activities of the p110α and p110β catalytic subunits of class Ia phosphoinositide 3-kinases. *Biochem J* **350**: 353-359.

Bertrand, F., A. Atfi, A. Cadoret, G. L'Allemain, H. Robin, et al., 1998. A role for nuclear factor kappaB in the antiapoptotic function of insulin. *J Biol Chem* **273**:2931-2938.

Bezprozvanny, I. B., K. Ondrias, E. Kaftan, D. A. Stoyanovsky and B. E. Ehrlich. 1993. Activation of the calcium release channel (ryanodine receptor) by heparin and other polyanions is calcium dependent. *Mol Biol Cell* **4**:347-352.

Bikopoulos, G., R. B. Ceddia, G. Sweeney and A. J. Hilliker. 2004. Insulin reduces apoptosis and increases DNA synthesis and cell size via distinct signalling pathways in *Drosophila* Kc cells. *Cell Prolif* **37**:307-316.

Blasina, A., B. D. Price, G. A. Turenne and C. H. McGowan. 1999. Caffeine inhibits the checkpoint kinase ATM. *Curr Biol* **9**:1135-1138.

Bose, A., A. Guilherme, S. Robida, S. M. C. Nicoloro, Q. L. Zhou, *et al.*, 2002. Glucose transporter recycling in response to insulin is facilitated by myosin Myo1c. *Nature* 420:821-824.

Brand, A. H. and N. Perrimon. 1993. Targeted gene expression as a means of altering cell fates and generating dominant phenotypes. *Development* **118**:401-415.

Brazil, D. P., and B. A. Hemmings. 2001. Ten years of protein kinase B signalling: a hard Akt to follow. *Trends Biochem Sci* **26**: 657-664.

Brodsky, M. H., J. J. Sekelsky, G. Tsang, R. S. Hawley and G. M. Rubin. 2000. mus304 encodes a novel DNA damage checkpoint protein required during Drosophila development. *Genes Dev* **14**:666-678.

Brogiolo, W., H. Stocker, T. Ikeya, F. Rintelen, R. Fernandez *et al.*, 2001. An evolutionarily conserved function of the Drosophila insulin receptor and insulin-like peptides in growth control. *Curr Biol* **11**:213-221.

Bruns, R. F., G. H. Lu and T. A. Pugsley. 1986. Characterization of the A2 adenosine receptor labeled by [3H]NECA in rat striatal membranes. *Mol Pharmacol* **29**:331-346.

Cantrell, D. A. 2001. Phosphoinositide 3-kinase signalling pathways. *J Cell Sci* **114**:1439-1445.

Daly, J. W., P. Butts-Lamb and W. Padgett. 1983. Subclasses of adenosine receptors in the central nervous system: interaction with caffeine and related methylxanthines. *Cell Mol Neurobiol* **3**:69-80.

Daniel, P. B., W. H. Walker and J. F. Habener. 1998. Cyclic AMP signaling and gene regulation. *Annu Rev Nutr* **18**:353-383.

Demaurex, N. and C. Distelhorst. 2003. Apoptosis - the calcium connection. *Science* **300**:65-67.

De Gubareff, T. and W. Sleator Jr. 1965. Effects of caffeine on mammalian atrial muscle, and its interaction with adenosine and calcium. *J Pharmacol Exp Ther* **148**:202-213.

Della Fazia, M. A., G. Servillo and P. Sassone-Corsi. 1997. Cyclic AMP signalling and cellular proliferation: regulation of CREB and CREM. *FEBS Let* **410**:22-24.

Du, C., M. Fang, Y. Li, L. Li and X. Wang. 2000. SMAC, a mitochondrial protein that promotes cytochrome C dependent caspase activation by eliminating IAP inhibition. *Cell* **102**:33-42.

Edgar, B. A. 1999. From small flies come big discoveries about size control. *Nat Cell Biol* **1**:E191-193.

Fernandez, M. J., A. Lopez and A. Santa-Maria. 2003. Apoptosis induced by different doses of caffeine on Chinese hamster ovary cells. *J Appl Toxicol* **23**:221-224.

Foukas, L. C., N. Daniele, C. Ktori, K. E. Anderson, J. Jensen *et al.*, 2002. Direct effects of caffeine and theophylline on p110δ and other phosphoinositide 3-kinases. *J Biol Chem* **277**: 37124-37130.

Franke, T. F., C. P. Hornik, L. Segev, G. A. Shostak and C. Sugimoto. 2003. PI3K/Akt and apoptosis: size matters. *Oncogene* **22**:8983-8998.

Fredholm, B. B. 1982. Adenosine receptors. *Med Biol* **60**:289-293.

Fredholm, B. B., A. P. Ijzerman, K. A. Jacobson, K. N. Klotz and J. Linden. 2001. International Union of Pharmacology. XXV. Nomenclature and classification of adenosine receptors. *Pharmacol Rev* **53**:527-552.

Fredholm, B. B. and T. V. Dunwiddie. 1988. How does adenosine inhibit transmitter release? *Trends Pharmacol Sci* **9**:130-134.

Fruman, D. A., R. Meyers and L. C. Cantley. 1998. Phosphoinositide kinases. *Annu Rev Biochem* **67**:481-507.

Gao, Z., T. Chen, M. J. Weber and J. Linden. 1999. A_{2B} adenosine and $P2Y_2$ receptors stimulate mitogen-activated protein kinase in human embryonic kidney-293 cells: cross-talk between cyclic AMP and protein kinase C pathways. *J Biol Chem* **274**:5972–80.

Gilbert, R. M. 1984. Caffeine Consumption. *Prog Clin Biol Res.***158**:185-213.

Gilman, A. G. 1987. G proteins: transducers of receptor-generated signals. *Annu Rev Biochem* 56:615-649.

Golic, K. G. and S. L. Lindquist. 1989. The FLP recombinase of yeast catalyzes site-specific recombination in the Drosophila genome. *Cell* **59**: 499-509.

Hanson, C. J., M. D. Bootman and R. Llewelyn. 2004. Cell Signalling: IP3 receptors channel calcium into cell death. *Curr Biol* **14**:933-935.

He, Z., W. Ma, T. Hashimoto, A. M. Bode, C. S. Yang *et al.*, 2003. Induction of apoptosis by caffeine is mediated by p53, Bax, and Caspase 3 pathways. *Cancer Res* **63**:4396-4401.

Henderson, D. S. 1999. DNA repair defects and other (mus)takes in Drosophila melanogaster. *Methods* **18**:377-400.

Jacobson, K. A., C. Hoffmann, F. Cattabeni and M. P. Abbracchio. 1999. Adenosine-induced cell death: evidence for receptor-mediated signalling. *Apoptosis* **4**:197-211.

Jafari, M., and A. Rabbani. 2000. Dose and time effects of caffeine on superoxide release, cell survival, and DNA fragmentation of alveolar macrophages from rat lung. *Toxicology* **149**: 101-108.

Katso, R., K. Okkenhaug, K. Ahmadi, S. White, J. Timms et al., 2001. Cellular function of phosphoinositide 3-kinases: implications for development, homeostasis, and cancer. *Annu Rev Cell Dev Biol* **17**:615-675.

Koulen, P. and B. E. Erlich. 2000. Reversible block of the calcium release channel/ryanodine receptor by protamine, a heparin antidote. *Mol Biol Cell* **11**:2213-2219.

Krasilnikov, M. A. 2000. Phosphatidylinositol-3 kinase dependent pathways: the role in control of cell growth, survival, and malignant transformation. *Biochemistry (Mosc)* **65**: 59-67.

Lam, K., C. L. Carpenter, N. B. Ruderman, J. C. Friel and K. L. Kelly. 1994. The phosphatidylinositol 3-kinase serine kinase phosphorylates IRS-1. *J Biol Chem* **269**: 20648-20652.

Lau, C. C. and A. B. Pardee. 1982. Mechanism by which caffeine potentiates lethality of nitrogen mustard. *Proc Natl Acad Sci USA* **79**:2942-2946.

Lee-Kwon, W., D. Park, P. V. Baskar, S. Kole and M. Bernier. 1998. Antiapoptotic signalling by the insulin receptor in Chinese hamster ovary cells. *Biochemistry* **37**:15747-15757.

Linden, J., T. Thai, H. Figler, X. Jin and A. S. Robeva. 1999. Characterization of Human A_{2B} Adenosine Receptors: Radioligand binding, western blotting, and coupling to G_q in human embryonic kidney 293 cells and HMC-1 mast cells. *Mol Pharmacol* **56**: 705-713.

Lizcano, J. M., S. Alrubaie, A. Kieloch, M. Deak, S. J. Leevers *et al.*, 2003. Insulin-induced Drosophila S6 kinase activation requires phosphoinositide 3-kinase and protein kinase B. *Biochem J* **374**:297-306.

Londos, C., D. M. Cooper and J. Wolff. 1980. Subclasses of external adenosine receptors. *Proc Natl Acad Sci USA* **77**:2551-2554.

Mandel, H.G. 2002. Update on caffeine consumption, disposition and action. *Food Chem Toxicol* **40**:1231-1234.

McPherson, P. S., Y-K. Kim, H. Valdivia, C. M. Knudson, H. Takekura, *et al.*, 1991. The brain ryanodine receptor: caffeine-sensitive calcium release channel. *Neuron* **7**:17-25.

Merighi, S., P. Mirandola, K. Varani, S. Gessi, E. Leung, *et al.*, 2003. A glance at adenosine receptors: novel target for anticancer therapy. *Pharmacol Ther* **100**:31-48.

Mignery, G. A., T. C. Sudhof, K. Takei and P. De Camilli. 1989. Putative receptor for inositol 1,4,5-trisphosphate similar to ryanodine receptor. *Nature* **342**:192-195.

Nishijima, H., H. Nishitani, N. Saito and T. Nishimoto. 2003. Caffeine mimics adenine

and 2'-deoxyadenosine, both of which inhibit the guanine-nucleotide exchange activity of RCC1 and the kinase activity of ATR. *Genes to Cells* **8**:423-435.

Osaki, M., M. Oshimura and H. Ito. 2004. PI3K-Akt pathway: its functions and alterations in human cancer. *Apoptosis* **9**:667-676.

Palade, P., C. Dettbarn, B. Alderson and P. Volpe. 1989. Pharmacologic differentiation between inositol-1,4,5-trisphosphate-induced Ca^{2+} release and Ca^{2+}- or caffeine-induced Ca^{2+} release from intracellular membrane systems. *Mol Pharmacol* **36**:673-680.

Palmer, T. M., T. W. Gettys and G. L. Stiles. 1995. Differential interaction with and regulation of multiple G-proteins by the rat A_3 adenosine receptor. *J Biol Chem* **270**:16895-16902.

Pan, Z., D. Damron, A-L. Nieminen, M. B. Bhat and J. Ma. 2000. Depletion of intracellular Ca^{2+} by caffeine and ryanodine induces apoptosis of chinese hamster ovary cells transfected with ryanodine receptor. *J Biol Chem* **275**:19978-19984.

Rauth, A. M. 1967. Evidence for dark reactivation of ultra-violet light damaged DNA in mouse L cells. *Radiat Rès* **31**:121-138.

Rondinone, C. M., E. Carvalho, T. Rahn, V. C. Manganiello, E. Degerman *et al.*, 2000. Phosphorylation of PDE3B phosphatidylinositol 3-kinase associated with the insulin receptor. *J Biol Chem* **275**: 10093-10098.

Rousseau, E., J. LaDine, Q-Y. Liu and G. Meissner. 1988. Activation of the Ca^{2+} release channel of skeletal muscle sarcoplasmic reticulum by caffeine and related compounds. *Arch Biochem Biophys* **267**: 75-86.

Sakaria, J. N., E. C. Busby, R. S. Tibbetts, P. Roos, Y. Taya, *et al.*, 1999. Inhibition of ATM and ATR kinase activities by the radiosensitizing agent, caffeine. *Cancer Res* **59**:4375-4382.

Saris, N. E. and E. Carafoli. 2005. A historical review of cellular calcium handling, with emphasis on mitochondria. *Biochem (Mosc)* **70**:187-194.

Schlegel, R. and A. B. Pardee. 1986. Caffeine-induced uncoupling of mitosis from the completion of DNA replication in mammalian cells. *Science* **232**:1264-1266.

Schulte, G. and B. B. Fredholm. 2003. Signalling from adenosine receptors to mitogen-activated protein kinases. *Cell Signal* **15**:813-827.

Shepherd, P. R. 2005. Mechanisms regulating phosphoinositide 3-kinase signalling in insulin-sensitive tissues. *Acta Physiol Scand* **183**:3-12.

Silva, E. A. 2002. Generation and characterization of chemical-sensitive cell cycle checkpoint mutants in *Drosophila.* M.Sc. Thesis. *Department of Biological Sciences* University of Alberta, Edmonton.

Stowers, R. S. and T. L. Schwarz. 1999. A genetic method for generating Drosophila eyes composed exclusively of mitotic clones of a single genotype. *Genetics* **152**: 1631-1639.

Susin, S. A., H. K. Lorenzo, N. Zamzami, I. Marzo, B. E. Snow, *et al.*, 1999. Molecular characterization of mitochondrial apoptosis-inducing factor. *Nature* **397**:387-389.

Tenzer, A., and M. Pruschy. 2003. Potentiation of DNA-damage-induced cytotoxicity by G2 checkpoint abrogators. *Curr Med Chem Anticancer Agents* **3**:35-46.

van Calker, D., M. Muller and B. Hamprecht. 1978. Adenosine inhibits the accumulation of cyclic AMP in cultured brain cells. *Nature* **276**:839-841

van Calker, D., M. Muller and B. Hamprecht. 1979. Adenosine regulates via two different types of receptors, the accumulation of cyclic AMP in cultured brain cells. *J Neurochem* **33**:999-1005.

Vanhaesebroeck, B., S. J. Leevers, G. Panayatou and M. D. Waterfield. 1997. Phosphoinositide 3-kinases: a conserved family of signal transducers. *Trends Biochem Sci* **22**:267-272.

Vernikos-Danellis J. and C. G. Harris III. 1968. The effect of *in vitro* and *in vivo* caffeine, theophylline and hydrocortisone on the phosphodiesterase activity of the pituitary median eminence, heart and cerebral cortex. *Proc Soc Exp Biol Med* **128**:1016-1021.

Wang, Z-B., Y-Q. Liu and Y-F. Cui. 2005. Pathways to caspase activation. *Cell Biol Intl* **29**:489-496.

Waring, P. 2005. Redox active calcium ion channels and cell death. *Arch Biochem Biophys* **434**:33-42.

Weinert, T., and L. Hartwell. 1989. Control of G2 delay by the rad9 gene of Saccharomyces cerevisiae. J Cell Sci Suppl 12:145-148.

Wolff, T., and D. F. Ready. 1993. Pattern formation in the *Drosophila* retina. Pp. 1277-1325 in *The Development of Drosophila melanogaster*. Cold Spring Harbour Laboratory Press.

Wymann, M. P., and R. Marone. 2005. Phosphoinositide 3 kinase in disease: timing, location, and scaffolding. *Curr Opin Cell Biol* **17**:141-149.

Yakel, J. L., R. A. Warren, S. M. Reppert and R. A. North. 1993. Functional expression of adenosine A_{2b} receptor in *Xenopus* oocytes. *Mol Pharmacol* **43**:277-280.

Yao, K. M., M. L. Samson, R. Reeves and K. White. 1993. Gene elav of Drosophila melanogaster: a prototype for neuronal-specific RNA binding gene family that is conserved in flies and humans. *J Neurobiol* 24:723-739.

Yenush, L., C. Zanella, T. Uchida, D. Bernal and M. F. White. 1998. The pleckstrin homology and phosphotyrosine binding domains of insulin receptor substrate 1 mediate inhibition of apoptosis by insulin. *Mol Cell Biol* **18**:6784-6794.

Zhou, Q. Y., C. Li, M. E. Olah, R. A. Johnson, G. L. Stiles *et al.*, 1992. Molecular cloning and characterization of an adenosine receptor: the A3 adenosine receptor. *Proc Natl Acad Sci USA* **89**:7432-7436.

Zhou, B-B. S., P. Chaturvedi, K. Spring, S. P. Scott, R. A. Johanson, *et al.*, 2000. Caffeine abolishes the mammalian G2/M DNA damage checkpoint by inhibiting Ataxia-Telangiectasia-mutated kinase activity. *J Biol Chem* **275**:10342-10348.

Zucchi, R., and S. Ronca-Testoni. 1997. The sarcoplasmic reticulum Ca^{2+} channel/ryanodine receptor: modulation by endogenous effectors, drugs and disease states. *Pharmacol Rev* **49**:1-51.

Chapter 2: The Mapping and Identification of *huc*95^{E}

Section 2-1: Introduction

In order to elucidate the molecular nature of the *huc*95DE mutation and to determine the reasons for caffeine sensitivity, it was necessary to identify which gene on the right arm of the third chromosome was associated with this phenotype. Furthermore, determining the identity of *huc*95DE could help to assess the success of this screen regarding its original intent, which was to identify novel cell cycle checkpoint functions. Originally, *huc*95DE was mapped cytologically by deletion mapping and complementation analysis to the cytological region of 95D11-95F15, because *huc*95DE failed to complement the deficiencies *Df*(3R)*crb87-4* (extending from 95D11-E2 to 96A2) and *Df*(3R)*crbF89-4* (extending from 95D7-11 to 95F15), respectively (Silva, 2002). Further refinement of the position to 95D11 to 95E6-7 was determined by complementation testing of *huc*95DE with the synthetic deficiency *Df*(3R)*slo*3, which has a large deletion on the right arm of the third chromosome (extending from 94D4-10 to 96A18) and the proximal portion (94D4-10 to 95E7-F1) of this deleted region duplicated, inverted, and inserted into the second chromosome at position 57B3-5 (see Figure 2-6A). These results had narrowed the number of potential candidates down to 26 genes (see Table 2-2). Out of this initial list, *huc*95DE was found to complement the genes *Syntaxin 1A* (*Syx1A* at position 95E1), *Tuberous sclerosis complex 1* (*Tsc1* at 95E4), and *Adenomatous polyposis coli 2* (*Apc2* at 95E6), thereby limiting the number of candidates at the start of this project to 23 predicted genes within this region.

Besides deficiency mapping and complementation analysis, several other strategies are available to further narrow down and map *Drosophila* mutations in a cost

effective and efficient manner. One such strategy is the genetic mapping of the relative positions of genes by recombination frequency analysis. This can be done with a classical three point cross whereby the position of a mutation is mapped with respect to two other mutations on the same chromosome. Another method that is useful in mapping is to mobilize *P*-elements to synthesize flanking deletions that when mapped, can be used to narrow down the location of a gene expressing a particular trait. This method involves isolating *P*-element-induced recombinants and using segregation patterns of recessive markers flanking the mutation to determine whether the mutation segregates proximal or distal to the site of insertion (Chen *et al.*, 1998). Determination of the molecular breakpoints of flanking deletions of recombinants that segregate with the mutation can then be used to narrow down the region to where the mutation exists on the chromosome. This is an informative method, as even determining the breakpoints of recombinants that do not segregate with the mutation can also be used to exclude candidate genes lying within the region. Another method is the molecular analysis and sequencing of candidate genes. This method takes advantage of the completed *Drosophila* genome sequence of predicted genes and allows for the identification and analysis of sequence alterations in a search for putative candidates. This method could not only identify *huc*95^{DE}, but also elucidate the molecular nature of the mutation associated with the gene. Although it did not seem to be very practical to sequence all 23 candidates within this initial region, this method would become useful if this region was further narrowed down by any of the other methods previously described (so that only a few remaining candidates would remain to be sequenced), or could become useful in the confirmation and analysis of a particular candidate. Furthermore, obvious candidates for which a plausible mechanism

could be proposed for caffeine sensitivity (such as gene candidates involved in apoptosis, caffeine metabolism, or genes involved with cellular proliferation or cell cycle checkpoints) could be directly analyzed by this method in the absence of any available mutants for these genes. Each of the above methods were attempted in order to determine the location of the *huc*95^{DE} mutation. This chapter will discuss each approach and the information that I obtained from them.

Section 2-2: Materials and Methods

Section 2-2a: Fly stocks and crosses

All *Drosophila* mutants and fly stocks used in the experiments described within this chapter are listed in Table 2-3. All fly stocks and crosses (unless otherwise stated) were raised on standard molasses and cornmeal media and grown either at room temperature or at 25°C in either vials or plastic fly bottle with volumes of 6 ml and 60 ml media, respectively. For crosses involving caffeine treatment in vials, caffeine-containing food was prepared by scoring the media with a clean metal spatula and adding 250 μL of caffeine (dissolved in distilled water) at an appropriate concentration (normally from a 50 mM caffeine stock solution for a final concentration of 2 mM) to yield the desired concentration in vials. This volume was previously empirically calculated to ensure complete absorption of the caffeine. Prepared vials were allowed to soak over night after which flies were tipped into this media and allowed to lay eggs for approximately 24 hours prior to tipping again to a new vial. Alternatively, fly crosses were set up within the vials and allowed to lay eggs for 24 hours after which time the flies were tipped into a new vial. The media was then scored and caffeine added as described above. This method was done to address any concerns about flies not laying in

caffeine-tainted media because of perceived sensitivity to the media. However, both methods yielded similar results and approximately equivalent amounts of progeny, indicating that either method was suitable for the caffeine experiments described in this chapter.

*huc*95DE hemizygotes were originally produced by either crossing *huc*95DE*/TM3 Ser-GFP* to either *Df*(3R)*crb87-4/TM3 Ser-GFP* or *Df*(3R)*crbF89-4/TM3 Ser-GFP*, and selecting non-Ser adults or non-GFP third instar larvae. Because of the incomplete penetrance and cryptic nature of the *Ser* marker, and problems involving damage or loss of wings in the media, crosses involving *huc*95DE*/TM3 Sb*, *Ser* and *Df*(3R)*crb87-4/TM3 Sb*, *Ser*, *Df*(3R)*crbF89-4/TM3 Sb*, *Ser*, or *Df*(3R)*W6/TM6C Sb*, *Tb* were later used, selecting for absence of Sb in adult flies. To detect hemizygous 2nd and 3rd instar larvae, crosses involving *huc*95DE*/TM6B Sb*, *Tb*, *e* and *Df*(3R)*crb87-4/TM6B Sb*, *Tb*, *e* were used, selecting for non-Tb larvae. Crosses to generate deletion mutants through *P*-element mobilization are outlined in Figure 2-3.

Section 2-2b: PCR and sequencing

DNA used in PCR and sequencing reactions was obtained by homogenizing adult flies of the appropriate genotype in genomic DNA homogenization buffer (100 mM NaCl, 0.2 M sucrose, 100 mM Tris pH 9.5, 50 mM EDTA, and 0.05% SDS) and incubated at 65°C for 30 minutes, followed by addition of 8 M of potassium acetate and further incubation on ice for 30 minutes. Following centrifugation at ~ 12000 rpm (17211 xg) for 10 minutes, 0.7 volumes of isopropanol was added to the supernatant, incubated on ice for an additional 30 minutes, and centrifuged at ~ 8000 rpm (7649 xg) for 10 minutes. The pelleted DNA was then washed in 70% ethanol, resuspended in TE

Buffer (10 mM Tris-Cl pH 7.5 and 1mM EDTA), and treated with RNase A at 37°C for 30 minutes. RNase and any remaining protein were removed through phenol-chloroform extractions (as described in Sambrook *et al.*, 1989), followed by isopropanol/ethanol precipitations (as described above but using 7.5 M ammonium acetate), and resuspension in sterile water. The resultant DNA was then quantified by spectrophotometry or gel quantification analysis. All PCR reactions were carried out for 30 cycles utilizing the appropriate primer pairs for given genes and sequences at concentrations of 1 mM (see Appendix for list of primers). PCR reaction mixes containing 10X PCR Buffer, 50 mM $MgCl_2$ solution, and *Thermus aquaticus* DNA polymerase were obtained from Invitrogen, as well as all primers used. Sequencing reactions were performed using the Big Dye Terminator V3.1 sequencing mix and sequencing primers listed in the appendix for the various genes listed. For large genomic regions, overlapping template sequences of approximately 2000 to 3000 nucleotides were amplified. Sequencing reactions were conducted using 100 – 500 ng of template DNA, 5 pmol of sequencing primer, 4 μL of sequencing pre-mix buffer (consisting of 200 mM Tris, pH 9.0 and 5 mM $MgCl_2$), and 4 mL of the BigDye premix in a total volume of 20 μL. PCR reactions were then run with a denaturation temperature of 95°C for 30 sec, annealing temperature of 50°C for 15 sec, and an extension temperature of 1 min for 30 cycles. The Molecular Biology Sciences Unit at the University of Alberta then resolved the sequencing reactions by gel electrophoresis using an ABI 3700 automated DNA sequencer, and the resulting sequences were analyzed using the sequence analysis program Gene Tools 2.

Section 2-2c: Embryo DNA Preparation and PCR

The extent of the *Df*(3R)*W6* deletion was determined using DNA isolated from embryos collected on grape juice plates after 1 day of egg laying from a *Df*(3R)*W6/TM3C Sb, Tb* stock. Each embryo was then macerated in 10 μL of homogenization buffer (10 mM Tris-HCl pH 8.0, 1 mM EDTA pH 8.0, 25 mM NaCl, and freshly added Proteinase K at 200 μg/ml), incubated for 30 minutes at 37°C (for Proteinase K digestion), followed by heat inactivation of Proteinase K at 99°C for 10 minutes. *Df*(3R)*W6* homozygote embryo DNA samples were identified by the inability to amplify fragments from *Apc2* and *Tsc1*, known to reside within the deficiency, and the ability to amplify fragments from *Myt1*, which was known to reside outside of the deleted region. 1 μL of this mixture was immediately used as a template in PCR reactions performed as described above utilizing the primer sets for *Myt1*, *Tsc1*, *Apc2*, *mRpS24*, *CG13605*, *CG13606*, *CG13607*, *CG6129*, *CG6178*, *CG6182*, *CG5463*, *CG5510*, *CG18428*, and *CHORD* (see appendix).

Section 2-2d: RT-PCR and RNA isolation

RNA for RT-PCR analysis was isolated using the Qiagen RNAasy Mini Kit (catalogue number 74104). Total RNA was obtained by macerating adult flies or larvae of the appropriate genotype in the provided lysis buffer using a mortar and pestle, and homogenizing the lysate by passage through a 20 gauge sterilized needle. The resultant suspension was then processed directly according to the protocol provided with the kit for isolation of total RNA. The isolated RNA was then used for RT-PCR using the One Step RT-PCR Kit (catalogue number 210210) and subjected to reverse transcription reaction for 30 minutes at 50°C, an initial PCR activation step of 95°C for 15 minutes, followed by

PCR denaturation, annealing, and extension reactions at appropriate temperatures as described above for 40 cycles. A final extension time of 10 minutes at 72°C was also programmed to ensure complete extension of desired templates. Results were then analyzed by gel electrophoresis on a 0.5% Tris Borate EDTA (TBE) or 1% Tris Acetate EDTA (TAE) agarose gel.

Section 2-2e: Synthesis and mapping of transgenic rescue lines

The restriction enzymes *Eco*RI, *Sca*I, *Eco*RV, and *Xho*I, and T4 DNA ligase, all used in the cloning of a *myo*95E rescue construct, were obtained from Invitrogen. Genomic DNA for the *myo*95E genomic rescue construct was excised from the Bacterial Artificial Chromosome BACR29F06, obtained from BACPAC resources at the Children's Hospital Oakland Research Institute. The genomic rescue plasmid for *myo*95E was constructed by excising a 8039 bp fragment from BACR29F06 using a blunt ended restriction enzyme *Sca*I, and a sticky ended cutter *Xho*I (Figure 2-12). This fragment was predicted by the *Drosophila* genome project to encompass the whole *myo*95E gene (including all 15 introns, 3', and 5' untranslated regions) as well as most of the downstream region up to the next gene (but did not contain the upstream genomic region). To add an *Eco*RI restriction site, which would be used for insertion into the transformation vector *pUAST*, this 8039 bp fragment was subcloned into the vector *pBluescript* cut with *Eco*RV and *Xho*I. To include regulatory elements upstream of *myo*95E, a 3672 bp fragment containing the upstream genomic region was also excised from BACR29F06 using *Xho*I restriction sites, and ligated to the *pBluescript* plasmid containing the 8039 bp fragment restricted with *Xho*I. Plasmid contructs containing the 3672 bp fragment ligated within the correct orientation were identified by PCR using

primers that flanked the ligation site, and the resulting 11711 bp fragment (8039 bp + 3672 bp) was sequenced to confirm its integrity. The 11711 bp fragment was then excised using *Eco*RI and *Xho*I, and cloned into the transformation vector *pUAST* (described by Brand and Perrimon, 1993). Transformation through injection into pre-blastoderm embryos was carried out as described by Rubin and Spradling (1982) with the construct concentrated and purified to a concentration of 5 μg/10 μL, along with a Δ 2-3 helper plasmid at 1 μg/10 μL that was microinjected into stage 4 bleach-dechorionated embryos from *yw* flies. First instar survivors were then raised on instant *Drosophila* media, and were subsequently crossed to *yw* flies as adults. Two putative transformants (identified by orange eye colour due to expression of the white gene present in the P-transformation vector *pUAST*) were obtained and the rescue construct was subsequently mapped in both transformants to the third chromosome. Because *huc*95^{DE} also mapped to the third chromosome, recombinants were generated using the strategy shown in Figure 2-13A that contained the genomic rescue construct and *Df(*3R)*crb87-4* on the same chromosome. Putative recombinants were selected on the basis of inheritance of $P[w^+]$ transgene carrying the rescue construct and *e* from the deficiency chromosome with a third chromosomal balancer and then tested for complementation against the deficiency to identify recombination events that linked the construct (evident by the presence of $[w^+]$ gene expression) and the *e* recessive mutation without the deficiency. Recombinant chromosomes carrying both the transgene and deficiency were then tested for complementation with *huc*95^{DE} mutants in the presence and absence of 2 mM caffeine, as described in Figure 2-13B.

Section 2-3: Results

Section 2-3a: Mapping of *huc95^{DE}* through Recombination

Because of the caffeine-sensitive conditional lethality of *huc*95DE hemizygotes, a strategy was devised to map *huc*95DE through the classical method of constructing three factor crosses and determining recombination frequencies. This strategy involved the use of two unconditional recessive embryonic lethal mutants for the genes *syntaxin 1A* (*syx1A*) and *crumbs* (*crb*) (mapping to 95E1 and 95F10-11, respectively), as well as the deficiency *Df*(3R)*crb87-4* which spanned the region containing these genes and *huc*95DE (see Figure 2-1 for the crossing scheme). Syx1A is a presynaptic membrane protein present in several tissues but most highly expressed within cells of the nervous system where it is thought to act as a receptor for synaptic vesicle docking and fusion (Broadie *et al.*, 1995). *syx1A* null mutant embryos fail to secrete most or all cuticle, exhibit abnormal gut morphology, and have subtle defects in axonal morphology (with axon bundles of segmental and intersegmental nerves appearing thickened and irregular in shape). In addition, there is a complete failure to evoke endogenous neurotransmitter release, resulting in an absence of synaptic transmission (Schulze *et al.*, 1995). The *crb* gene encodes an apical transmembrane protein that is involved in determining the apical-basolateral polarity of epithelial cells - an important process in the organization and establishment of compartmentalization in multicellular organisms (Tepass *et al.*, 1990). Consequently, *crb* mutants exhibit embryonic lethality shortly after gastrulation (a period when extensive epithelial movement and reorganization occurs to form the three germ layers, eventually giving rise to body axis and organogenesis).

The fact that both *syx1A* and *crb* mutants were able to complement *huc*95DE allowed for a strategy to be devised whereby the caffeine sensitivity phenotype could be used to map *huc*95DE with respect to these two genes (see Figure 2-1). In this strategy, the frequency of forming *huc*95DE-*syx1A*, *huc*95DE-*crb*, and *syx1A-crb* recombinant double mutants was determined by crossing flies with the genotypes *huc*95DE/*syx1A*, *huc*95DE/*crb*, and *syx1A*/*crb* to *Df*(3R)*crb87-4/ TM3 Sb, Ser* in the presence of caffeine and looking for progeny that did not inherit the *TM3* balancer. Since the *huc*95DE hemizygotes exhibited caffeine-sensitive lethality while *crb* and *syx1A* hemizygotes exhibit embryonic lethality, the only non-balancer progeny that would survive would be those that have previously undergone a recombination event to create a wildtype chromosome (Figure 2-1). Using a concentration of 2 mM caffeine (the concentration used in the screen that resulted in the isolation of these mutants), crosses involving *huc*95DE/ *crb* females with *Df*(3R)*crb87-4/ TM3 Sb* males resulted in a recombination frequency of 0.021 (n=5007) for flies not containing the *Sb* balancer. Crosses between *huc*95DE/ *syx 1A* females with *Df*(3R)*crb87-4/TM3 Sb* males resulted in a recombination frequency of 0.07 (n=3937), while crosses between *syx 1A/ crb* resulted in a recombination frequency of 0.017 (n=9541). Analysis of these frequencies suggested that *huc*95DE might be closer to the *crb* locus than the *syx1A* locus (0.021 cM from *huc*95DE to *crb* as compared to 0.07 cM from *huc*95DE to *syx 1A*). However, the map distance determined between the loci of *syx 1A* and *huc*95DE (0.07 cM) did not add up to the sum of the proposed distances of *syx 1A* to *crb*, and *crb* to *huc*95DE (0.038 cM) (Figure 2-2) suggesting possible inaccuracies in the data. Furthermore, these results suggested that *huc*95DE mapped to the right of *crb* (which is located cytologically at 95F10-11), which conflicts with the original mapping of *huc*95DE

to the cytological regions of 95D-E through deficiency mapping. An explanation for these anomolous results is that perhaps some of the recombinants isolated were *huc*95DE hemizygotes who escaped the lethal effects of caffeine and managed to complete development to adulthood. This would artificially boost the recombination frequency by increasing the number of putative recombinants, thereby increasing the proposed map distance between the respective genes. To test for this, male recombinants from each of these crosses were collected and subjected to single male crosses with *Df*(3R)*crb87-4/TM3 Sb* virgin females in the presence and absence of 2 mM caffeine to test if they were true recombinants. If these flies were recombinants, then the non-balancer progeny of such a cross should be able to grow and develop normally on caffeine-containing medium. Alternatively, if the flies were escapers, non-balancers would be susceptible to caffeine sensitivity and not be sensitive in its absence. Out of 10 putative *huc*95DE/*crb* recombinant males tested, 5 behaved as recombinants while 5 behaved as escapers. Similar results were also obtained with crosses done with 23 *huc*95DE-*syx 1A* putative recombinants, which yielded 10 possible escapers and 4 recombinants (with the remaining unclassifiable due to lack of progeny in these crosses). From these tests, it could be concluded that the genetic map is most likely affected by escapers artificially increasing the recombination frequency, which supports the inability of the map distances to add up as well as the original mapping data.

Section 2-3b: Mapping of *huc95^{DE}* through P-element mobilization and flanking deletion synthesis

Another strategy to map the location of the *huc*95DE mutation was to synthesize flanking deletions by mobilizing transposable *P*-elements within the 95D-E region. To

synthesize a library of flanking deletions, stocks carrying four different *P*-element insertions mapping within the cytological regions of 95D-E were crossed to males containing a transposase source and third chromosomal recessive markers *claret* (*ca*, located cytologically at 99B8-10) and *ebony* (*e*, located cytologically at 93C7-D1). The *P*-element lines used for this experiment were *P{EP}Syx1A*^{EP3215} (mapped cytologically to 95E1, inserting 556 bp upstream from *syx 1A*), *P{EP}CG6178*^{EP3637} (mapped cytologically to 95E5-6, inserting 206 bp upstream of *CG6178* and 820 bp upstream of *Mpk2*), *P{EP}mask*^{EP601} (mapped cytologically to 95F3-5, inserting 2995 bp within the gene ***m**ultiple **a**nkyrin repeats **s**ingle **K**H domain* (*mask*)), and *P{GT1}*CG33100^{BG01713} (mapped cytologically to 95E1, inserting 3197 bp upstream of *syx1A*). Males containing the transposase source and one of these *P*-element insertions, were then crossed to homozygous *ca* and *e* females to detect *P*-element transposase-associated recombination events, scored by the absence of either *ca* or *e* in the resulting progeny (see Figure 2-3). Crossing these recombinants to *huc*95DE mutants in the presence and absence of caffeine to identify recombinants that were caffeine sensitive could then identify useful recombinant lines containing flanking deletions that deleted *huc*95DE. The putative deletions within these caffeine-sensitive recombinants would then be molecularly mapped by inverse PCR to narrow down the region of interest. In such a strategy, mapping the breakpoints of deletions of recombinants that do not exhibit caffeine lethality would also be informative, as mapping these would allow the exclusion of candidate genes from the region.

Males containing the transposase source on the second chromosome with the balancer *CyO*, and a third chromosomal dominant mutation *Sb* over a 2-3 translocation

dominant mutation (apterous xasta (ap^{xa})), were crossed to females from a homozygous stock consisting of *e* and *ca* markers (Figure 2-3). Males from this cross were identified by the inheritance of *Sb* (and thus, the transposase source as a result of co-segregation of the second and third chromosomes in this cross due to the translocation) and crossed to each of the four *P*-element lines. Resultant progeny males, which had inherited the transposase source and *P*-element, were crossed again to the homozygous *e*, *ca* stock to identify events of recombination that presumably would have taken place within these males. Upon examination of all progeny from several trials of this final cross (amounting to up to 5 bottles for each *P*-element line), no recombinants were obtained (as evidenced by the inability to recover only *ca* or *e* progeny). It was also noticed that in flies harbouring both the transposase source and the *P*-element, the expected mottling of eye colour (whereby pigmentation within the eye appears patchy due to position effect variegation) was not evident, suggesting that the transposase source used might be very weak or even non-functional. This would explain the difficulty in obtaining male recombinants since this strategy had depended upon functional transposase expression in order to induce *P*-element excision events. To address this problem, another stock with a stronger transposase transgene inserted on the third chromosome and known to transpose efficiently was obtained and used in the crossing scheme presented in Figure 2-4. In this scheme, males containing the transposase source marked with *Sb* were crossed to the *P*-element insertion line and then crossed to a stock with a third chromosomal balancer that did not contain the dominant mutation *Sb*. The resulting progeny would then be crossed to the $huc95^{DE}$ stock (or a deficiency that deleted $huc95^{DE}$) and tested for caffeine sensitivity to determine if they complement $huc95^{DE}$. Such flies could carry a new

deletion containing *huc*95DE caused by excision of the *P*-element. This strategy would not be as informative as the previous one, since negative results could not also be used to rule out possible gene candidates. This method did, however, have the advantage of taking fewer generations of crosses to obtain results since no recessive markers would have to be crossed in to identify recombinants. Unfortunately, all attempts to generate males containing the transposase insertion and the *P*-element line *P{EP}CG6178*^{EP3637} failed, possibly due to second site lesions which might have existed on both third chromosomes harbouring the *P*-element and transposase source. Since this *P*-element corresponded to a gene that mapped within the smallest region that *huc*95DE had been mapped to (defined by *Df*(3R)*W6*, as discussed later), excision events from this *P*-element line had the greatest opportunity of generating useful deletions with which to map *huc*95DE. Rather than testing the other lines or devising alternative strategies for recombinational mapping, more time and focus was devoted to other types of experiments as discussed below.

Section 2-3c: Deficiency Mapping and Complementation Analysis

When I started this project, *huc*95DE was already mapped to cytologically to 95D-E by crosses to chromosomal deletions. Complementation tests with mutants affecting three genes in this region limited the candidates to 23 genes. To further narrow down the number of candidates, a complementation test was done with *Df*(3R)*crb87-4* (a deficiency extending from 95D11-E2 to 96A2 that did not complement *huc*95DE) and *Df*(3R)*mbc-R1* (extending from 95A6-7 to 95D6-11 and did complement *huc*95DE) to see if these deficiencies overlap. These two deficiencies failed to complement, suggesting that they overlap. Since *Df*(3R)*mbc-R1* complements *huc*95DE, if the extent of the

overlap of this deletion could be determined, then genes within this overlap could be eliminated as candidates. *syx1A*, one of the previous genes which was tested and shown to complement the *huc*95DE mutation and which mapped cytologically to 95E1, was unable to complement *Df*(3R)*mbc-R1*, suggesting that this gene resided within this region. As a result, any possible candidates which localized upstream of *syx1A* could be excluded since this gene was localized in a deficiency which complemented *huc*95DE. These results eliminated one gene upstream of *syx1A*, further refining the number of candidates to 22 genes.

The region where *huc*95DE maps was further narrowed down by complementation tests with another deficiency called *Df*(3R)*W6*, reported to delete the gene *Adenomatous polyposis coli 2* (*Apc2*) which mapped to 95E6 (Ahmed *et al.*, 2002). *huc*95DE failed to complement *Df*(3R)*W6*, suggesting that *Df*(3R)*W6* contained the gene associated with caffeine sensitivity. Complementation tests involving *Df*(3R)*W6* and mutants of the *Tsc1* gene (mapped at 95E4) and the *Syx1A* gene (mapped at 95E1) had showed that *Df*(3R)*W6* failed to complement 4 different alleles of *Tsc1*, but did complement an allele of *Syx 1A*, suggesting that the deletion extended cytologically to 95E4 (deleting *Tsc1*), but not past 95E1. To further narrow down the possible candidates, the next logical step was to determine the approximate extent of the W6 deletion and the genes that it contained.

Because *Df*(3R)*W6* was maintained over a balancer containing the larval marker *Tubby* (*Tb*) (which results in shorter third instar larvae and as a result, shorter pupal cases), and because no non-Tb pupal cases were seen in any of the stock bottles, *Df*(3R)*W6* was lethal in a homozygous state (which was not surprising since this deficiency deleted *Tsc1* and *Tsc1* homozygotes die as second instar larvae). If *Df*(3R)*W6*

homozygotes were capable of surviving as embryos however, it would be possible to obtain homozygous *Df*(3R)*W6* embryonic DNA to test for the presence or absence of specific genes by PCR amplification (Figure 2-5A). To do this, DNA was extracted from embryos deposited over a 12 hour collection period and *Df*(3R)*W6* homozygotes were identified by two criteria: 1) the ability to amplify a 1650 bp fragment from *Myt1* (localized to 64E7, as a positive control) and 2) the inability to amplify 575 bp and 540 bp fragments from *Tsc*1 and *Apc*2 since genetic tests described earlier had demonstrated that *Df*(3R)*W6* contained these genes (Figure 2-5B). Subsequently, systematic tests were conducted to determine that *Df*(3R)*W6* deleted the genes *CG13607* and *CG5510*, but not *CG13605* or *CG13606*, genes upstream and downstream from *CG13607* and *CG5510*, respectively (see molecular evidence - Figure 2-6). Furthermore, PCR tests for *CG18428* and *CHORD* (genes upstream and downstream of *CG13605* and *CG13606*, respectively) had also shown amplification, confirming that *Df*(3R)*W6* did not extend past *CG13605* and *CG13606* (data not shown). Even though both *CG13605* and *CG13606* displayed amplification, the possibility still existed that *Df*(3R)*W6* could have extended into the 5' untranslated region or important upstream regions that were important for expression and function of these genes. As a result, these genes were still considered as candidates and defined *Df*(3R)*W6* as extending cytologically from 95E1 to 95E7-E8, a region containing 18 predicted genes (see Figure 2-7B). Since *Apc*2 and *Tsc*1 were previously shown to complement *huc*95^{DE} mutants (see Table 2-2), the number of potential candidate genes for the *huc*95^{DE} mutation was reduced to 16 genes from a total of 23 original candidates, which prompted a renaming of the *huc*95^{DE} mutant to *huc*95^{E}.

For further analysis of candidate genes within the region, *P*-element insertion lines associated with the genes *kal-1*, *CG6164*, *sec10*, *CG6178*, and *CG6182* were obtained and tested against *huc*95^{E} for complementation. The gene *kal-1* is the *Drosophila* homologue of the extracellular matrix cell-adhesion protein anosmin-1, which is associated with the human X-linked genetic disorder Kallmann syndrome (Andrenacci *et al.*, 2004). This disease is characterized by anosmia (no sense of smell), hypogonadism, and sterility, and is thought to arise because anosmin-1 is suspected to play a role in the formation of the olfactory bulb and in the targeting and migration of axons of olfactory neurons and gonadotropin-releasing-hormone neurons into the brain (thus explaining the phenotypes as gonadotropin is the hormone responsible for gonad and genital development) (Lutz *et al.*, 1993; Hardelin *et al.*, 1999). Sec10 is a component of the exocyst complex, which is an important macromolecule in the secretory pathway, purported to play a role in the trafficking of secretory vesicles to the plasma membrane (Lloyd *et al.*, 2000). The genes *CG6164*, *CG6178*, and *CG6182* are novel genes with no known function or homologues that are also *huc*95^{E} candidates because they reside in the region deleted by *Df*(3R)*W6*. The insertion points for the *P*-insertion elements associated with *kal-1*, *CG6164*, *sec10*, and *CG6182* were located 71 bp, 2358 bp, 37 bp, and 313 bp upstream of the 5' untranslated region, respectively. None of these *P*-element insertion lines were sensitive to caffeine in initial tests and they all complemented *huc*95^{E} mutants for caffeine sensitivity. To confirm that the P-element insertions associated with these genes had affected gene function, RT-PCR of homozygous viable lines of P-element insertions associated with *kal-1*, *CG6164*, and *CG6182*^{Ey08283} was performed and revealed expected amplification products, suggesting that these genes were still being

transcribed in the homozygous lines. Since insertion of a *P*-element within the 5' untranslated region often inhibits or reduces gene function by interfering with transcription, the genes *kal-1*, *CG6164*, and *CG6182*^{Ey08283} cannot conclusively be eliminated as candidates. *sec10* however, was not a homozygous viable *P*-insertion mutant and crosses to other deficiencies encompassing the 95D-E region also failed to produce viable hemizygotes, suggesting that the P-element insertion that created this mutant was a lethal insertion in that chromosome. Since the P-element only mapped 37 bp upstream of *sec10* and had resulted in a lethal insertion, it is highly likely that this P-element disrupts the function of this gene by inserting into the 5'-untranslated region. Furthermore, knockdown of *Drosophila sec10* expression, which was previously done using a transgenic RNAi approach, resulted in post-embryonic lethality with larvae dying as second larval instars, suggesting that *sec10* is an essential gene (Andrews *et al.*, 2002). Since this P-insertion maps only within 37 bp of the upstream region (and thus is predicted to disrupt transcription and expression of *sec10*) and is associated with homozygous lethality, consistent with knockdown studies reducing Sec10 expression, this *P*-element insertion line can be considered a true *sec10* mutant and conclusively ruled out as a candidate of *huc*95^{E} through complementation. Complementation tests were also done with several other *P*-element insertion lines *P{EP}CG6178*^{EP3637}, *P{EP}CG6178*^{EP3251}, *P{EPgy2}CG6178*^{EY07693} and *P{Sup or P}CG6178*^{KG05318}, all of which are associated with the gene *CG6178*, inserting 206 bp, 65 bp, 212 bp, and 214 bp upstream of this gene, respectively. All of these lines also complemented *huc*95^{E} suggesting that this gene was not a candidate, or that the *P*-element insertions associated with this gene do not completely disrupt the function of this gene. To examine this

possibility, I performed RT-PCR on RNA isolated from these lines and was able to amplify *CG6178* mRNA, suggesting that these *P*-elements do not knock out the function of this gene.

Section 2-3d: Sequencing of candidate genes

In addition to the strategies described earlier for determining which gene candidates could be associated with *huc*95^{E}, candidates whose known or proposed functions could plausibly explain the caffeine sensitive phenotype were sequenced and analyzed for sequence alterations. One attractive candidate was the *Mpk2* gene (also known as *p38a*), which encodes a **M**itogen **A**ctivated **P**rotein **K**inase (MAPK) with homology to the mammalian MAPK p38. These kinases are known to have roles in response to various forms of cellular stress such as osmotic stress, inflammatory cytokines, presence of lipopolysaccharide, and UV irradiation (Seger and Krebs, 1995; Ono and Han, 2000; Johnson and Lapadat, 2002). The MAPK signal transduction pathway is conserved from yeast to mammals and consists of a complex cascade that involves activation of MAPK by MAPK kinases (MKK) that have been activated by MKK kinases (MAP3K) upon exposure to environmental stress, growth factors, cytokines or other mitogenic factors (Ono and Han, 2000). All p38 MAPKs are activated by dual phosphorylation from MKKs at a Thr-Gly-Tyr (TGY) motif and once activated, regulate the activity of transcription factors to control gene expression (Ono and Han, 2000). In mammalian systems, *p*38 MAPKs participate in innate immunity, inflammatory response, and stress-induced signalling events including a link with cell cycle checkpoint regulation. Previously, *p*38 was implicated in mediating a caffeine-insensitive (and thus an ATM/ATR independent) G_2 delay following UV irradiation

through phosphorylation of cdc25B and *p*53 (Bulavin *et al.*, 2001; Goldstone *et al.*, 2001; Bulavin *et al.*, 1999). This suggests that *p*38 is involved in a separate checkpoint pathway that does not involve ATR or ATM (Bulavin *et al.*, 2001; Bulavin *et al.*, 2002). Because the premise of the original screen that identified *huc*95^{E} was to discover potential checkpoint components, *p38a* seemed like an ideal candidate, as one could conceive a scenario whereby the MAPK pathway (which normally responds to environmental stress or pathogenic invasion) might also serve a back-up role in cell checkpoint control and cell cycle arrest. By this reasoning, *huc*95^{E} flies might be sensitive to caffeine because they had lost this function, due to simultaneous loss of MAPK-mediated and ATR/ATM-mediated checkpoint arrests as a result of caffeine's inhibition of ATR/ATM (see Figure 2-8). To address this possibility, the coding region of *Mpk2* was tested for any single base pair mismatches by annealing single strands of *Mpk2* coding sequences amplified from *huc*95^{E} to wild type genomic DNA and determining the annealing time (with the expectation that if there was a mutation, the annealing time would be altered) (Silva, 2002). By this test, no alterations appeared to exist within this region. To further test the possibility that alterations existed in the noncoding or regulatory regions of *Mpk2*, 5645 base pairs encompassing this entire gene including exons and the 5' and 3' untranslated regions (making up 2795 base pairs) were sequenced. No sequence alterations exist within this gene and its outlying regions, thus eliminating this gene as a candidate. Later, complementation tests were performed with a *Mpk2* homozygous null mutant that was created by mobilization of a nearby *P*-element *P{EP}CG6178*^{EP3637}, 820 bp upstream of the *Mpk2* locus (creating a new line containing a second *P*-element insertion 263 base pairs downstream of the *Mpk2* locus), followed by

the simultaneous excision of both elements to create a precise 1.9 kb deletion that completely removed *Mpk2* (Craig *et al.*, 2004). RT-PCR analysis, as well as PCR of genomic DNA isolated from this stock, had confirmed the absence of *Mpk2* and verified this mutant line. This homozygous null mutant failed to display any sensitivity to caffeine and was able to complement *huc*95^{E} for caffeine sensitivity, confirming that *Mpk2* was not responsible for the caffeine sensitivity of these mutants. Recently another putative gene, known as *p38c* with sequence homology to *Mpk2*, was also found to exist in the region immediately adjacent to the left of *Mpk2*. This gene was thought to arise as a result of a duplication event of *Mpk2* (due to its sequence homology and proximity to *Mpk2*). However, *p38c* contains changes within its sequence at conserved motifs, which would interfere with its function as a MAPK, suggesting that p38c is actually a pseudogene. In particular, the invariant dual phosphorylation motif TGY was changed to a TDH by a replacement of the conserved tyrosine residue by a histidine in p38c (Craig, 2003). Also, changes within its catalytic loop, as well as the fact that no expressed sequence tags were found, suggested that *p38c* is likely a pseudogene. In case this putative MAPK did have some function that could be related to Mpk2 in other systems, the coding region of this gene was also sequenced in the *huc*95^{E} hemizygotes and compared to wildtype sequences. This gene was also found to contain no sequence alterations within the coding regions, suggesting that this gene was not *huc*95^{E}. Because sequencing of the coding regions did not exclude the possibility that mutations might exist within the regulatory region, qualitative RT-PCR was performed to determine if the *p38c* gene was expressed. Results from this test showed that *p38c* is expressed, eliminating this putative gene as a candidate (see Figure 2-9). Although no expressed

sequence tags have been reported thus far for this gene, this evidence for expression might be the result of the amplification process, which would serve to enhance undetectable amounts of RNA.

Another gene that was eliminated by genomic sequencing was *mRpS24,* localized at 95E6. This gene, which is predicted to encode a mitochondrial ribosomal protein, was easy to sequence because the reported size of this gene was only 718 bp with no introns. Furthermore, being a ribosomal protein localized in the mitochondrion (which is known to be linked to pathways involving programmed cell death), a scenario could be imagined whereby a mutation in this gene causes caffeine sensitivity that results in apoptosis. Sequencing results revealed no sequence alterations within the coding region of this gene and qualitative RT-PCR also showed that this gene was expressed in both wildtype and hemizygote flies, suggesting that this gene is not a candidate for the *huc*95^{E} mutation (Figure 2-9).

CG6178 is another candidate for sequencing that has a putative role in acyl-CoA biosynthesis (Oba *et al.*, 2004). CG6178 shares a high similarity to firefly luciferase ($e=8^{-113}$), a bifunctional enzyme that has monooxygenase (mediating bioluminescence) and a fatty acyl-CoA synthetase activity. *In vitro* catalytic tests have revealed that CG6178 does not exhibit luciferase activity, but is capable of synthesizing fatty acyl-CoA in the presence of ATP, Mg^{2+}, and CoA (Oba *et al.*, 2004). Acyl-CoA and its derivatives can mediate cellular signalling by release Ca^{2+} from RyR channels and possibly stimulating Ca^{2+} reuptake at IP_3R channels (Faergeman and Knudsen, 1997; Fitzsimmons *et al.*, 2000). Because caffeine also evokes a Ca^{2+} release from RyR channels and could theoretically affect Ca^{2+} signalling from IP_3R channels (by affecting PKC signalling

through adenosine GPCRs), this gene was also a plausible candidate (Rousseau *et al.*, 1988; McPherson *et al.*, 1991). Upon sequencing 4743 bp for this gene, no sequence alterations were found, eliminating this gene as a candidate.

Other candidates that were sequenced and had displayed no sequence alterations were the genes *CG31133* and *CG6182*, respectively (Table 2-2). Both of these genes have unknown functions and are not obvious candidates for *huc*95^{E} other than residing within the deleted region. Nonetheless, opportunity arose for these genes to be sequenced and as a result, were successfully eliminated as candidates for *huc*95^{E}.

A gene encoding a novel class I myosin called *myo*95E was also a possible candidate even though it was not an obvious candidate in terms of being implicated in cell cycle checkpoint regulation. However, a mutation in a myosin gene could exhibit caffeine sensitivity, as myosins are often regulated by calcium containing molecules such as calmodulin. Myosins are molecular motors that transduce energy from ATP hydrolysis into mechanical movement along actin filaments. They are known to be involved in several different processes including cell locomotion, muscle contraction, cytokinesis, endo/exocytosis, vesicle and organelle transport, signal transduction, and establishment of polarity (Berg *et al.*, 2001; Krendel and Mooseker, 2005). There are currently 17 known classes of myosins, based upon whether they function as dimers or monomers, as well as particular domains and motifs that are related to specialized functions (Tzolovsky *et al.*, 2002). Structurally, all myosins are characterized by the presence of an N-terminal heavy chain that harbours a conserved 80 kDa catalytic domain containing an ATP-hydrolyzing domain and actin-binding sites, required for movement of the myosin (Berg *et al.*, 2001). The catalytic domain consists of three

conserved loops (the P-loop, switch-1 region, and switch-2 region, respectively) with consensus sequences that surround the active site (Yamashita *et al.*, 2000). The conservation of these functional domains has been instrumental in the identification of other myosins, of which 13 have been identified in *Drosophila* (Yamashita *et al.*, 2000; Berg *et al.*, 2001; Tzolovsky *et al.*, 2002). The P-loop serves as an ATP binding site, while the switch-1 region and switch-2 region interact together to hydrolyze ATP and transmit this energy beyond the active site (Smith and Rayment, 1996; Onishi *et al.*, 1998; Furch *et al.*, 1999). Following this N-terminal motor domain is an α-helical light chain, "neck" region that contains anywhere from 0 to 6 tandem isoleucine-glutamine (IQ) motifs, which serves as a binding site for regulatory proteins such as calmodulin or other members of the EF-hand containing family (Tzolovsky *et al.*, 2002). This family of regulatory proteins is characterized by the presence of helix-loop-helix motifs that contain highly conserved residues in the loop region for the binding of Ca^{2+} (Kawasaki *et al.*, 1998). It is thought that interaction of these regulatory proteins with Ca^{2+} affects the affinity of these proteins for IQ motifs in the regulatory neck region of the myosin. In general, unconventional myosins (which are all myosin classes that are not of the typical class II muscle myosins) bind calmodulin with higher affinity when it is not associated with Ca^{2+} (Tzolovsky *et al.*, 2002). This Ca^{2+}-sensitive binding of regulatory proteins to IQ motifs contributes to the regulation of these molecular motors, with the neck region postulated to act as a lever arm to amplify small movements in the motor domain to create the power stroke (Howard, 1997). In addition, the neck region of many myosins is the site of alternative splicing to produce myosin variants with different numbers of IQ motifs, adding further complexity to the regulation of these proteins. Following the neck

region is the highly divergent C-terminal tail region, which has been known to contain various different motifs such as coiled-coil α-helical domains (eg. class II myosins) for dimerization of myosin monomers, Src homology 3 (SH3) domains (found in many intracellular or membrane-associated proteins that mediate diverse processes including the formation of multiprotein complexes, altering subcellular localization, or mediating the local accumulation of proteins), GAP domains, band F ezrin-radixin-moesin homology (FERM) domains (which are involved in localizing proteins to the plasma membrane), Pleckstrin homology (PH) domains (which target proteins to the plasma and internal membranes through association with phosphoinositides), and Myosin tail homology (MyTH) domains, to name a few (Oliver *et al.*, 1999). These diverse tail or cargo domains are thought to either target the myosin to different cellular localizations, to anchor the myosin thereby allowing it to move actin filaments within the cell, or to interact with particular cargo molecules and facilitate their transport to other locations by movement along actin filaments. Some tails also have kinase domains, PH domains or GTPase activating domains, suggesting that these myosins may also play a role in signal transduction.

By sequence homology and structural organization, *myo*95E encodes a class I myosin (Tzolovsky *et al.*, 2002). These were the first unconventional myosins (ie. non-muscle myosins) discovered and have been implicated in several processes including establishment and maintenance of cortical tension, motility, endocytosis and exocytosis (Osherov and May, 2000; Wu *et al.*, 2000). They lack a coiled-coil protein interaction domain within the tail region, suggesting that these myosins act as monomeric filaments. The tail also has a domain consisting of many basic amino acid residues referred to as the

Tail **h**omology **1** (TH1) region. This TH1 domain has been shown to bind phospholipid vesicles *in vitro* and is thought to play a role in tethering some class I myosins to membranes *in vivo* (Osherov and May, 2000). In addition to *myo*95E, *Drosophila* also contains 2 other class I myosin genes named *myo1A* and *myo1B*. *myo1A* and *myo1B* were discovered by a PCR-based hybridization approach, using degenerate primers to two highly conserved head domain regions (Morgan *et al.*, 1994). *myo1A* was localized to the cytological region of 31D-F and contains two IQ motifs, while *myo1B* was localized cytologically to 61F and contains three IQ motifs. Both of these class I myosins are associated with the brush border of the alimentary canal in both larval and adult stages, with Myo1A predominantly localizing to the sub-apical terminal web domain and Myo1B localizing to the apical microvillar domain (Morgan *et al.*, 1995). Like other brush-border myosins in vertebrates, both Myo1A and Myo1B are thought to be involved in vesicle transport and regulation of membrane dynamics, possibly acting as structural elements within the brush border.

*myo*95E is a recently discovered class I myosin that was initially missed in the preliminary annotation of the *Drosophila* genome. Originally, the predicted sequence for this gene was unusually short for a myosin, encoding only 59 amino acids, which was later revealed to be the result of the gene being predicted incorrectly (Tzolovsky *et al.*, 2002). As a result, the sequence for this gene was manually assembled using expressed sequence tags (ESTs), the reported *Drosophila* genomic DNA sequence, and homology to other myosins. Two different splicing prediction programs theoretically predicted the splicing of this gene and the artificially assembled sequence was then used to design primers for RT-PCR amplification. The resulting cDNA was sequenced and it was

determined that the *myo*95E gene consists of 16 exons and produces at least 3 different types of transcripts that are expressed during oogenesis, larval, and adult stages. It was also determined by homology searches that the myosins produced from this gene share 33% identity (53% similarity) to vertebrate brush border class I myosins – even more so than to the two other class I myosins in *Drosophila* (Tzolovsky *et al.*, 2002). *myo*95E also contains a 281 amino acid insertion within the N-terminal region, resulting from an unusually long exon 3, that is similar to an AAA (**A**TPase **A**ssociated with various cellular **A**ctivities) domain (Berg *et al.*, 2001; Tzolovsky *et al.*, 2002). Such domains exist in a wide variety of proteins in different organisms and are characterized by a conserved region of about 220 amino acids containing an ATPase domain that utilizes energy from ATP hydrolysis to carry out such processes as proteolysis, protein folding, membrane trafficking, cytoskeletal organization, organelle biogenesis, DNA replication, and intracellular motility (Hanson and Whiteheart, 2005). AAA motifs have also been identified in the molecular motor dynein, a microtubule-based motor required for chromosome movement, organelle transport, and ciliary/flagellar beating (Vale, 2000). AAA domains have not been previously found in myosins, which usually contain small motor domains with only one ATP binding site that are thought to modulate their activity by a different mechanism than dynein (Hanson and Whiteheart, 2005). It is believed that this domain modulates the hydrolysis of ATP as it is inserted into loop 1 of the motor domain, which harbours the other region for ATP hydrolysis. Myo95E has also been found to contain 2 IQ motifs with two different variants due to alternative splicing (Tzolovsky *et al.*, 2002).

When I sequenced *myo*95E from genomic DNA isolated from *huc*95^{E} hemizygotes, I found that the mutant allele contained a single nucleotide alteration that changed a guanine residue to an adenine residue. This mutation was confirmed in both the sense and anti-sense sequences, using two different primer sets on two different sequencing templates and is consistent with those commonly caused by EMS mutagenesis as methylation of G residues to O^6-ethyl-G mispairs with T during replication, resulting in G/C to A/T transitions (Bentley *et al.*, 2000). Analysis of this alteration revealed that this mutation existed at the junction of intron 8 and exon 9, mutating a normal AG splicing acceptor site to AA (see Figure 2-10A). This mutation identified in *myo*95E is predicted to prevent splicing at this acceptor site, resulting in a severely truncated protein due to the presence of a TAA stop codon within the original reading frame 54 bp downstream of exon 8 in intron 8. Such a defect would result in loss of approximately half of the protein, including the terminal part of the motor domain, the entire neck domain (crucial for regulation) and the tail domain (crucial for function through interaction with specific cargo for transport or cellular components for anchoring). Consequently, the prediction is that this would result in a non-functional myosin. Furthermore, alternative splicing linking exon 8 to exon 10 (essentially bypassing the mutated splicing acceptor site at the junction of intron 8 and exon 9) would still result in a truncated protein that would be lacking the neck and tail regions due to a stop codon being formed in frame 233 bp in exon 10 with this processing (Figure 2-11A). Similarly, fusion of exon 8 to exon 11 would result in a myosin with no regulatory IQ motifs and splicing products eliminating exon 8 would also eliminate the switch-2 motif that is needed for ATP hydrolysis (Figure 2-

11A). Only class XIV myosins do not contain any IQ motifs and are found only in Apicomplexan parasites such as *Toxoplasma gondii* and *Plasmodium falciparum* (Heintzelman & Schwartzman, 1997; Hettmann *et al*, 2000). Class XIV myosins are required to mediate a unique substrate-dependent gliding motility involving circular and forward twisting movements. Although it is not certain that a Myo95E isoform without IQ motifs would be nonfunctional, it is likely, as the only class of myosins lacking these motifs are involved in a specific type of movement for a single cellular organism. Furthermore, it could be possible that some other form of alternative splicing exists which does not use these typical splicing acceptor sites to result in a functional protein but based upon known acceptor sites, myosin functions, and sequence, myosins resulting from this mutation are predicted to be nonfunctional. In fact, all predicted full-length transcripts of *myo*95E (with the exception of one transcript which results in a severely truncated protein due to a stop codon in exon 5 and is thought to be inactive (Tzolovsky *et al*., 2002)) utilize this particular splicing acceptor site, suggesting that if alternative splicing occurs, it does not involve this particular site (Figure2-11B).

To confirm that this splicing defect was actually present and determine if the *myo*95E gene was expressed, RT-PCR was performed on total RNA isolated from adult *huc*95^{E} hemizygote flies and compared with third chromosome isogenized wild type flies using primers that flanked the intron (see Figure 2-10B). From this analysis, it was clear that hemizygotes were only capable of amplifying a 376 bp fragment (representing an unspliced transcript), whereas wild type controls displayed both the 376 bp fragment (in a stoichiometrically lower amount, possibly relating to the efficiency of the splicing reaction) and a 279 bp fragment (which resulted from the removal of a 97 bp intron by

splicing). These results implicated *myo*95E as a possible candidate for *huc*95^{E}, a hypothesis I pursued further by the following approach.

Section 2-3e: Transgenic rescue experiments

To test the possibility that *myo*95E is the gene associated with the *huc*95^{E} caffeine sensitivity phenotype, a genomic rescue plasmid containing the entire *myo*95E gene along with 2672 bp of the upstream and 1579 bp of the downstream regions was constructed utilizing the strategy outlined in Figure 2-12 and used to obtain transformants. Two putative transformants were obtained and the *P* transposon insertions associated with the two lines were subsequently mapped to the third chromosome. Since the *huc*95^{E} mutation also existed on the third chromosome, crosses were set up with *Df*(3R)*crb87-4* as shown in Figure 2-13A, to produce recombinants that would contain both the transgenic rescue construct and the deficiency. Putative recombinants were selected on the basis of inheritance of w^{+} gene (associated with the construct) and *e* (associated with the deficiency) over *TM3 Sb, e* and tested for their inability to complement *Df*(3R)*crb87-4*, thereby selecting against recombination events that linked the construct and the *e* recessive mutation without the deficiency. Recombinants were then crossed to *huc*95^{E} mutants and tested in the presence and absence of caffeine (Figure 2-13B). Unfortunately, the construct did not rescue the caffeine sensitivity of the *huc*95^{E} mutants. There are two possibilities for this result: either *myo*95E is not the *huc*95^{E} gene, or the rescue construct was either not functional or not expressed properly to mediate caffeine tolerance. To determine if the rescue construct was expressed, RT-PCR experiments were performed on RNA isolated from recombinants containing the rescue construct isolated in the absence of caffeine. The results of this experiment indicated that these

flies exhibited a *myo*95E splicing pattern similar to that in wild type *myo*95E controls, suggesting that the construct was expressing *myo*95E mRNA normally (Figure 2-14). However, although the results suggest that the rescue construct is being properly spliced, it is unknown whether or not the RNA is being translated or expressed sufficiently in the cells necessary to mediate caffeine tolerance (if in fact *myo*95E corresponds to *huc*95^{E}).

Section 2-4: Discussion

At present, the identity of the gene responsible for caffeine sensitivity in *huc*95^{E} mutants and the underlying mechanism involved, remains elusive. Out of an initial list of 23 genes, I have managed to narrow the number of remaining possible candidates to 9, with one (*myo*95E) showing particular promise as a candidate gene. I have determined though sequencing of genomic DNA isolated from hemizygous *huc*95^{E} mutants that *myo*95E has a single transition mutation of a G to an A within a AG splicing acceptor site at the junction of intron 8 and exon 9. This mutation is predicted to result in a truncated protein where the terminal portion of the head domain (important for the motor action and generation of power for myosin movement), the neck domain (required for regulation of the myosin), as well as the cargo domain (for interacting with the structures or components to be moved) as a consequence of a premature stop codon located 54 bp down from the splice site. Alternative splicing products using splicing acceptor sites of other known exons are also predicted to result in nonfunctional proteins. RT-PCR utilizing primers flanking the splice site (see Figure 2-10B) confirmed this splicing defect, demonstrating both that this gene was expressed and that hemizygotes bearing this mutation had lacked the proper splicing of this intron. Unfortunately, rescue experiments to confirm that this gene is associated with *huc*95^{E} caffeine sensitivity have failed; even

though RT-PCR experiments confirm expression of the construct and splicing within *huc*95^{E} hemizygotes expressing the transgene. There are several possible reasons as to why the rescue construct might have failed to rescue the caffeine sensitivity of the *huc*95^{E} mutants. One possibility is that the transgene could have inserted within a region of the chromosome that affected levels of its expression or function. Another possibility is that other regulatory elements required for sufficient *myo*95E expression were missing within the rescue construct. As such, position effects, or failure to include upstream or downstream elements that are crucial in the regulation of the expression of this gene could explain the failure of this construct to rescue the *huc*95^{E} mutant phenotype.

Class I myosins have been implicated in vesicle transport and fusion to the plasma membrane, motility, and the establishment and maintenance of cortical tension (Osherov and May, 2000; Wu *et al.*, 2000). Myo95E in particular, shares higher similarity and identity (53% and 33%, respectively) with vertebrate brush border class I myosins compared to the two other class I myosins identified in *Drosophila* (Tzolovsky *et al.*, 2002). These similarities suggest a function for *myo*95E in exo or endocytic events and vesicle transport, as class I myosins within the brush border have been implicated in processes involving absorption of nutrients (Skowron *et al.*, 1998). Furthermore, recent findings in 3T3-L1 adipocytes have implicated a class I myosin, myo1C, in the fusion of vesicles containing the GLUT4 glucose transporter receptor, to the plasma membrane (Bose *et al.*, 2002). PI3K signalling was found to regulate this process as inhibition of PI3K prevented fusion of these vesicles (Bose *et al.*, 2002; Bose *et al.*, 2004). Interestingly, overexpression of *myo1C* was shown to mediate fusion of vesicles containing the GLUT4 receptor to the plasma membrane, even when PI3K was inhibited

(Bose *et al.*, 2002; Bose *et al.*, 2004). One of the many effects of caffeine is that it interferes with PI3K activity by inhibiting the p110 catalytic subunit of PI3K. Since PI3K is an important signalling molecule involved in processes such as apoptosis, cellular proliferation, and cell growth, perhaps the reason for caffeine sensitivity within the *huc*95DE mutants is that caffeine-induced inhibition of PI3K interferes with these processes, which require *huc*95^{E} function. If *huc*95^{E} is *myo*95E, then a possible reason for the conditional lethality of *huc*95^{E} mutants in the presence of caffeine could be that *myo*95E expression is required to overcome the caffeine-induced insult (analogous to the overexpression of *myo1C* overriding PI3K inhibition). Although myo95E is classified as a class I myosin because it contains a basic tail, it differs from all other class 1 myosins discovered to date in that it also contains a partial AAA domain within the head region of the protein (Tzolovsky *et al.*, 2002). The significance of this domain (ie. whether it is a functional domain and what it is used for) remains unclear, however. Proteins containing such domains have been implicated in a wide variety of processes such as protein degradation, DNA replication, membrane fusion, and movement of microtubule motors. Perhaps this domain is crucial for the function of *myo*95E and (if *myo*95E is the gene associated with the *huc*95^{E} mutation) its ability to impart caffeine tolerance. In addition to this, several different isoforms based upon alternative splicing have been found for *myo*95E, which might suggest that this gene might be involved in producing several different functions of this class I myosin. Consequently, *myo*95E remains an attractive candidate for *huc*95^{E}.

Besides *myo*95E, the genes *CG13605*, *CG13607*, *CG6129*, *CG6164*, *CG5463*, *kal-1*, *CG5510* and *CG13606* are also possible candidates that have yet to be eliminated.

CG5510 might have putative roles in secretion and intracellular transport and could result in a caffeine sensitivity phenotype whereby the transport of a particular component or processes involved may be required to address the caffeine insult (similar to the conjecture of *myo*95E being a candidate). *CG6129* is an attractive candidate because it has homology to *Homo sapiens* **C**entrosomal **N**IMA-**r**elated **K**inase 2 (Nek2) **A**ssociated **P**rotein **1** (C-Nap1) ($e=2.0^{e-27}$). The NIMA (**N**ever **I**n **M**itosis in ***A**spergillus nidulans*) protein kinases were originally discovered in the filamentous fungus *Apergillus nidulans* where they are required for regulating the onset of mitosis in collaboration with the cyclin dependent protein kinase Cdk1 (Oakley and Morris, 1983). Overexpression of NIMA causes premature mitotic events (such as chromatin condensation and formation of the mitotic spindle) and expression of *Apergillus nidulans* NIMA in *Schizosaccharomyces pombe*, *Xenopus*, and humans also induces premature mitotic events, suggesting that NIMA related pathways also exist in these organisms (Osmani and Ye, 1996). Nek2 is the most closely related mammalian homologue to NIMA and has been found to localize to the centrosome, the major microtubule organizing centre responsible for facilitating intracellular transport and imparting shape and polarity during interphase, as well as ensuring bipolarity and spindle orientation through formation of the spindle poles in mitosis (Fry *et al.*, 1998a). Nek2 is also required for centrosomal splitting at the G_2-M transition, due to its ability to phosphorylate C-Nap1 (a core centrosomal protein that is responsible for holding the centrioles together during interphase), resulting in its displacement (Rapley *et al.*, 2005; Fry *et al.*, 1998a; Fry *et al.*, 1998b). Interestingly Nek11, another related NIMA kinase, has been implicated in a DNA replication/damage and genotoxic stress checkpoint that exists downstream of a caffeine-sensitive pathway

(Noguchi *et al.*, 2002). Because of homology to C-Nap1, its proposed role in cell cycle regulation, and the possibility that related proteins could exist in a caffeine sensitive pathway, *CG6129* is an interesting candidate for *huc*95^{E}.

Amongst the other candidates, 3 genes (CG13607, CG6164, and CG13606, respectively) exist with no known homologues or putative function (see Table 2-2) and, as such, might be interesting candidates for possible novel functions, which may be potentially related to caffeine or cell cycle checkpoint control. The fastest way to determine the identity of *huc*95^{E} is probably to sequence these remaining candidates as this would serve to directly confirm or eliminate these genes as possibilities. Also, isolation of more *huc*95^{E} alleles could help to confirm any putative candidates by searching for mutations within these alleles. As such, efforts are continuing to identify *huc*95^{E} by sequencing and a screen is being planned for the isolation of more alleles of this mutant. As a result, the identity of *huc*95^{E} will not remain elusive for long.

Section 2-5: Literature cited

Ahmed, Y., A. Nouri and E. Wieschaus. 2002. *Drosophila* Apc1 and Apc2 regulate Wingless transduction throughout development. *Development* **129**:1751-1762.

Andrenacci, D., S. Le Bras, M. R. Grimaldi, E. Rugarli and F. Graziani. 2004. Embryonic expression pattern of the *Drosophila* Kallman syndrome gene *kal-1*. *Gene expression Patterns* 5:67-73.

Andrews, H. K., Y. Q. Zhang, N. Trotta and K. Broadie. 2002. *Drosophila* Sec10 is required for hormone secretion but not general exocytosis or neurotransmission. *Traffic* **3**: 906-921.

Berg, J. S., B. C. Powell and R. E. Cheney. 2001. A millennial myosin census. *Mol Biol Cell* **12**:780-794.

Bose, A., A. Guilherme, S. Robida, S. M. C. Nicoloro, Q. L. Zhou, *et al.*, 2002. Glucose transporter recycling in response to insulin is facilitated by myosin Myo1c. *Nature* **420**:821-824.

Bose, A., S. Robida, P. S. Furcinitti, A. Chawla, K. Fogarty *et al.*, 2004. Unconventional myosin 1c promotes membrane fusion in a regulated exocytic pathway. *Mol Cell Biol* **24**:5447-5458.

Brand, A. H. and N. Perrimon. 1993. Targeted gene expression as a means of altering cell fates and generating dominant phenotypes. *Development* **118**:401-415.

Broadie, K., A. Prokop, H. J. Bellen, C. J. O'Kane, K. L. Schulze *et al.*, 1995. Syntaxin and synaptobrevin function downstream of vesicle docking in *Drosophila*. *Neuron* **15**:663-673.

Bulavin, D. V., S. A. Amundson and A. J. Fornace. 2002. p38 and Chk1 kinases: different conductors for the G_2/M checkpoint symphony. *Curr Opin Genet Dev* **12:** 92-97.

Bulavin, D. V., Y. Higashimoto, I. J. Popoff, W. A. Gaarde, V. Basrur *et al.*, 2001. Initiation of a G_2/M checkpoint after ultraviolet radiation requires p38 kinase. *Nature* **411:** 102-107.

Bulavin, D. V., S. Saito, M. C. Hollander, K. Sakaguchi, C. W. Anderson *et al.*, 1999. Phosphorylation of human p53 by p38 kinase coordinates N-terminal phosphorylation and apoptosis in response to UV radiation. *EMBO J* **18:** 6845-6854.

Chen, B., T. Chu, E. Harms, J. P. Gergen and S. Strickland. 1998. Mapping of

Drosophila mutations using site-specific male recombination. *Genetics* **149**:157-163.

Craig, C. 2003. *Personal communication to flybase*.

Craig, C. R., J. L. Fink, Y. Yagi, Y. T. Ip and R. L. Cagan. 2004. A *Drosophila p38* orthologue is required for environmental stress responses. *EMBO Rep* **5**:1058-1063.

Faergeman, N. J. and J. Knudsen. 1997. Role of long-chain fatty acyl-CoA esters in the regulation of metabolism and in cell signalling. *Biochem J* **323 (Pt 1):** 1-12.

Fitzsimmons, T. J., I Gukovsky, J. A. McRoberts, E. Rodriguez, F. A. Lai *et al.*, 2000. Multiple isoforms of the ryanodine receptor are expressed in rat pancreatic acinar cells. *Biochem J* **351:** 265-271.

Fry, A. M., T. Mayor, P. Meraldi, Y. D. Stierhof, K. Tanaka *et al.*, 1998a. C-Nap1, a novel centrosomal coiled-coil protein and candidate substrate of the cell cycle-regulated protein kinase Nek2. *J Cell Biol* **141**:1563-1574.

Fry, A. M., P. Meraldi and E. A. Nigg. 1998b. A centrosomal function for the human Nek2 protein kinase, a member of the NIMA family of cell cycle regulators. *EMBO J* **17**:470-481.

Furch, M., S. Fujita-Becker, M. A. Geeves, K. C. Holmes and D. J. Manstein. 1999. Role of the salt-bridge between switch-1 and switch-2 of *Dictyostelium* myosin. *J Mol Biol* **290**:797-809.

Goldstone, S., S. Pavey, A. Forrest, J. Sinnamon and B. Gabrielli. 2001. Cdc25-dependent activation of cyclin A/cdk2 is blocked in G_2 phase arrested cells independently of ATM/ATR. *Oncogene* **20**: 921-932.

Hanson, P. L. and W. Whiteheart. 2005. AAA+ proteins: have engine, will work. *Nature Rev* **6**:519-529.

Hardelin, J. P., A. K. Julliard, B. Moniot, N. Soussi-Yanicostas, C. Verney *et al.*, 1999. Anosmin-1 is a regionally restricted component of basement membranes and interstitial matrices during organogenesis: implications for the developmental anomalies of X chromosome-linked Kallmann syndrome. *Dev Dyn* **215**:26-44.

Heintzelman, M. B. and J. D. Schwartzman. 1997. A novel class of unconventional myosins from *Toxoplasma gondii*. *J Mol Biol* **271**:139-146.

Hettman, C., A. Herm, A. Geiter, B. Frank, E. Schwarz *et al.*, 2000. A dibasic motif in the tail of a class XIV apicomplexan myosin is an essential determinant of plasma membrane localization. *Mol Biol Cell* **11**:1385-1400.

Howard, J. 1997. Molecular motors: structural adaptations to cellular functions. *Nature* **389:** 561-567.

Johnson, G. L. and R. Lapadat. 2002. Mitogen-activated protein kinase pathways mediated by ERK, JNK, and p38 protein kinases. *Science* **298:** 1911-1912.

Kawasaki, H. S. Nakayama and R. H. Kretsinger. 1998. Classification and evolution of EF-hand proteins. *Biometals* **11**: 277-295.

Krendel, M. and M. S. Mooseker. 2005. Myosins: tails (and heads) of functional diversity. *Physiology* **20**:239-251.

Lloyd T. E., P. Verstreken, E. J. Ostrin, A. Phillippi, O. Lichtarge *et al.*, 2000. A genome-wide search for synaptic vesicle cycle proteins in *Drosophila*. *Neuron* **26**:45-50.

Lutz, B., S. Kuratani, E. I. Rugarli, G. Eichelè, and A. Ballabio. 1993. X-linked Kallmann syndrome. A neuronal targeting defect in the olfactory system? *Fed Eur Biochem Soc Lett* **352**:128–134.

McPherson, P. S., Y. K. Kim, H. Valdivia, C. M. Knudson, H. Takekura *et al.*, 1991. The brain ryanodine receptor: a caffeine-sensitive calcium release channel. *Neuron* **7**: 17-25.

Morgan, N. S., D. M. Skovronsky, S. Artavanis-Tsakonas and M.S. Mooseker. 1994. The molecular cloning and characterization of *Drosophila melanogaster* myosin-1A and myosin-1B. *J Mol Biol* **239**:347-356.

Morgan, N. S., M. B. Heintzelman and M. S. Mooseker. 1995. Characterization of myosin-1A and myosin-1B, two unconventional myosins associated with the *Drosophila* brush border cytoskeleton. *Dev Biol* **172**: 51-71.

Noguchi, K. H. Fukazawa, Y. Murakami and Y. Uehara. 2002. Nek11, a new member of the NIMA family of kinases, involved in DNA replication and genotoxic stress responses. *J Biochem* **277**:39655-39665.

Oakley, B. R., and N. R. Morris. 1983. A mutation in *Aspergillus nidulans* that blocks the transition from interphase to prophase. *J Cell Biol* **96**:1155-1158.

Oba, Y., M. Ojika and S. Inouye. 2004. Characterization of CG6178 gene product with high sequence similarity to firefly luciferase in *Drosophila melanogaster*. ***Gene*** **329**: 137-145.

Oliver, T. N., J. S. Berg and R. E. Cheney. 1999. Tails of unconventional myosins. *Cell Mol Life Sci* **56**: 243-257.

Onishi, H., S-I. Kojima, K. Katoh, K. Fujiwara, H. M. Martinez and M. F. Morales. 1998. Functional transitions in myosin: formation of a critical salt-bridge and transmission of effect to the sensitive tryptophan. *Proc Natl Acad Sci USA* **95:** 6653-6658.

Ono, K. and J. Han. 2000. The p38 signal transduction pathway: activation and function. *Cell Signal* **12**: 1-13.

Osherov, N. and G. S. May. 2000. *In vivo* function of class I myosins. *Cell Motil Cytoskeleton* **47**: 163-173.

Osmani, S. A. and X. S. Ye. 1996. Cell cycle regulation in *Aspergillus* by two protein kinases. *Biochem J* **317 (Pt 3)**: 633-641.

Rapley, J., J. E. Baxter, J. Blot, S. L. Whattam, M. Casenghi et al., 2005. Coordinate regulation of the mother centriole component nlp by nek2 and plk1 protein kinases. *Mol Cell Biol* **25**:1309-1324.

Rousseau, E., J. Ladine, Q. Y. Liu and G. Meissner. 1988. Activation of the Ca^{2+} release channel of skeletal muscle sarcoplasmic reticulum by caffeine and related compounds. *Arch Biochem Biophys* **267**: 75-86.

Rubin, G. M., and A. C. Spradling. 1982. Genetic transformation of *Drosophila* with transposable element vectors. *Science* **218**:348-353.

Sambrook, J., E. F. Fritsch, and T. Maniatis. 1989. Molecular Cloning, A Laboratory Manual. Second edition. Cold Spring Harbor Laboratory Press. pp.

Schulze, K. L., K. Broadie, M. S. Perin and H. J. Bellen. 1995. Genetic and electrophysiological studies of *Drosophila* Syntaxin-1A demonstrate its role in nonneuronal secretion and neurotransmission. *Cell* **80**:311—320.

Seger, R. and E. G. Krebs. 1995. The MAPK signaling cascade. *Faseb J* **9**: 726-735.

Silva, E. A. 2002. Generation and characterization of chemical-sensitive cell cycle checkpoint mutants in *Drosophila,* M.Sc Thesis. *Department of Biological Sciences*. University of Alberta, Edmonton.

Skowron, J. F., W. M. Bement and M. S. Mooseker. 1998. Human brush border myosin-I and myosin-Ic expression in human intestine and Caco-2_{BBe} cells. *Cell Motil Cytoskeleton* **41**: 308-324.

Smith, C. A., and I. Rayment. 1996. Active site comparisons highlight structural similarities between myosin and other P-loop proteins. *Biophysics J* **70**:1590-1602.

Tepass, U., and E. Knust. 1990. Phenotypic and developmental analysis of mutations at

the *crumbs locus*, a gene required for the development of epithelia in *Drosophila melanogaster*. *Roux's Arch Dev Biol* **199**:189-206.

Tzolovsky, G., H. Millo, S. Pathirana, T. Wood and M. Bownes. 2002. Identification and phylogenetic analysis of *Drosophila melanogaster* myosins. *Mol Biol Evol* **19**:1041-1052.

Vale, R. D. 2000. AAA proteins. Lords of the ring. *J Cell Biol* **150**: F13-19.

Wu, X., G. Jung and J. A. Hammer 2000. Functions of unconventional myosins. *Curr Opin Cell Biol* **12**: 42-51.

Yamashita, R. A., J. R. Sellers, and J. B. Anderson. 2000. Identification and analysis of the myosin superfamily in *Drosophila*: a database approach. *J Muscle Res Cell Motil* 21: 491-505.

Table 2-1: Predicted genes in region 95DE of the third chromosome.

Gene name	Map position	Putative Function	Similar gene sequences
CG10694	95E1	DNA repair protein	*S. cerevisiae RAD23* (e=1.2e-21)
syntaxin 1A	95E1	exocytosis	* *syx1A* alleles complement huc^{95D-E}
CG18428	95E1	unknown	-----
CG13605	95E1	protein ubiquitination	------
CG13607	95E1	unknown	------
CG6129	95E1-E3	Ciliary rootlet component	*H. sapiens* NEK2-assoc. protein (e=2.0e-27)
CG5463	95E3-E4	tRNA amidotransferase	*H. sapiens* Gln-tRNA (e=1.6e-102)
Tsc1	95E4	cell cycle regulator	* *Tsc1* alleles complement huc^{95D-E}
sec10	95E4-E5	exocytosis	*H. sapiens* secretory protein (e=5.7e-148)
CG6164	95E5	unknown	-----
kal-1	95E5	cell adhesion	*H. sapiens* anosmin-1 (e=4.9e-31)
Mpk2	95E5	protein kinase	*M. musculans* p38 MAPK 14 (e=5.2e-134)
p38c	95E5	putative protein kinase	-----
CG6178	95E5-E6	enzyme	*P. pennsylvanica* monooxygenase (e=1.0e-101)
*myo*95E	95E6	myosin ATPase	-----
CG6182	95E6	unknown	------
mRpS24	95E6	ribosomal protein	*H. sapiens mRpS24* (e=3.4e-24)
Apc2	95E6	microtubule function	* $Apc2^{DeltaS}$ complements huc^{95D-E}
CG5510	95E6	glycoprotein	*H. sapiens* GP36B (e=1.7e-75)
CG13606	95E7-E8	unknown	------
CHORD	95E8	zinc binding	------
CG5515	95E8	unknown	*H. sapiens CGI-24* (e=4.9e-32)
CG5524	95E8-F1	DNA repair protein	*S. pombe rad18* (e=1.6e-71)
CG6204	95F1	unknown	*S. pombe* putative ATP binding protein (e=6.0e-53)
CCR4	95F1-F2	transcription factor	*S. cerevisiae CCR4*
CG17786	95F2	unknown	------

Table 2-2: Putative transcripts that map to the *Df(3R)W6* region

Gene name	Map position	Putative function	*huc*95^{E} candidacy
CG13605	95E1	Protein ubiquitination	?
CG13607	95E1	Unknown	?
CG6129	95E1-E3	ciliary rootlet component	?
CG5463	95E3-E4	glutamyl tRNA amidotransferase	?
Tsc1	95E4	cell cycle regulator	Complements huc95^{E}
Sec10	95E4-E5	component of exocyst	Complements huc95^{E}
CG6164	95E5	Unknown	?
kal-1	95E5	homologue of cell adhesion protein anosmin-1	?
CG31133	95E5	Unknown	No sequence alterations
p38c	95E5	putative mitogen activated protein kinase	No sequence alterations
mpk2	95E5	mitogen activated protein kinase	No sequence alterations
CG6178	95E5-E6	acyl-CoA biosynthesis	No sequence alterations
myo95E	95E6	class I myosin	Putative splicing defect
CG6182	95E6	Unknown	No sequence alterations
mRpS24	95E6	mitochondrial ribosomal protein	No sequence alterations
Apc2	95E6	β-catenin chaperone protein	Complements huc95^{E}
CG5510	95E6	intracellular protein transport	?
CG13606	95E7-E8	Unknown	?

Table 2-3: Relevant fly stocks used in the mapping of *huc*95^{E}

Stock genotype	Stock No.	Experiment	Donor
Df(3R)crb87-4	2362	Deficiency mapping Recombination	Bloomington stock center
Df(3R)crbF89-4	4432	Deficiency mapping Recombination	Bloomington stock center
Df(3R)mbc-R1	2585	Deficiency mapping	Bloomington stock center
Tp(3;2)slo3	------	Deficiency mapping	Bruce Ganetzky
Df(3R)W6	7251	Deficiency mapping	Marianne Bienz
syx1A$^{\Delta 229}$	4379	Recombination Complementation	Bloomington stock center
crb^{2}	3448	Recombination Complementation	Bloomington stock center
Tsc1^{Q600X}	------	Complementation	Tian Xu
Tsc1^{29}	------	Complementation	Duojia Pan
Tsc1^{Q87X}	------	Complementation	Iswar Hariharan
Tsc1^{Q243X}	------	Complementation	Iswar Hariharan
Tsc1^{Q453X}	------	Complementation	Iswar Hariharan
Apc2$^{\Delta S}$	5917	Complementation	Bloomington stock center
Apc2^{d40}	6801	Complementation	Bloomington stock center
Mpk2^{1}	8822	Complementation	Bloomington stock center
Tp(2,3) ap^{Xa}*,ap*^{Xa}*/CyO, H{w*^{mC}*=PΔ23} HoP2.1; Sb*^{1}	6394	P-element deletion synthesis	Bloomington stock center
ecd^{1}*, st*^{1}*, red*^{1}*, e*^{4}*, ca*^{1}	4210	P-element deletion synthesis	Bloomington stock center
P{EP}Syx1A^{EP3215}	------	P-element deletion synthesis	Szeged Drosophila collection
P{EP}CG6178^{EP3637}	------	P-element deletion synthesis	Szeged Drosophila collection
P{EP}mask^{EP601}	------	P-element deletion synthesis	Szeged Drosophila collection
P{GT1}CG33100^{BG01713}	12631	P-element deletion synthesis	Bloomington stock center
w;Sp/CyO;Δ2-3 Sb,e/TM6, Ubx	------	P-element deletion synthesis	Scott Hanna
y^{1}*,w*^{67c23}*; P{w*^{mC} *y*^{mDint2}*=EPgy2} CG6182*^{EY08283}	16885	Complementation	Bloomington stock center
w^{1118}*; P{w*^{mC}*=XP} kal-1*^{d01966}	19168	Complementation	Bloomington stock center
w^{1118}*; PBac{w*^{mC}*=WH} CG6164*^{f00379}	18323	Complementation	Bloomington stock center
P{EP}CG6178^{EP3251}	17104	Complementation	Bloomington stock center
P{EPgy2}CG6178^{EY07693}	17388	Complementation	Bloomington stock center
P{Sup or P}CG6178^{KG05318}	13992	Complementation	Bloomington stock center

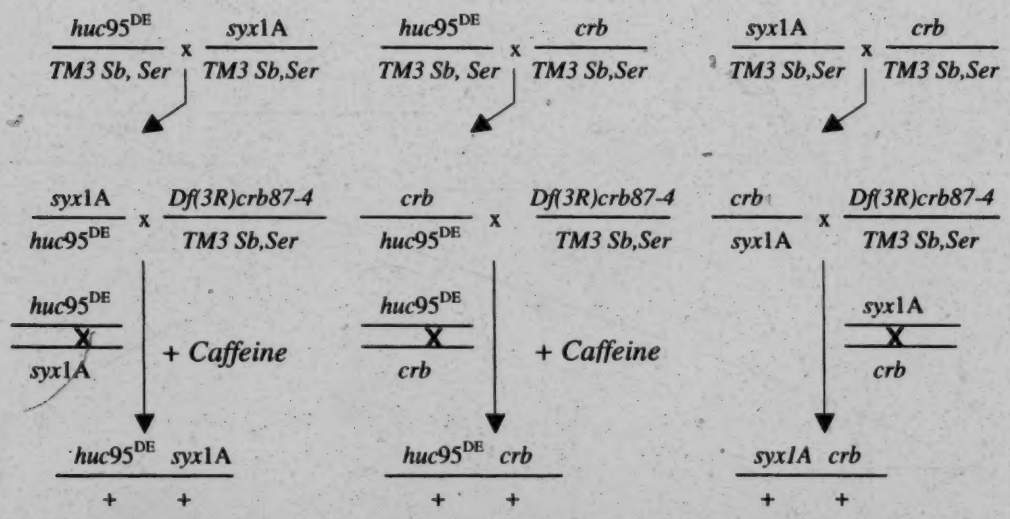
huc95DE / TM3 Sb, Ser x syx1A / TM3 Sb,Ser
huc95DE / TM3 Sb, Ser x crb / TM3 Sb,Ser
syx1A / TM3 Sb,Ser x crb / TM3 Sb,Ser
syx1A / huc95DE x Df(3R)crb87-4 / TM3 Sb,Ser
crb / huc95DE x Df(3R)crb87-4 / TM3 Sb,Ser
crb / syx1A x Df(3R)crb87-4 / TM3 Sb,Ser
huc95DE / syx1A
+ Caffeine
huc95DE / crb
+ Caffeine
syx1A / crb
huc95DE syx1A
+ +
huc95DE crb
+ +
syx1A crb
+ +

Select non-TM3 Sb (Ser) as evidence of recombination under presence of caffeine

Figure 2-1. Strategy to map *huc*95DE through recombination. Crosses of the *huc*95DE mutation over a balancer containing TM3, *Sb* are crossed to stocks containing the recessive lethal mutants *syx1A* and *crb* in order to select for progeny flies containing both the *huc*95DE mutation and recessive lethal marker (by selecting against inheritance of the balancer). These flies are then crossed to a deficiency which uncovers both the huc95^{DE} and recessive lethal mutations, and the progeny reared under caffeine, such that the only non-balancer containing flies that survive must have undergone a recombination event between the *huc*95DE and recessive lethal mutation to create a wildtype complimentary chromosome. Note that caffeine treatment is not required for crosses involving the two recessive lethal mutations as these mutants are not caffeine sensitive.

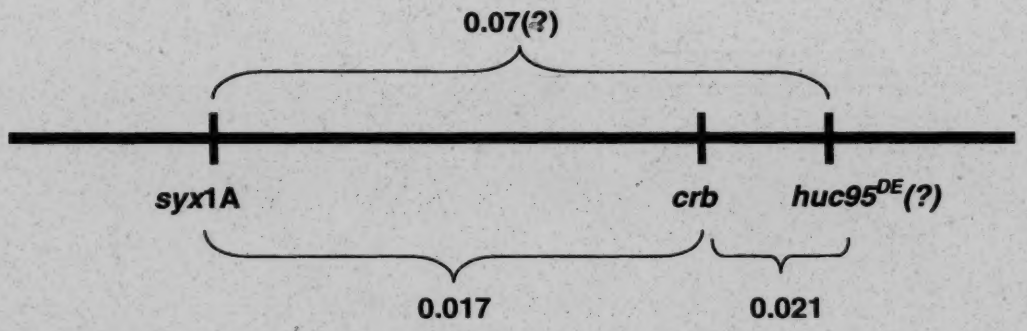

Figure 2-2. Resultant recombination map of *huc*95DE mapping strategy. The positions of *syx1A*, *crb*, and *huc*95DE were determined through the recombination frequencies derived from crosses between combinations of double mutants with a deficiency that had uncovered all of these mutations. The distance between *huc*95DE and *syx1A* was determined out of a total of 3937 flies, and 5007 flies for *huc*95DE to *crb*. The distance between *syx1A* and *crb* was determined out of a total of 9541 flies.

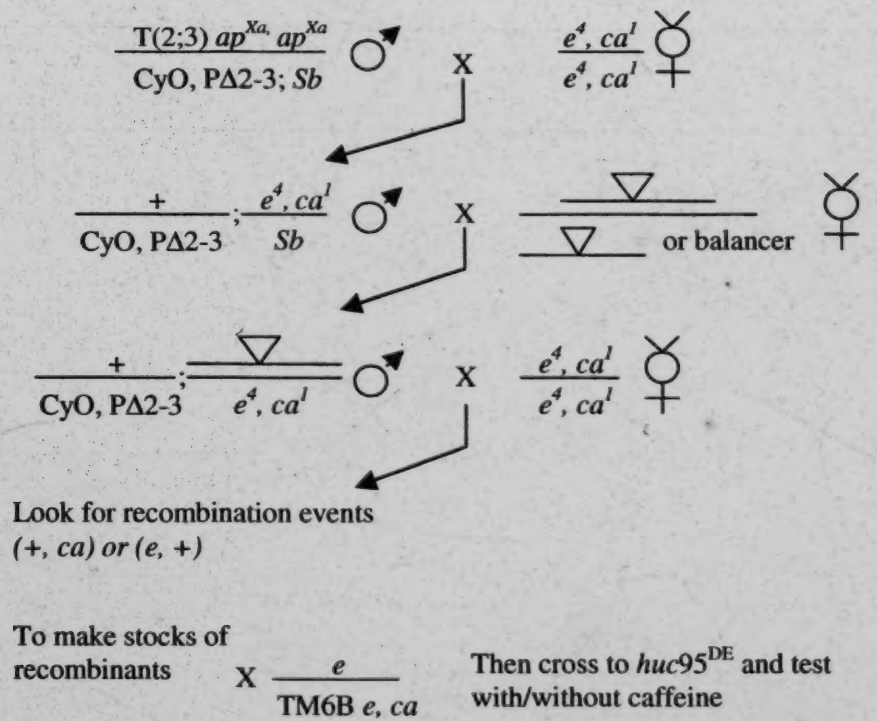

Figure 2-3. *P*-element strategy for mapping *huc*95DE. Males containing a Δ2-3 transposase source element on the second chromosome (associated with the balancer CyO) and recessive markers (*e* and *ca*) to screen for recombinants on the third chromosome are generated and crossed to lines containing *P*-elements on the third chromosome within the vicinity of the gene to be mapped. The use of a translocation of the second and third chromosome marked with the dominant wing mutation apterous^{xasta} ensures inheritance of both the Δ2-3 element and associated third chromosome (marked by *Sb)* together. Males containing the *P*-element, Δ2-3 element, and recessive markers are then crossed to mutant females and the progeny screened for inheritance of only one of the recessive markers. Stocks of these recombinants are then constructed and crossed to the mutant in the presence and absence of caffeine. Those that fail to complement the mutant in the presence of caffeine might harbour a flanking deletion, which extends into this gene region that can be mapped through molecular methods.

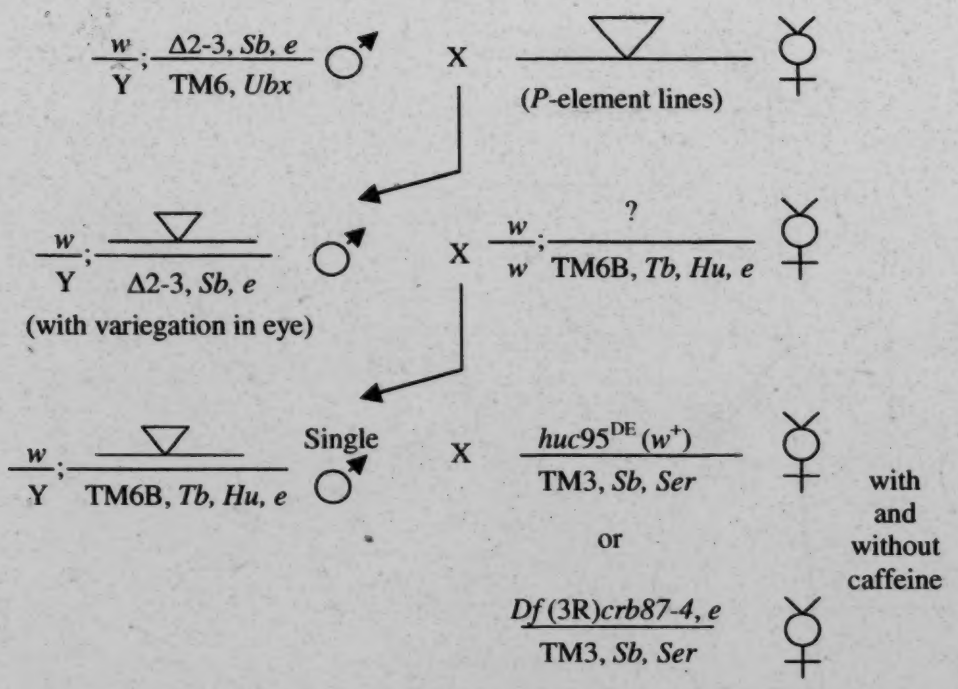
w / Y ; Δ2-3, Sb, e / TM6, Ubx
X
(P-element lines)
w / Y ; Δ2-3, Sb, e
(with variegation in eye)
X
w / w ; ? / TM6B, Tb, Hu, e
w / Y ; TM6B, Tb, Hu, e
Single
X
huc95DE (w+) / TM3, Sb, Ser
or
Df (3R)crb87-4, e / TM3, Sb, Ser
with and without caffeine

Figure 2-4: **Alternative crossing scheme for *P*-element strategy to map *huc*95DE.** In this strategy, a stronger Δ2-3 element present on the third chromosome is used by directly crossing this stock to lines containing *P*-elements within the vicinity of the gene to be mapped. Flies with exhibiting variegation in the eye (evidence for P-element transposition) are then crossed to a stock containing a suitable balancer (producing both a stock of these flies and segregating away the transposase source) and tested against the mutant in the presence or absence of caffeine.

A

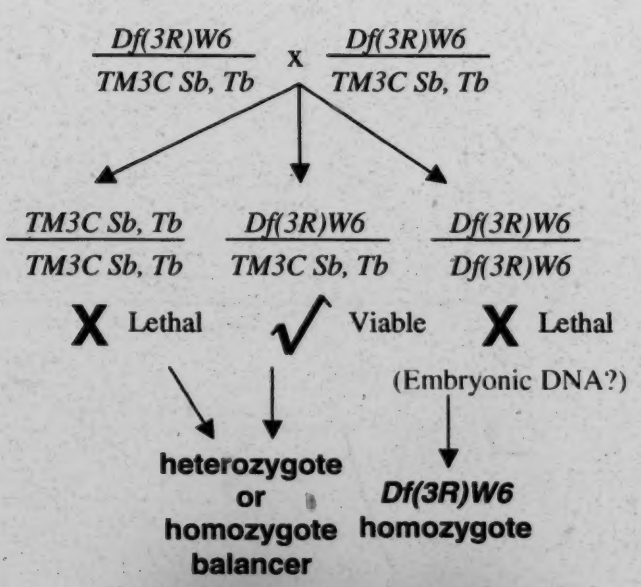

B

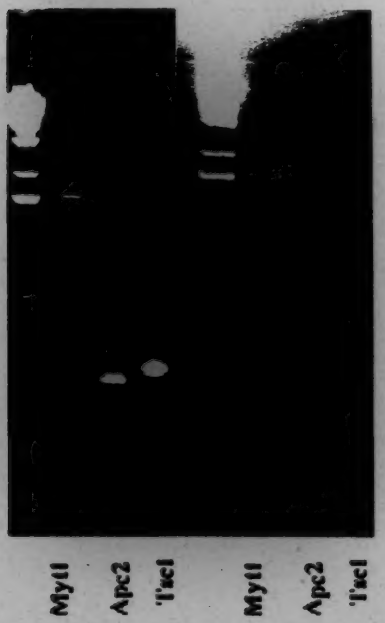

Figure 2-5: **Isolation of homozygous *Df(3R)W6* DNA for delineation of the region uncovered by *Df(3R)W6*.** **A)** In a *Df(3R)W6/TM3C Sb, Tb* stock, homozygous *Df(3R)W6* embryos can be identified (even though larvae are nonviable) from PCR on embryonic DNA. **B)** *Df(3R)W6* homozygous embryonic DNA is identified by ability to amplify a 1650 bp fragment from *Myt1*, and inability to amplify 575 bp and 540 bp fragments of *Tsc1* and *Apc2*, respectively.

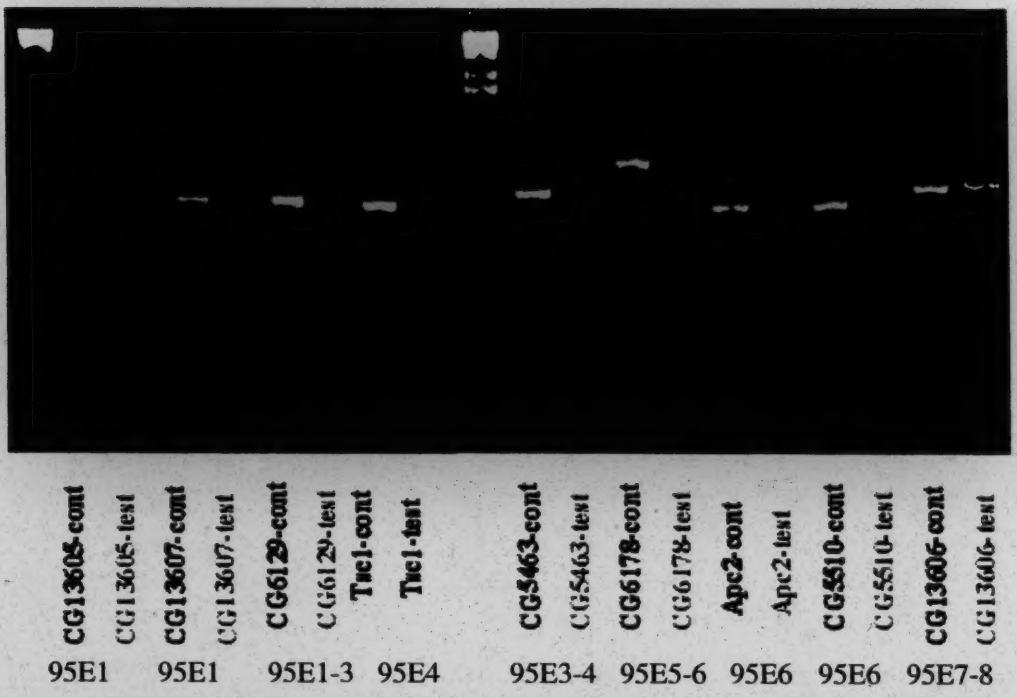

Figure 2-6: **Determination of the extent of *Df(3R)W6*.** ***Df(3R)W6/TM3CSb,Tb*** (control reactions shown in black) and ***Df(3R)W6*** (test reactions shown in red) embryonic DNA were tested for the ability to amplify a 544 bp, 572 bp, 598 bp, 575 bp, 589 bp, 775 bp, 532 bp, 529 bp, and 586 bp fragment from *CG13605, CG13607, CG6129, Tsc1, CG5463, CG6178, Apc2, CG5510*, and *CG13606*, respectively. The cytological region for each of the genes tested is listed below the corresponding lanes.

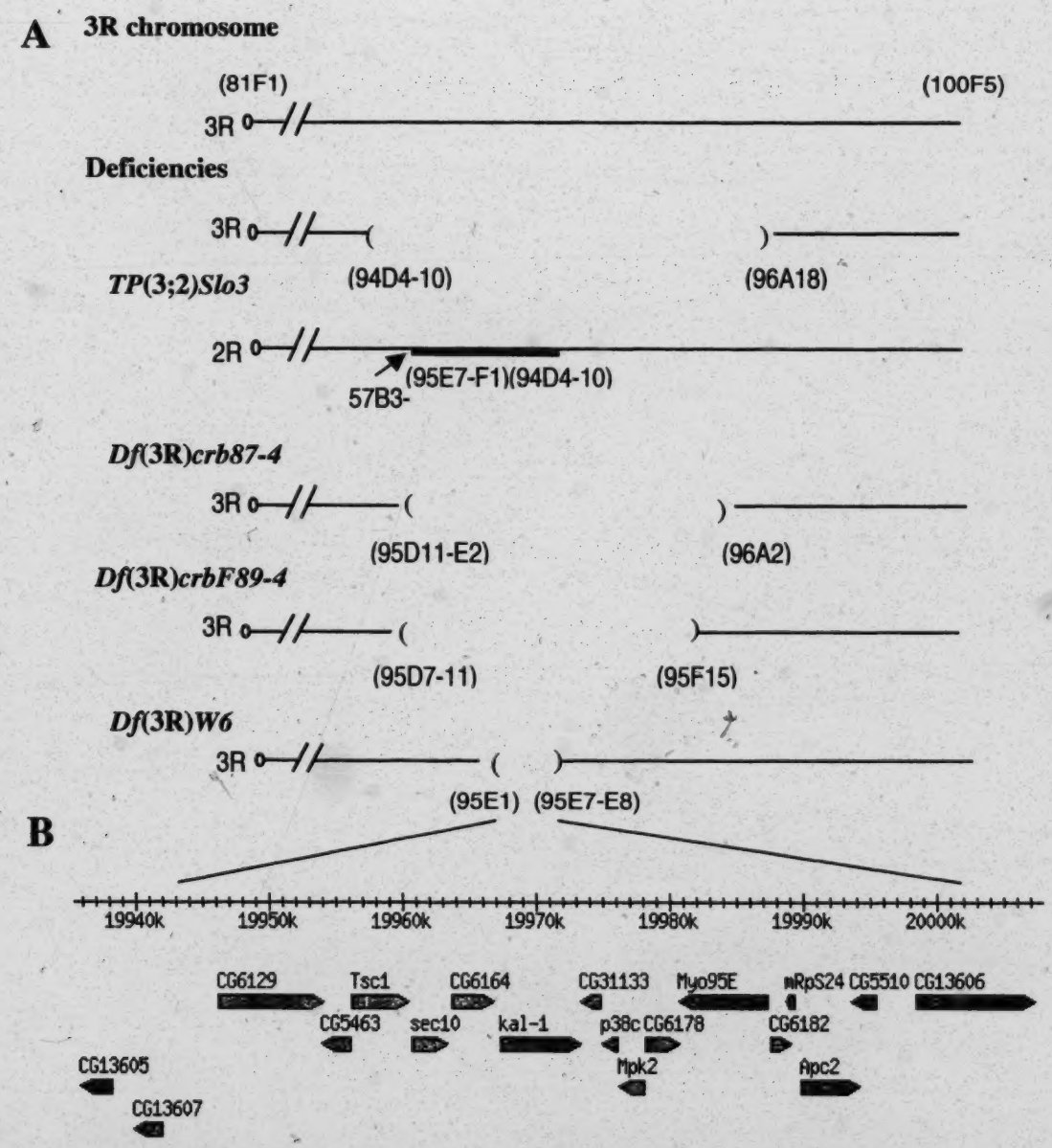

Figure 2-7: Localization of the *huc*95DE mutation to the cytological region of 95E1-E7-E8. A) The *huc*95DE mutation was mapped cytologically by the inability to complement *Df*(3R)*crb87-4* and *Df*(3R)*crbF89-4*, and the ability to complement the synthetic deficiency *Df*(3R)*slo*3 (containing a deletion extending from 94D4-10 to 96A18, and the proximal portion of this deleted region (94D4-10 to 95E7-F1) duplicated, inverted, and inserted into the second chromosome at position 57B3-5). Further refinement was obtained by its inability to complement *Df(3R)W6*, which was later determined to contain the genes listed in **B**.

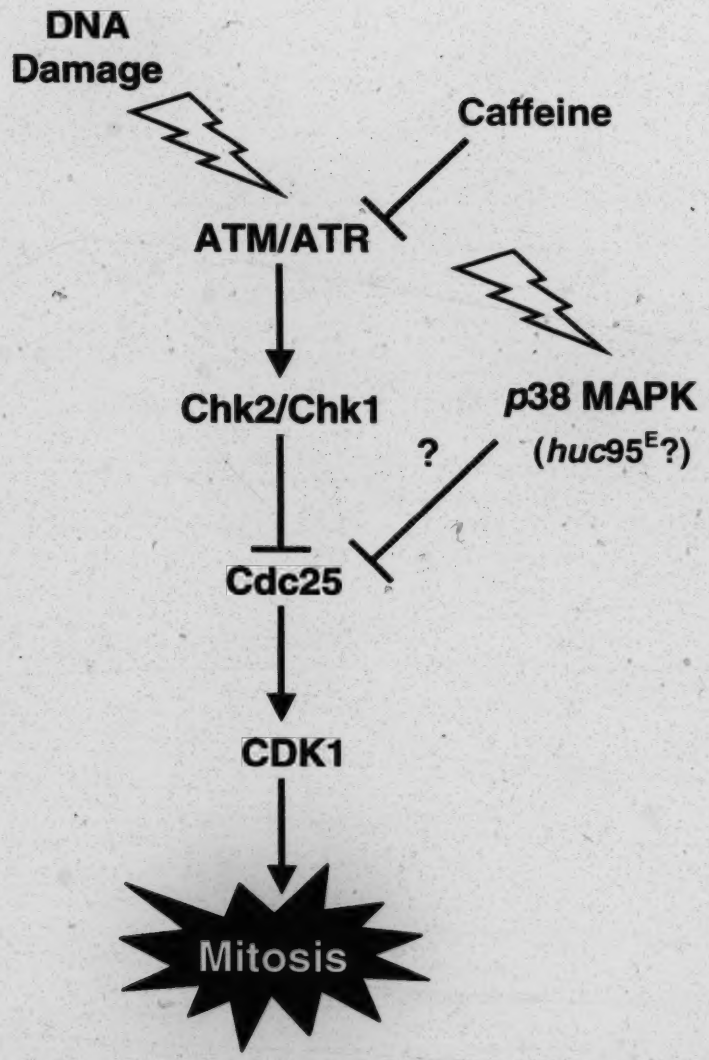

Figure 2-8: Possible model for a p38 mitogen activated protein kinase (MAPK) as a candidate for *huc*95^{E}. Because p38 MAPKs are involved in stress response and have been implicated in an ATM/ATR independent checkpoint pathway, a possible scenario for caffeine sensitivity is that p38 might be involved in an ATR/ATM independent pathway and can instigate a checkpoint when proper checkpoint regulation by ATM/ATR is compromised by caffeine. Hence, a mutation in p38 could render cells sensitive to damage if caffeine is used to inhibit ATM and ATR.

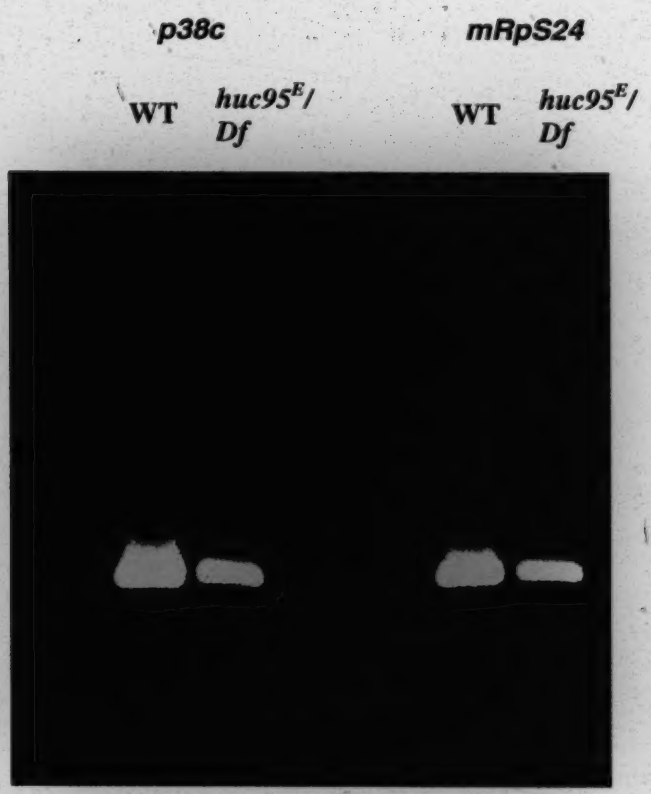

Figure 2-9: ***p38c* and *mRpS24* are expressed in *huc*95^{E} hemizygotes**. RT-PCR was performed on total RNA isolated from an isogenized third chromosome wildtype stock used for the original screen and from *huc*95^{E} hemizygotes using primers that amplified a 154 bp and 178 bp fragment of the genes *p38c* and *mRpS24*, respectively.

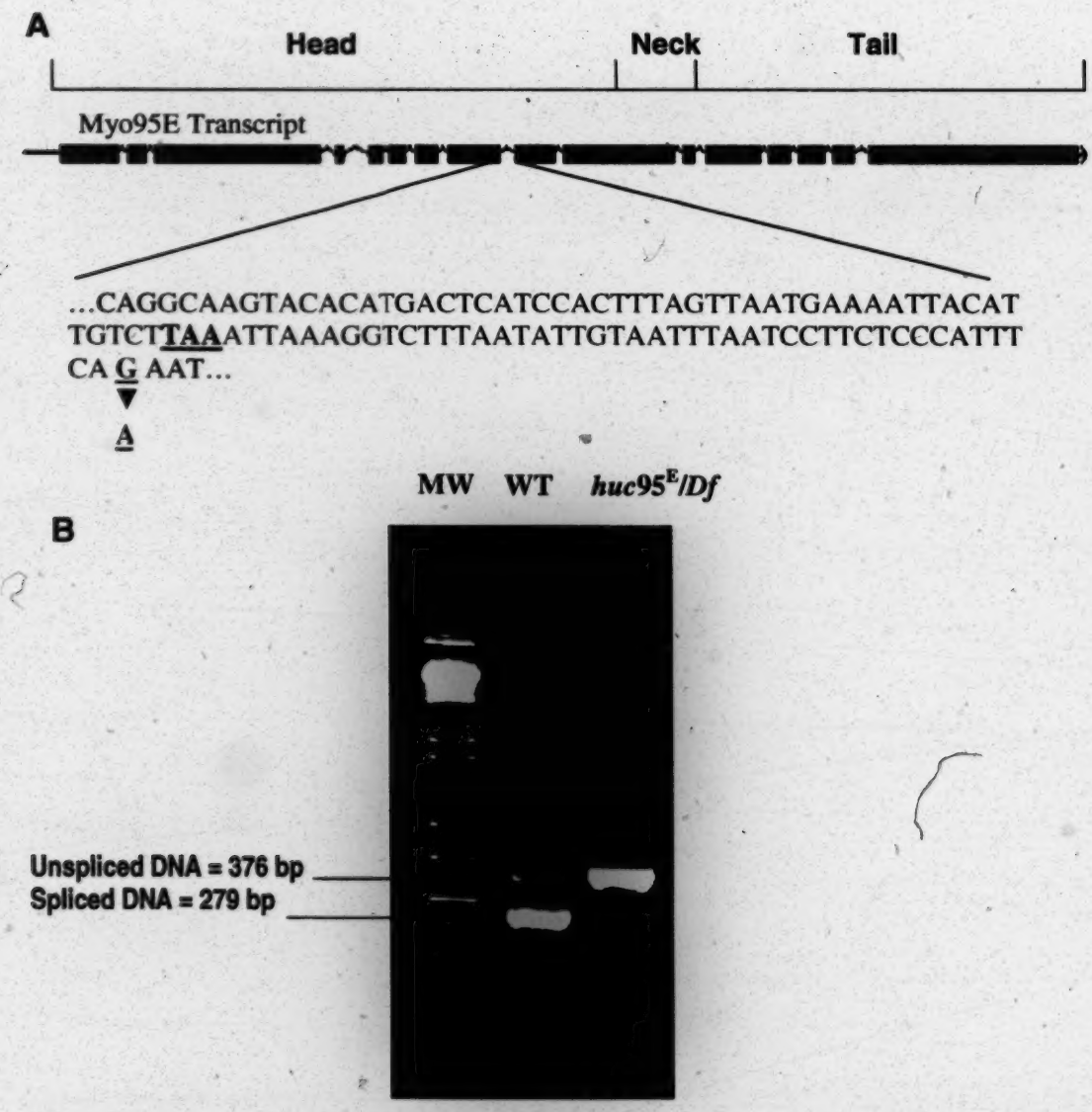

Figure 2-10: Splicing defect in *myo*95E in *huc*95^{E} hemizygotes. **A)** *huc*95^{E} hemizygotes exhibit a mutation within the eighth intron (in blue) in *myo*95E whereby a guanine at the intron 8-exon 9 junction is mutated to an adenine (shown in red), abolishing the proposed splicing acceptor site. Such a mutation would result in a severely truncated protein missing the terminal portion of the head region and the entire neck and tail region due to a premature stop codon (shown in green) along the original reading frame. **B)** Qualitative RT-PCR analysis demonstrating the splicing defect. RT-PCR was performed on total RNA isolated from an isogenized third chromosome stock used for the initial screen (lane 1) and from *huc*95^{E} hemizygotes using primers that flanked the intron (lane 2).

A

Exon 8 translation:

VQETAQLLNMEAQILINCLTRANSTNSAQEDVGCEMDARQAATNRNTLCR
TLYSRLFTWLVNKINESLKSTQREKNLALLDFYGFEALDHNSFEQFAINYS
AEKIHQ

Exon 10 translation: reading frame from exon 9

IRHYASVVNYSIHRFLEKNSDMLPKYISAAFYQSKLSLVQSLFPEGNPRRQVT
KKPSTLSSNIRTQLQTLLAIVKHRRSHYVFCIKPNEGKQPHQFDMALVQHQV
RYMSLMPLVHLCRTGHCYHLLHVKFFHRYKLLNSLTWPHFHGGSQVEGIALI
IRNLPLPSAEFTIGTKNVFVRSPRTVYELEQFRRLRISELAVLIQTMFRMYHAR
KRFQRMRHSQMIISSAWRTWR

Exon 10 translation: reading frame from exon 8

DSSLCKCSELLNTSVSRKELRHAAEVHKRCLLSEQTFFGAKPIPRGESPS
TGYQKAQHVEFEYPHPIADAAGHR*

B

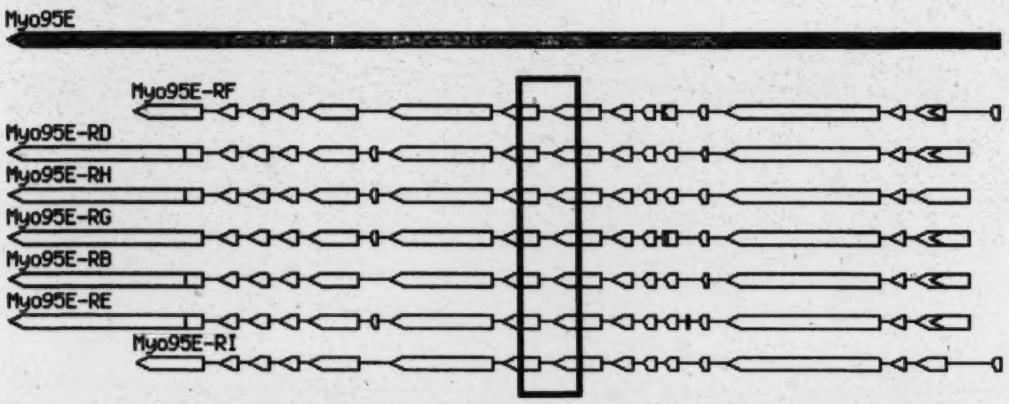

Figure 2-11: Analysis of alternative splicing in *myo*95E that bypasses splicing of exon 9. A) The translated protein sequence of exon 8 is listed in red with the switch-2 motif shown in blue. Splicing of the intron between exon 9 and 10 would result in translation of exon 10 shown in green with the IQ motif shown in blue. Bypassing exon 9 results in a truncated protein as a result of a stop codon being formed (represented by the asterisk) in frame from translation of exon 8. **B)** The putative transcripts of *myo*95E. The red box designates intron 8, which is utilized in all of the putative full length transcripts (note that translation of *myo*95E-RG encounters a stop codon in exon 5 and also lacks the switch-1 and switch-2 motifs, probably making this truncated protein non-functional as a myosin.

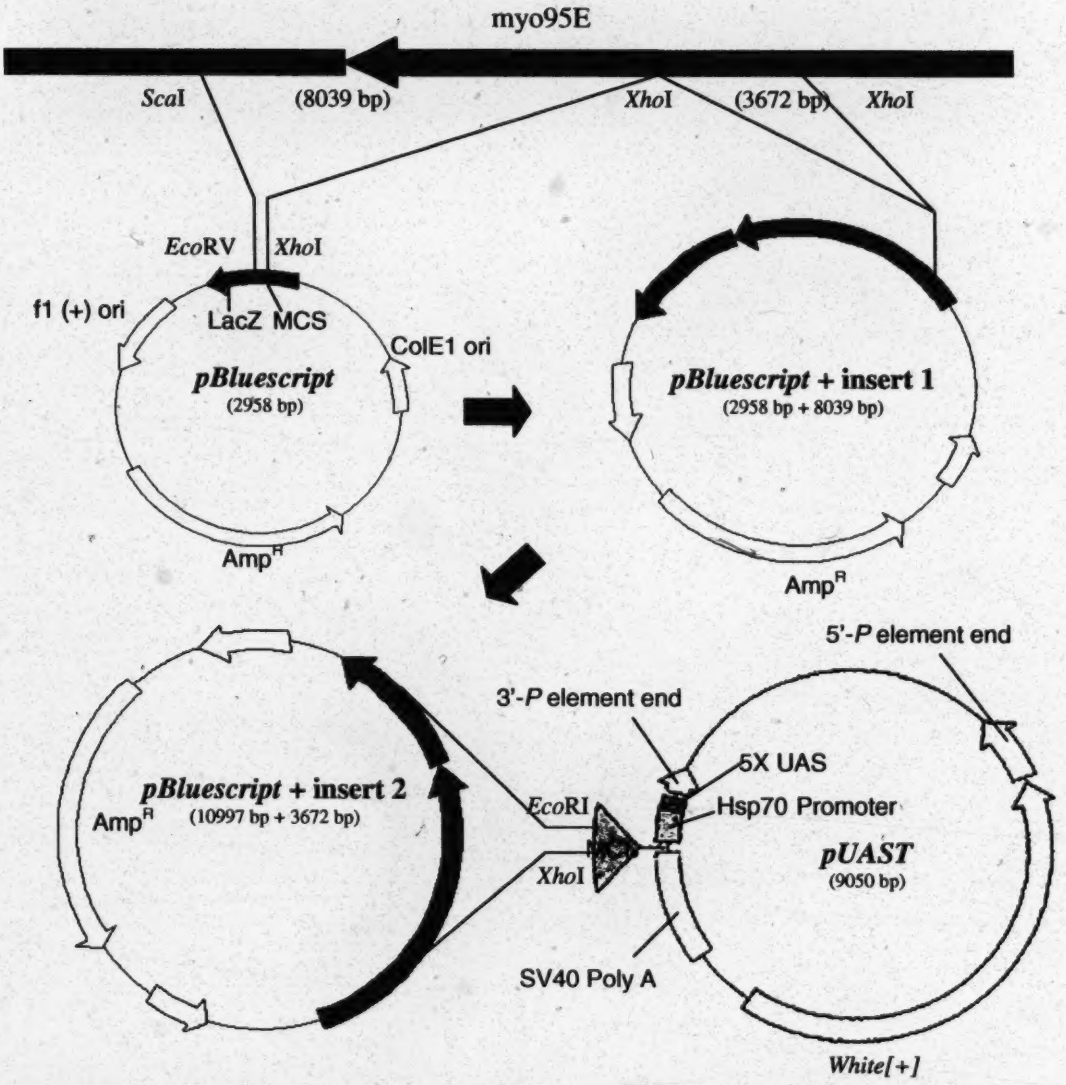

Figure 2-12: Creation of *myo*95E genomic rescue construct. A 8039 bp fragment containing *myo*95E and most of the downstream genomic region was excised from BACR29F06 using *ScaI* and *XhoI* restriction sites and cloned into *pBluescript* cut with *EcoRV* and *XhoI*. 3672 bp of the upstream genomic region was excised from BACR29F06 using *XhoI* restriction sites and cloned into the *pBluescript* containing the insert. Constructs containing the 3672 bp fragment ligated with the correct orientation were identified by PCR, and a 11711 bp fragment containing *myo*95E and upstream and downstream regions was excised using *EcoRI* and *XhoI*, and cloned into the transformation vector *pUAST*.

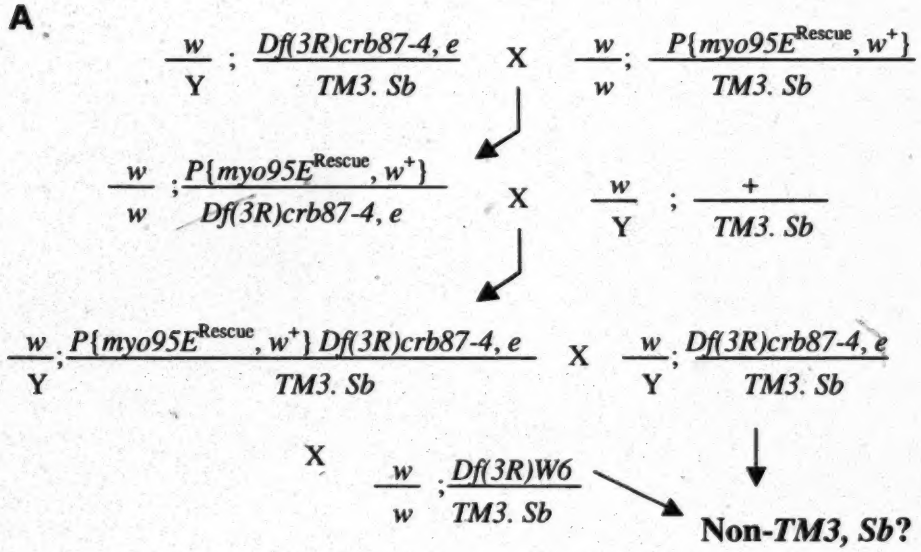
A
w / Y ; Df(3R)crb87-4, e / TM3. Sb X w / w ; P{myo95E^Rescue, w+} / TM3. Sb
w / w ; P{myo95E^Rescue, w+} / Df(3R)crb87-4, e X w / Y ; + / TM3. Sb
w / Y ; P{myo95E^Rescue, w+} Df(3R)crb87-4, e / TM3. Sb X w / Y ; Df(3R)crb87-4, e / TM3. Sb
X w / w ; Df(3R)W6 / TM3. Sb
Non-TM3, Sb?

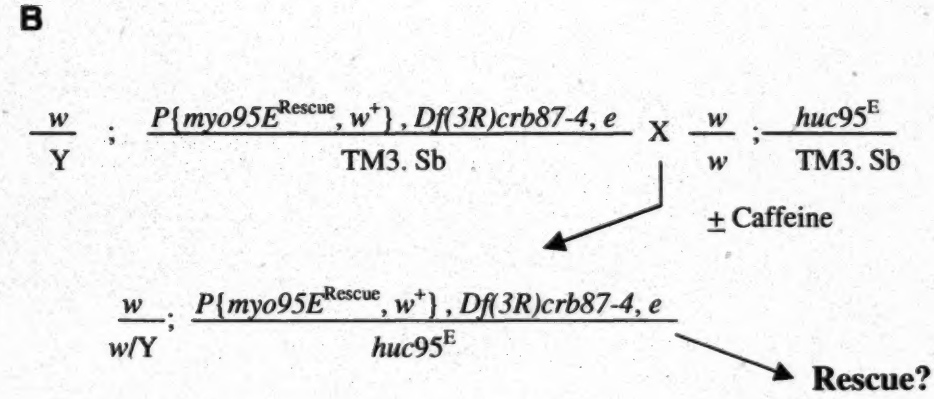

Figure 2-13: ***myo*95E transgenic rescue test for *huc*95^E hemizygote caffeine sensitivity**. **A)** To make an appropriate rescue line for the test, a recombinant stock was made containing both a deficiency that uncovered *huc*95^E and the *myo*95E rescue construct and tested for lethality with deficiencies that uncovered *huc*95^E to ensure integrity of the deficiency. Recombinants that fail to complement these deficiencies are crossed to *huc*95^E mutants in the rescue test shown in **B)** in the presence and absence of caffeine, and the viability of hemizygotes carrying the genomic rescue construct assessed.

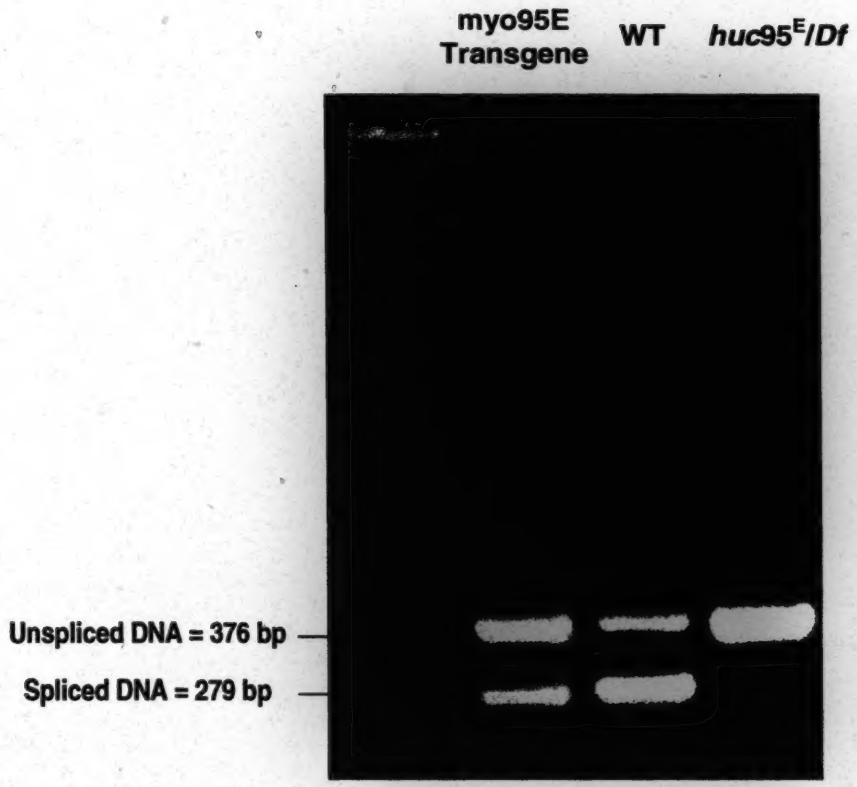

Figure 2-14: Hemizygotes expressing the rescue construct exhibit splicing of intron 8 in *myo*95E. Total RNA was isolated from *huc*95^{E}/ P{*myo*95E}, *Df(3R)crb87-4, e* and subjected to RT-PCR using primers that span the splice site of intron 8. Results are similar to RT-PCR performed with wild type flies and demonstrate splicing of intron 8 as compared to RNA isolated from hemizygotes.

Chapter 3: The Characterization of the *Drosophila huc95*^{E} Mutants

Section 3-1: Introduction

In addition to attempts at mapping and identifying the gene responsible for the *huc*95^{E} mutation, some work was also done to further characterize these mutants. The initial identification and classification of the *huc* mutants was based upon the sensitivity of adult eye development to 2 mM caffeine and 3 mM HU treatment in a screen utilizing the EGUF-GMR-*hid* system for creating homozygous ommatidial clones (hence the name *huc* for **h**ydroxy**u**rea and **c**affeine sensitive mutants) (Silva, 2002). When using this system, *huc*95^{E} mutants have compound eyes with severely reduced ommatidia that are occasionally fused and irregular (Figure 1-12). These mutants were subsequently found to be primarily sensitive to 2 mM caffeine, as treatment with 3 mM HU alone produced little discernible contribution to the phenotype (Silva, 2002). Furthermore, *huc*95^{E} hemizygotes survived to adulthood with no visible developmental abnormalities when grown on normal media, but undergo pupal lethality when grown on media containing caffeine concentrations as low as 0.5 mM. This suggests that *huc*95^{E} is a conditional mutant, implying that the *huc*95^{E} gene is not required for viability under normal growth conditions, but is necessary for development in the presence of caffeine.

The adult external structures emerge out of specialized, compartmentalized epithelial sacs called imaginal discs, which invaginate from the body wall during embryogenesis and proliferate rapidly without differentiating inside the larval body cavity (Cohen, 1993). These discs become spatially patterned along the body axis throughout larval development and upon pupariation (following the complete differentiation of these discs), they evert, resulting in the emergence of developed adult

structures. The severe eye phenotype seen in the huc95E mutants prompted examination of the eye-antennal imaginal discs from *EGUF*/+; *FRT82B huc*95^{E}/*FRT82B GMR-hid*3R third instar larvae grown in both normal media and media containing HU and caffeine (Silva, 2002). The eye-antennal discs were smaller and more fragile in larvae reared in the presence of HU and caffeine as compared to larvae grown on normal media. To determine if there were any abnormalities in the differentiation of ommatidia in these mutants, these discs were stained with antibodies to a neuronal RNA-binding protein called **e**mbryonic **l**ethal, **a**bnormal **v**isual (ELAV) (Figure 1-12) (Silva, 2002). This protein is required for normal maintenance and development of all neurons within the central nervous system, and interacts directly with neuronal RNA, such that ELAV antibody staining serves as a marker for those cells that have undergone neuronal differentiation (Yao *et al.*, 1993). ELAV staining revealed that the differentiation of ommatidial precursors still initiates within these discs, with no change in the size of the individual pre-clusters (Figure 1-12). This suggests that the reduction in size of these discs is due to fewer, normal sized cells being present and not that the disc is composed of smaller cells (Silva, 2002). The pattern of pre-clusters also appeared to be disrupted, with clusters being more tightly packed and less evenly spaced as compared to heterozygous controls. This disorganization however, could be due to the fragility of the eye discs under HU and caffeine and thus, might be an artefact of dissection (Figure 1-12, compare C and E to D and F). To determine if there were any defects in the synchronization or coordination of cell cycles within the developing disc, the pattern of bromodeoxyuridine (BrdU) incorporation was examined in eye-antennal imaginal discs from *EGUF*/+; *FRT82B huc*95^{E}/*FRT82B GMR-hid*3R third instar larvae and compared to

eye imaginal discs from *EGUF/+*; *FRT82B huc*95^E*/TM3 Ser* third instar larvae in the presence of caffeine (Figure 1-13). BrdU is a base analog similar in structure to the nucleoside thymidine and is used to identify cells in S phase. Because cell cycles are synchronized at G_1 within the morphogenetic furrow, with unspecified cells undergoing a coordinated single division following the furrow (referred to as the second mitotic wave), BrdU staining could possibly reveal defects in cell cycle coordination. Homozygous mutant eye-antennal discs had fewer cells labelled with BrdU as compared to heterozygous controls, and had a staining pattern that was disrupted and more diffuse, suggesting that fewer cells are undergoing replication, or that cells are dying prematurely, or are arrested prior to undergoing replication. However, it is unknown whether or not these cells were capable of undergoing mitosis or if the cells that did not undergo S-phase were arrested and capable of undergoing mitosis later on.

To further characterize the *huc*95^E mutants, I performed experiments to analyze the sensitivity of these mutants to development in the presence of caffeine. Since the sensitivity of *huc*95^E hemizygotes was only tested with caffeine concentrations as low as 0.5 mM, the approximate limit of caffeine sensitivity on the viability of *huc*95^E hemizygotes was determined to test the acute sensitivity of these mutants. Also, since the intent of the screen that had isolated *huc*95^E was to discover possibly novel cell cycle checkpoint mutants that would have remained hidden due to redundancy in checkpoint pathways, the effects of ionizing radiation on viability of *huc*95^E hemizygotes was also examined. Furthermore, because *huc*95^E hemizygotes die as pupal lethals in the presence of caffeine, the gene associated with this phenotype might have a temporal role in development (as the mutation does not immediately kill larvae grown in the presence of

caffeine, but allows persistence to the pupal stage). The appearance of fewer ommatidia within mutants exposed to caffeine also suggested that cells within the eye imaginal disc that would eventually develop into ommatidia were unable to efficiently proliferate, or had undergone apoptosis, or both. As a result, experiments were done to look at the effects of caffeine treatment on cell proliferation and apoptosis during the development of the imaginal discs.

Section 3-2: Materials and Methods

Section 3-2a: Caffeine titration

Reciprocal crosses between *huc*95^{E}*/TM3 Sb, Ser* and *Df*(3R)*crb87-4/TM3 Sb, Ser* were set up in vials and bottles containing 0.5 mM, 0.25 mM, 0.125 mM, 0.06 mM, and 0 mM caffeine respectively, and the proportions of hemizygotes determined from the progeny of these crosses. Caffeine-containing food was prepared by scoring the media in vials and bottles with a clean metal spatula and adding 250 µl or 2.5 ml respectively, of an appropriate concentration of caffeine (dissolved in distilled water) to yield the desired concentration.

Section 3-2b: Ionizing Irradiation Sensitivity Assay

Reciprocal crosses consisting of *huc*95^{E}*/TM3, Ser-GFP* and *Df*(3R)*crb87-4/TM3 Ser-GFP*, were set up and allowed to develop to third instar larvae (to ensure that the larvae were as robust and mature as they could be in order to survive the irradiation treatment). The larvae were exposed for 0, 45, 90, 180, or 360 seconds in a cobalt^{60} gamma source, to mediate exposure to 0, 5, 10, 20 and 40 Grays (Gy) of ionizing radiation, respectively. The crosses were then left to develop at 22°C and the progeny sorted and tabulated following eclosion.

Section 3-2c: Imaginal Disc Antibody staining

Third instar wandering larvae of an appropriate genotype were dissected in 0.01 M phosphate-buffered saline (PBS) and fixed in 3.7% formaldehyde, 0.1% polyoxyethylene sorbitan monolaurate (tween 20), and 0.01 M PBS (PBST) for 20 minutes. The discs were then rinsed three times in PBST for 5 minutes and blocked in 5% bovine serum albumin (BSA) in PBST for 30 minutes. Primary antibodies of choice at the appropriate dilutions were then added to discs soaking in 5% BSA in 1% PBST and incubated with gentle agitation on a rotating nutator at 4°C overnight. Following three 10-minute rinses in PBST, the discs were then incubated in the appropriate secondary antibodies at a dilution of 1 in 1000, in 5% BSA with no light at room temperature for 1 hour. Samples were then rinsed again in PBST three times for 10 minutes and stained with hoechst dye for 5 minutes at a dilution of 1 in 500. Following a final rinse for 10 minutes in PBST, imaginal discs or brains were then dissected out from inverted larval cuticles in PBS and mounted on microscope slides with 80% glycerol in PBS. The dilution for anti-mouse Phospho-Histone 3 (Ser10) antibody (Upstate Biotechnology Cat No. 05-598) was 1/1000, while the dilution for anti-rabbit cleaved human caspase-3 antibody (Cell signaling Cat No. 9661) was 1/800.

Section 3-3: Results

Section 3-3a: The viability of huc95^{E} hemizygotes is compromised at concentrations as low as 0.25 mM of caffeine

Originally, the viability of *huc*95^{E} hemizygotes was found to be sensitive to 0.5 mM caffeine, but the limits of this sensitivity were not determined (Silva, 2002). A caffeine titration experiment was performed to test sensitivity of hemizygotes to 0.25

mM, 0.125 mM, and 0.06mM caffeine (Figure 3-1) (Krause, 2003). At concentrations of 0.25 mM, the proportion of hemizygote survivors was similar to concentrations of 0.5 mM for both reciprocal crosses. At a caffeine concentration of 0.125 mM, the proportion of survivors drastically increases to approximately 9 times the proportion seen at a concentration of 0.25 mM in both reciprocal crosses, and is comparable to proportions seen at 0.06 mM caffeine. Proportions exhibit only a modest increase when no caffeine is added as compared to 0.06 mM caffeine in both reciprocal crosses, suggesting that the caffeine concentration sufficient to compromise the viability of *huc*95^{E} hemizygotes is between 0.25 mM and 0.125 mM caffeine.

Section 3-3b: Ionizing radiation does not substantially affect the viability of *huc95^{E}* hemizygotes

Because the original premise of the screen was to isolate potential cell cycle checkpoint mutants, it was logical to determine if the *huc*95^{E} mutants were defective in cell cycle checkpoint regulation. Since it was previously known that caffeine affected the viability of *huc*95^{E} hemizygotes, it was reasoned that if *huc*95^{E} was defective for a cell cycle checkpoint function, *huc*95^{E} hemizygotes might also exhibit increased sensitivity to DNA damaging agents. Ionizing radiation is an effective inducer of DNA checkpoint activation and has been commonly used to study the effects of cell cycle checkpoint response by mediating DNA damage such as double stranded breaks (Iliakis *et al*, 2003). As such, the sensitivity of hemizygotes to ionizing radiation was assessed to determine if the *huc*95^{E} mutation rendered it checkpoint defective. To test this, crosses and reciprocal crosses of *Df*(3R)*crb87-4/TM3 Ser-GFP* and *huc*95^{E}*/TM3 Ser-GFP* were set up and third instar larvae resulting from the cross were exposed to varying amounts of gamma

irradiation at 0, 5, 10, 20, and 40 Gy, respectively. After irradiation, the larvae were allowed to develop, and the proportion of hemizygotes determined (Figure 3-2). No progeny developed to adulthood when exposed to 40 Grays delineating this dosage as completely lethal, even to wildtype. Exposure to 20 Grays drastically reduced the total number of progeny that developed to adults and corresponded to a developmental delay of 3 days, which was not observed with lower dosages. There was no appreciable reduction in the number of hemizygotes that developed following gamma irradiation compared to unirradiated controls at dosages of 5 or 10 Gy, suggesting that hemizygotes are not sensitive to ionizing radiation. At 20 Gy, the proportion of hemizygotes does significantly decrease (with proportion levels approximately half of those at 10 Gy) however, the total number of flies was also reduced, suggesting that at this dosage, the viability of all the flies are affected, not just hemizygotes. Furthermore, *huc*95^{E} hemizygotes did not exhibit additional delays in development relative to their heterozygous siblings, further supporting the conclusion that these flies were not sensitive to ionizing irradiation.

Section 3-2c: *huc95^{E}* hemizygote third instar larvae display increased apoptosis in eye imaginal discs when reared in media containing 2 mM caffeine

To determine if the reduction in ommatidial cells and overall size of the eye observed in *EGUF/+; FRT82B huc*95^{E}*/FRT82B GMR-hid*3R mutants was due to caffeine-induced apoptosis, eye discs from *EGUF/+; FRT 82B huc*95^{E}*/FRT82B GMR-hid3R* larvae grown in the presence and absence of 2 mM caffeine, were stained with acridine orange to visualize cell death (Bradley, 2002). The results revealed more cell death towards the anterior of the morphogenetic furrow in caffeine-treated larvae as

compared to larvae grown in the absence of caffeine, suggesting that more cell death is occurring in larvae exposed to caffeine (Figure 3-3). Because the larvae contained GMR-*hid* (a construct containing the apoptosis-triggering gene ***h**ead **i**nvolution **d**efective* fused to the *Glass Multiple Reporter* promoter) which is expressed mainly in post-mitotic cells after the second mitotic wave, significant background staining was apparent posterior of the morphogenetic furrow (where *GMR* is active). To examine apoptosis without *GMR-hid*, *huc*95^{E} hemizygous larvae were grown in the presence and absence of caffeine, and dissected for eye-antennal imaginal disc analysis. Third instar *huc*95^{E} hemizygous larvae grown on caffeine-containing media had either no imaginal discs of any kind, or discs so small and fragile that they escaped detection. Furthermore, *huc*95^{E} hemizygotes died as pupal lethals with no apparent development of any adult structures within the pupal cases, consistent with my observation that these larvae had no imaginal discs. This suggests that the caffeine-induced lethality and sensitivity of *huc*95^{E} mutants is due to the loss of imaginal discs, which would eventually differentiate and evert to form developed adult structures.

When testing *huc*95^{E} hemizygous larvae in media containing caffeine, the caffeine was added to the fly media such that the embryos laid would be developing under the constant presence of caffeine. To determine if prolonged development in the presence of caffeine was necessary to produce these effects, I set up multiple vial crosses to obtain hemizygotes and subsequently added 2 mM caffeine to each vial 1 to 6 days after egg laying (AEL). Imaginal discs from hemizygotes were obtained after addition at days 5 to 6 in the presence of caffeine, corresponding to addition of caffeine at the third larval instar. This suggests that caffeine might have a role in either the prevention of the

formation of imaginal discs, or its destruction. If caffeine did result in degeneration of the imaginal discs, this might explain the increased acridine orange staining that was attained with *EGUF/+; FRT82B, huc*95^{DE}*/FRT82B, GMR-hid*3R larvae grown in the presence and absence of 2 mM caffeine. Another observation is that there was always a developmental delay of about 3 days after addition of caffeine, which is not surprising since toxic components or stress result in developmental delays. To see if caffeine was causing the destruction of imaginal discs, 2 mM caffeine was added after day 4, and the larvae were allowed to develop to the wandering third instar larval stage. Dissection of these larvae revealed no imaginal discs, however upon dissection of the larval brains and staining with an antibody to activated caspase 3, intense staining could be seen within tissues that would have resulted in imaginal leg and eye-antennal discs, suggesting that there were discs, but that they were in the process of deteriorating, thus becoming fragile and undetectable. (see Figure 3-4). The deterioration of these discs is accompanied by apoptosis, which might be a reason for the lack of imaginal discs and pupal lethality of these mutants. To further examine this possibility, 2 mM caffeine was added to the media after 4 days of development, and the larvae allowed to develop for an additional 2 days, after which, the larvae were dissected and imaginal eye-antennal and wing discs were stained with an antibody against phospho-histone-3 (PH-3) a histone protein that is phosphorylated in cells undergoing mitosis) and activated caspase 3 (see Figure 3-5 and Figure 3-6). When grown on normal media, *huc*95^{E} hemizygotes exhibited very little caspase-3 staining that was comparable to heterozygous controls reared on normal media (Figure 3-5 and Figure 3-6: compare panel A and I). In the presence of caffeine however, imaginal discs from *huc*95^{E} hemizygous larvae exhibited markedly more caspase-3

staining compared to heterozygous controls (which appeared only slightly increased relative to controls raised on normal media). Interestingly, imaginal discs dissected from heterozygous larvae also displayed a slight increase in caspase-3 staining (Figure 3-5 and Figure 3-6: compare panel I and M), however this staining was no where near the intensity of staining exhibited by imaginal discs from *huc*95^{E} hemizygous larvae reared in caffeine-containing media. Staining with PH-3 did not seem to show any differences in both huc95^{E} hemizygotes or heterozygous controls in either the presence or absence of caffeine. All imaginal discs in all conditions had exhibited a lot of PH-3 staining (consistent with the proliferative nature of third instar imaginal discs) conditions. Although PH-3 staining might appears to be different (ie. less abundant and more punctate) in the caffeine treated heterozygous controls and hemizygotes reared on normal media, this is believed to be an artefact of the staining procedure. As a result, these observations are preliminary and future work to quantify the number of PH-3 staining cells within better-dissected discs.

Section 3-4: Discussion

From this analysis, I determined that the viability of the *huc*95^{E} mutants raised in the absence of caffeine is not sensitive to ionizing radiation treatment implying that *huc*95^{E} is not likely to have a novel cell cycle checkpoint function. *huc*95^{E} cannot be conclusively ruled out as a novel cell cycle checkpoint mutant however, as any roles pertaining to cell cycle checkpoint regulation might be masked by redundant mechanisms that compensate for *huc*95^{E}. Alternatively, it also could be possible that *huc*95^{E} encodes a checkpoint component that is not involved in responses to ionizing radiation or DNA repair. *huc*95^{E} mutants are sensitive, however, to caffeine concentrations of down to 0.25

mM. In the presence of caffeine, hemizygotes die at the pupal stage and examination of the pupal lethals revealed no evidence of adult structures. Furthermore, examination of third instar hemizygous larvae reared in the presence of caffeine revealed no imaginal discs, suggesting that the pupal lethality observed in these mutants was due to the inability to complete metamorphosis. I determined that this inability to develop imaginal discs could be relieved if caffeine was added to the media at day 5 AEL. Upon staining third instar larval brains with caspase-3 from hemizygotes grown in media that had caffeine added at day 4, intense staining of tissues that would eventually result in imaginal discs was seen, suggesting that day 4-5 was the critical time period for exposure to caffeine. Furthermore, imaginal discs dissected from *huc*95^{E} hemizygotes grown in the presence of caffeine exhibit more caspase-3 staining compared to heterozygous controls and hemizygous controls reared in the absence of caffeine, indicating that the imaginal discs are deteriorating in the hemizygotes as a result of caffeine-induced apoptosis. No detectable changes were observed upon the staining of imaginal discs with the mitotic marker PH-3 in both *huc*95^{E} hemizygous larvae and heterozygous controls both reared in the presence and absence of caffeine, suggesting that the process of mitosis remains unaffected. This is just a preliminary observation however, and further work to quantify the number of cells undergoing mitosis in both hemizygous and heterozygous controls would serve to confirm this result.

Although it is clear that *huc*95^{E} mutants exhibit increased apoptosis upon exposure to caffeine, it is still unknown as to why and how caffeine induces cell death in these mutants. As a result, an interesting question to address is whether this occurs through the release of calcium. Calcium is an important signalling molecule and is

routinely kept at an intracellular concentration of approximately 100 nM in resting cells (Hanson *et al.*, 2004; Saris and Carafoli, 2005; Waring, 2005). Such concentrations are accomplished by controlling the entry or efflux of Ca^{2+} into, and out of the cell, and the active sequestration and storage of intracellular Ca^{2+} within the endoplasmic reticulum (ER) and mitochondria through various channels and transporters. Excessive or inappropriate calcium release that depletes intracellular Ca^{2+} ER stores, can lead to apoptotic events by triggering mitochondrial-mediated pathways of caspase activation and apoptosis through the release of cytochrome C into the cytoplasm (Hanson *et al.*, 2004). As a result, it would be interesting to stain imaginal discs from *huc*95^{E} hemizygotes exposed to caffeine with antibodies to cytochrome C and see if cytochrome C release is involved. Furthermore, RyRs (receptors that reside in the ER and play a role in the regulation of cytosolic Ca^{2+}) are sensitive to caffeine and evoke Ca^{2+} release upon exposure (Rousseau *et al.*, 1988; McPherson *et al.*, 1991). Treatment of Chinese hamster ovary cells with caffeine and ryanodine induces a release of calcium from the ER through its actions on RyR, resulting in apoptosis as ER stores of Ca^{2+} are depleted (Pan *et al.*, 2000). Thus, it would be interesting to see the reaction of *huc*95^{E} mutants to ryanodine. *Drosophila* has only one RyR gene (*Ryr44F*) but mutants in *Ryr44F* exhibit impaired muscle function and die as first larval instars (Sullivan *et al.*, 2000). However, it would be interesting to see whether any interaction between *Ryr* and *huc*95^{E} occurs by making a double mutant expressing a homozygous *ryr* mutant gene (using the *EGUF-GMR-hid* system) and hemizygous *huc*95^{E} in the absence of caffeine. Interestingly, genetic interaction studies in *Drosophila* involving *Ryr44F* and *Cam* (a gene located cytologically at 48F1 which encodes the Ca^{2+} sensor protein calmodulin) showed that the

one copy of a hypomorphic *Ryr* allele was capable of partially rescuing phenotypes mediated by the Cam^7 allele, which comprised of pupal lethality, pupal cases with deep indentations at larval segmental boundaries, and pharate adults with inverted heads inside the thorax (Wang *et al.*, 2003). Furthermore, the inhibition of phototransduction in *Drosophila* photoreceptors, mediated by treatment with ryanodine and caffeine, was rescued by the subsequent application of Ca^{2+}-calmodulin (Arnon *et al.*, 1997). These results suggest that calmodulin plays a role in RyR regulation and thus, it would be interesting to determine if *Cam* and $huc95^E$ interact and whether the *Cam* mutation could partially rescue the $huc95^E$ mutation in the presence of caffeine. Alternatively, experiments involving Ca^{2+} channel blockers may also serve to elucidate the role of calcium channels in the apoptosis response of these mutants.

Another possibility is caffeine's effect on the phosphoinositide 3-Kinase (PI3K): an important signalling enzyme that has been implicated in a wide variety of processes ranging from cellular proliferation, apoptosis, differentiation, and metabolic regulation (Foukas *et al.*, 2002; Katso, *et al.*, 2001; Osaki *et al.*, 2004; Franke *et al.*, 2003). One of the most well studied aspects of PI3K signal transduction is its role in the insulin-signalling pathway (Shepherd, 2005). The hormone insulin rapidly stimulates class I_A PI3K signalling, which regulates such events as glycogen synthesis, inhibition of lipolysis, stimulation of protein biosynthetic pathways, and the translocation of the GLUT4 glucose transporter (a receptor required for the intake of extracellular glucose in to the cell) to the plasma membrane (Shepherd, 2005; Bose *et al.*, 2002). In addition to regulating glucose metabolism, insulin signalling is also the principle regulator of cell growth and development in *Drosophila* and is highly conserved from *Drosophila* to

humans (Lizcano *et al.*, 2003; Bikopoulos *et al.*, 2004). *Drosophila* have one insulin receptor (DinR), seven insulin-like peptides, and several homologues of mammalian insulin receptor substrates such as PI3K, PTEN, PKB/Akt, and p70SK (Bikopoulos *et al.*, 2004). Expression of ***D**rosophila* **i**nsulin-**l**ike **p**eptide-**2** (DILP-2) results in an increase in body mass and growth in the developing eye when exclusively overexpressed in this tissue and inhibition of insulin signalling corresponds to a decrease in the overall size of the fly and a reduction in the development of imaginal discs (Edgar, 1999; Brogiolo *et al.*, 2001). These results reflect the ability of insulin signalling to inhibit apoptosis, thereby allowing continued growth of cells and tissues by preventing their destruction (Bertrand *et al.*, 1998; Lee-Kwon *et al.*, 1998; Yenush *et al.*, 1998).

Caffeine has been found to inhibit the lipid kinase activity of class I PI3Ks *in vitro* and block the ability of insulin to stimulate PKB (an important kinase that inhibits processes of apoptosis and regulates cell size) *in vivo* in CHO-IR cells and rat soleus muscle with IC_{50} values similar to those required for inhibition of PI3K activity (Foukas *et al.*, 2002). This suggests that caffeine can inhibit insulin signalling by inhibiting PI3K and could explain the reduced size of imaginal discs and the increased occurrence of apoptosis in the *huc*95^{E} hemizygotes grown in caffeine since insulin signalling regulates cell size and apoptotic events. Furthermore, apoptosis has also been consistently linked with a decrease in glucose transport (Moley and Mueckler, 2000). Glucose transport and metabolism can trigger apoptosis because decreased glucose uptake results in ATP depletion, which can stimulate the mitochondrial cell death cascade or can result in oxidative stress, which can trigger stress-activated and other signal transduction pathways that signal apoptosis (Moley and Mueckler, 2000). Alternatively, intracellular

hypoglycemia and hypoxia due to decreased glucose transport can increase expression of **h**ypoxia-**i**nducible **f**actor-**1α** (HIF-1α), which stabilizes p53 and activates p53-associated apoptotic response pathways (Moley and Mueckler, 2000). Because caffeine also blocks insulin-stimulated glucose transport in CHO-IR cells, caffeine could conceivably signal apoptosis by affecting glucose uptake and metabolism (Foukas *et al.*, 2002).

Upon stimulation by insulin, the class I myosin Myo1C is required to facilitate the fusion and allocation of vesicles containing GLUT4 receptors to the plasma membrane in 3T3-L1 adipocyte cell cultures, and inhibition of PI3K by the inhibitor LY294002 could block this fusion step, resulting in GLUT4-containing vesicles accumulating just beneath the plasma membrane (Bose *et al.*, 2002; Bose *et al.*, 2004). This block in fusion mediated by PI3K inhibition could be relieved however, by overexpression of Myo1C (Bose *et al.*, 2004). The *Drosophila* class I myosin *myo*95E exhibits a polymorphism suggestive of a splicing defect that is predicted to result in a non-functional protein in the *huc*95^{E} mutants. Structurally, Myo1C differs from Myo95E in that it contains three IQ motifs and a cargo domain that contains several proline-rich domains that are thought to interact with SH3 domains. In BLAST alignments however, Myo95E is more related to Myo1C than to the other two class I myosins within *Drosophila*, suggesting that these differences may not be relevant (Tzolovsky *et al.*, 2002). Accordingly, an explanation for caffeine sensitivity of the *huc*95^{E} mutation (if *myo*95E is the gene associated with the *huc*95^{E} mutation) is that the expression of *myo*95E is required to compensate for caffeine's inhibition of PI3K signalling (analogous to overexpression of Myo1C being required to overcome a block in fusion mediated by PI3K inhibition in cells). For instance, a possible model could be that caffeine's ability to inhibit PI3K signalling

results in a decrease in downstream signalling mediated by PIP_3, including the activation of PKB (which renders cells extra sensitive to caffeine's ability to signal apoptosis), and inhibition of glucose transport (which triggers apoptosis to occur) (Figure 3-7). This results in degeneration of the imaginal discs and the consequent pupal-lethality (as no imaginal discs would be present to allow further metamorphosis). Expression of *myo*95E may be required to alleviate this sensitivity, possibly by allowing for vesicular trafficking to continue and inhibit apoptosis from occurring by maintaining glucose transport. This might also suggest why the rescue construct was not successful in rescuing the caffeine sensitive phenotype as expression of the construct may be reduced to that of wildtype.

To test this model, it will be necessary to determine if caffeine is capable of inhibiting PI3K signalling in *Drosophila*. PI3K signalling also regulates autophagy: a conserved process whereby amino acids and other nutrients from long-lived proteins, cellular organelles and other components are recycled within autophagic lysosomes (Rusten *et al.*, 2004). The process of autophagy is generally activated in response to environmental stress and nutrient deprivation and sustains the viability of cells under suboptimal conditions by recycling non-essential macromolecules (Klionsky and Emr, 2000). In holometabolous insects, autophagy is also triggered temporally in conjunction with development and metamorphosis, as larval tissues and organs are degraded and reorganized into adult forming structures. In this context, autophagy occurs by compartmentalization of cytoplasmic components by a cisternal isolation membrane derived from a preautophagosomal structure (PAS) to form a double membrane-enclosed autophagosome (see Figure 3-8) (Baehrecke, 2002; Noda *et al.*, 2002). Fusion of the autophagosome with a lysosome forms an autolysosome: the site of degradation where

cytoplasmic components are recycled (Fengsrud *et al.*, 2000). The mechanisms underlying formation of the PAS have been elucidated from studies in yeast and involve two ubiquitin-like conjugation systems. Initially, a small ubiquitin-like protein Atg12, covalently attaches to another ubiquitin-like protein Atg5, to form an Atg12-Atg5 conjugate (Mizushima *et al.*, 1998). This conjugate requires another ubiquitin-like protein Atg8, conjugated to the phosphatidylethanolamine (PE), for localization to the PAS (Suzuki *et al.*, 2001). Both conjugates are required for the process of autophagy to occur and ultrastructure analysis has revealed that Atg5 and Atg8 (or its mammalian homologue Microtubule associated protein-1 **l**ight **c**hain **3** (LC3)) localize to the isolation membranes (Mizushima *et al.*, 2001). Upon closure however, Atg5 is lost while LC3 still remains, making LC3 a marker for newly formed autophagosomes. Activation of the insulin pathway, and the consequent stimulation of class I_A PI3K signalling, represses autophagy in mammalian cells and *Caenorhabditis elegans*, suggesting that PI3K has a negative role in the regulation of autophagy (Melendez *et al.*, 2003; Seglen and Bohley, 1992). This is consistent with insulin's role as a regulator of cell growth and apoptosis as the larval period is characterized by an increase in mass with growth occurring predominantly in larval-specific tissues such as the salivary gland, epidermis, musculature, and fat body. At the end of the larval stage, these tissues and organs are marked for developmentally programmed autophagy to make way for the formation of adult structures. The fat body is primarily capable of starvation-induced autophagy and acts as a sensor of nutritional status to maintain adequate nutrient levels within the haemolymph and ensure survival during unfavourable conditions. Larval starvation results in the rapid inactivation of PI3K yielding reduced levels of PIP_3 in the plasma membrane of fat body cells. Mutations

disrupting PI3K phenocopy many of the effects of starvation, including reduced larval growth, specific arrest of endoreplicative cell cycles, and aggregation of lipid vesicles within the fat body, suggesting a role for PI3K in repressing autophagy (Britton *et al.*, 2002; Colombani *et al.*, 2003). Alternatively, constitutive expression of PI3K within the fat body prevents these responses and results in reduced viability under starvation conditions, suggesting that autophagy of the fat body serves to provide adequate nutrient levels during times of stress (Britton *et al.*, 2002). The process of starvation-induced autophagy was recently studied using a technique whereby stages of autophagy can be visualized utilizing transgenic lines harbouring a UAS-LC3-GFP or UAS-Atg5-GFP construct and a GAL4 driver specifically expressed within the haemolymph or fat body (Rusten *et al.*, 2004). This technique, along with use of the vital dye lysotracker (which stains acidic vesicles), is capable of identifying three distinct compartments representing three populations within the autophagy pathway: autophagosomes (which contain Atg5 or Atg8 (LC3) and thus could be visualized through GFP staining), lysosomes (stained with lysotracker), and autolysosomes (which would involve vesicles that co-stained with both GFP and lysotracker). Utilizing this technique, premature autophagy was demonstrated on second and third instar feeding larvae (previously shown not to exhibit the effects of autophagy) that were starved for 4 hours on amino acid deficient sucrose medium (as evident from co-staining and the presence of larger, more acidic autolysosomes) as well as by treatment with the hormone ecdysone. Expression of dp110 (the catalytic subunit of PI3K) or dAkt (one of the substrates of PI3K signalling) also resulted in a strong reduction of GFP-LC3/lyostracker positive structures (in a similar manner to results involving ecdysone expression), and analysis of clones expressing of a dominant negative

ecdysone receptor had displayed higher levels of PI3K activity compared to neighbouring cells had correspondingly fewer and smaller acidic staining vesicles. Hence, this technique can provide a unique means by which one can determine if exposure to caffeine is capable of inhibiting the PI3K pathway *in vivo* in *Drosophila* larvae, by assaying the process of autophagy in the presence of caffeine.

Section 3-5: Literature cited

Arnon, A., B. Cook, C. Montell, Z. Selinger, and B. Minke. 1997. Calmodulin regulation of calcium stores in phototransduction of *Drosophila*. *Science* **275**: 1119-1121.

Baehrecke, E. H. 2002. How death shapes life during development. *Nat Rev Mol Cell Biol* 3:779-787.

Bertrand, F., A. Atfi, A. Cadoret, G. L'Allemain, H. Robin, et al., 1998. A role for nuclear factor kappaB in the antiapoptotic function of insulin. *J Biol Chem* **273**:2931-2938.

Bikopoulos, G., R. B. Ceddia, G. Sweeney and A. J. Hilliker. 2004. Insulin reduces apoptosis and increases DNA synthesis and cell size via distinct signalling pathways in *Drosophila* Kc cells. *Cell Prolif* **37**:307-316.

Bose, A., A. Guilherme, S. Robida, S. M. C. Nicoloro, Q. L. Zhou, *et al.*, 2002. Glucose transporter recycling in response to insulin is facilitated by myosin Myo1c. *Nature* **420**:821-824.

Bose, A., S. Robida, P. S. Furcinitti, A. Chawla, K. Fogarty *et al.*, 2004. Unconventional myosin 1c promotes membrane fusion in a regulated exocytic pathway. *Mol Cell Biol* **24**:5447-5458.

Bradley, J. 2002. *Personal communication.*

Britton, J. S., W. K. Lockwood, L. Li, S. M. Cohen and B. A. Edgar. 2002. *Drosophila*'s insulin/PI3-kinase pathway coordinates cellular metabolism with nutritional conditions. *Dev Cell* **2**:239-249.

Brogiolo, W., H. Stocker, T. Ikeya, F. Rintelen, R. Fernandez *et al.*, 2001. An evolutionarily conserved function of the Drosophila insulin receptor and insulin-like peptides in growth control. *Curr Biol* **11**:213-221.

Cohen, S. M. (1993). Imaginal disc development. In *Drosophila Development*, A. Martinez-Arias and M. Bate, eds. (Cold Spring Harbor: Cold Spring Harbor Press), pp. 747-841.

Colombani, J., S. Raisin, S. Pantalacci, T. Radimerski, J. Montagne *et al.*, 2003. A nutrient sensor mechanism controls *Drosophila* growth. *Cell* **114**:739-749.

Edgar, B. A. 1999. From small flies come big discoveries about size control. *Nat Cell Biol* **1**:E191-193.

Fengsrud, M., E. S. Erichsen, T. O. Berg, C. Raiborg, and P. O. Seglen. 2000.

Ultrastructural characterization of the delimiting membranes of isolated autophagosomes and amphisomes by freeze-fracture electron microscopy. *Euro J Cell Biol* **79**:871-882.

Foukas, L. C., N. Daniele, C. Ktori, K. E. Anderson, J. Jensen *et al.*, 2002. Direct effects of caffeine and theophylline on p110δ and other phosphoinositide 3-kinases. *J Biol Chem* **277**: 37124-37130.

Franke, T. F., C. P. Hornik, L. Segev, G. A. Shostak and C. Sugimoto. 2003. PI3K/Akt and apoptosis: size matters. *Oncogene* **22**:8983-8998.

Hanson, C. J., M. D. Bootman and R. Llewelyn. 2004. Cell Signalling: IP3 receptors channel calcium into cell death. *Curr Biol* **14**:933-935.

Iliakis, G., Y. Wang, J. Guan and H. Wang. 2003. DNA damage checkpoint control in cells exposed to ionizing radiation. *Oncogene* **22**: 5834-5847.

Katso, R., K. Okkenhaug, K. Ahmadi, S. White, J. Timms *et al.*, 2001. Cellular function of phosphoinositide 3-kinases: implications for development, homeostasis, and cancer. *Annu Rev Cell Dev Biol* **17**:615-675.

Klionsky, D. J. and S. D. Emr. 2000. Autophagy as a regulated pathway of cellular degradation. *Science* **290**:1717-1721.

Krause, C. 2003. *Personal communication.*

Lee-Kwon, W., D. Park, P. V. Baskar, S. Kole and M. Bernier. 1998. Antiapoptotic signalling by the insulin receptor in Chinese hamster ovary cells. *Biochemistry* **37**:15747-15757.

Lizcano, J. M., S. Alrubaie, A. Kieloch, M. Deak, S. J. Leevers *et al.*, 2003. Insulin-induced *Drosophila* S6 kinase activation requires phosphoinositide 3-kinase and protein kinase B. *Biochem J* **374**:297-306.

McPherson, P. S., Y. K. Kim, H. Valdivia, C. M. Knudson, H. Takekura *et al.*, 1991. The brain ryanodine receptor: a caffeine-sensitive calcium release channel. *Neuron* **7**:17-25.

Melendez, A., Z. Talloczy, M. Seaman, E. L. Eskelinen, D. H. Hall *et al.*, 2003. Autophagy genes are essential for dauer development and life-span extension in *C. elegans*. *Science* **301**:1387-1391.

Mizushima, N., T. Noda, T. Yoshimori, Y. Tanaka, T. Ishii *et al.*, 1998. A protein conjugation system essential for autophagy. *Nature* **395**:395-398.

Mizushima, N., A. Yamamoto, M. Hatano, Y. Kobayashi, Y. Kabeya *et al.*, 2001.

Dissection of autophagosome formation using Apg5-deficient mouse embryonic stem cells. *J Cell Biol* **152**:657-668.

Moley, K. H. and M. M. Mueckler. 2000. Glucose transport and apoptosis. *Apoptosis* **5**:99-105.

Noda, T., K. Suzuki and Y. Ohsumi. 2002. Yeast autophagosomes: *de novo* formation of a membrane structure. *Trends Cell Biol* **12**:231-235.

Osaki, M., M. Oshimura and H. Ito. 2004. PI3K-Akt pathway: its functions and alterations in human cancer. *Apoptosis* **9**:667-676.

Pan, Z., D. Damron, A-L. Nieminen, M. B. Bhat and J. Ma. 2000. Depletion of intracellular Ca^{2+} by caffeine and ryanodine induces apoptosis of chinese hamster ovary cells transfected with ryanodine receptor. *J Biol Chem* **275**:19978-19984.

Rousseau, E., J. LaDine, Q-Y. Liu and G. Meissner. 1988. Activation of the Ca^{2+} release channel of skeletal muscle sarcoplasmic reticulum by caffeine and related compounds. *Arch Biochem Biophys* **267**: 75-86.

Rusten, T. E., K. Lindmo, G. Juhasz, M. Sass, P. O. Seglen *et al.*, 2004. Programmed autophagy in the *Drosophila* fat body is induced by ecdysone through regulation of the PI3K pathway. *Dev Cell* **7**:179-192.

Saris, N. E. and E. Carafoli. 2005. A historical review of cellular calcium handling, with emphasis on mitochondria. *Biochem (Mosc)* **70**:187-194.

Seglen, P. O. and P. Bohley. 1992. Autophagy and other vacuolar protein degradation mechanisms. *Experientia* **48**:158-172.

Shepherd, P. R. 2005. Mechanisms regulating phosphoinositide 3-kinase signalling in insulin-sensitive tissues. *Acta Physiol Scand* **183**:3-12.

Silva, E. A. 2002. Generation and characterization of chemical-sensitive cell cycle checkpoint mutants in *Drosophila*. University of Alberta.

Sullivan, K. M., K.Scott, C. S. Zuker and G. M. Rubin. 2000. The ryanodine receptor is essential for larval development in *Drosophila melanogaster*. *Proc Natl Acad Sci USA* **97**:5942-5947.

Suzuki, K., T. Kirisako, Y. Kamada, N. Mizushima, T. Noda *et al.*, 2001. The pre-autophagosomal structure organized by concerted functions of APG genes is essential for autophagosome formation. *EMBO J* **20**:5971-5981.

Tzolovsky, G., H. Millo, S. Pathirana, T. Wood and M. Bownes. 2002. Identification and phylogenetic analysis of *Drosophila melanogaster* myosins. *Mol Biol Evol*

19:1041-1052.

Wang, B., K. M. Sullivan and K. Beckingham. 2003. *Drosophila* calmodulin mutants with specific defects in the musculature or in the nervous system. *Genetics* **165**:1255-1268.

Waring, P. 2005. Redox active calcium ion channels and cell death. *Arch Biochem Biophys* **434**:33-42.

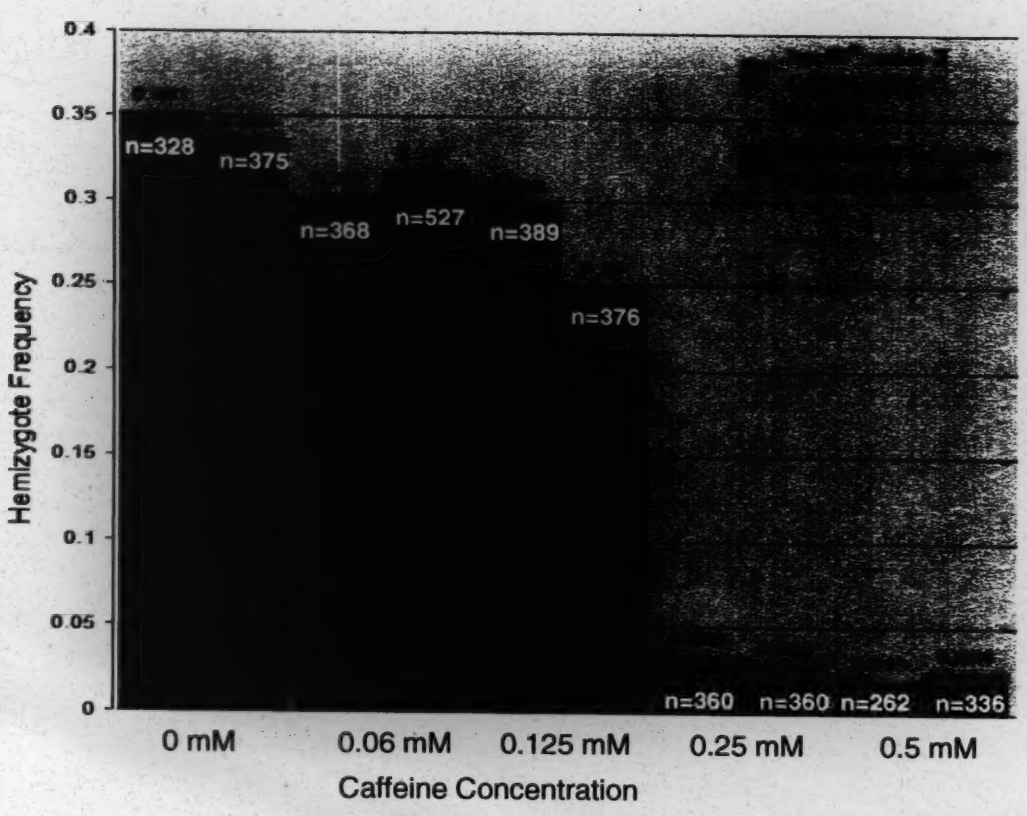

Figure 3-1: Caffeine sensitivity of *huc*95^{E} hemizygotes. Reciprocal crosses were set up between *huc*95^{E}*/ TM3 Sb, Ser* and *Df*(3R)*crb87-4/ TM3 Sb, Ser* in fly media containing the caffeine concentrations listed. The proportion (listed above the bars) of *huc*95^{E} hemizygotes that survived to adulthood was determined from the total progeny (listed in white in the bars)

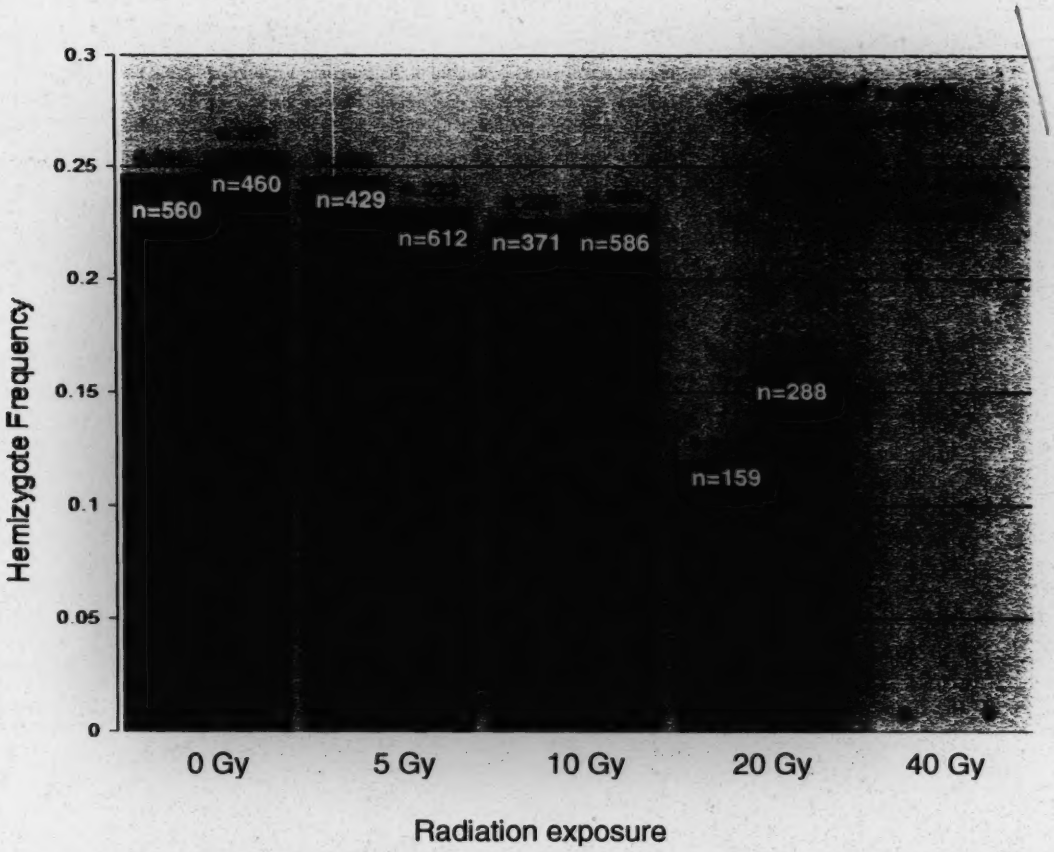

Figure 3-2: Effects of ionizing radiation on huc95^{E} hemizygote viability. Reciprocal crosses were set up between *huc*95^{E}*/ TM3 Ser-GFP* and *Df*(3R)*crb87-4/ TM3 Ser-GFP*, allowed to develop to third instar larvae, and irradiated at the exposures specified using a Co^{60} gamma source. The proportion (listed above the bars) of *huc*95^{E} hemizygotes that survived to adulthood was determined from the total progeny (listed in white in the bars)

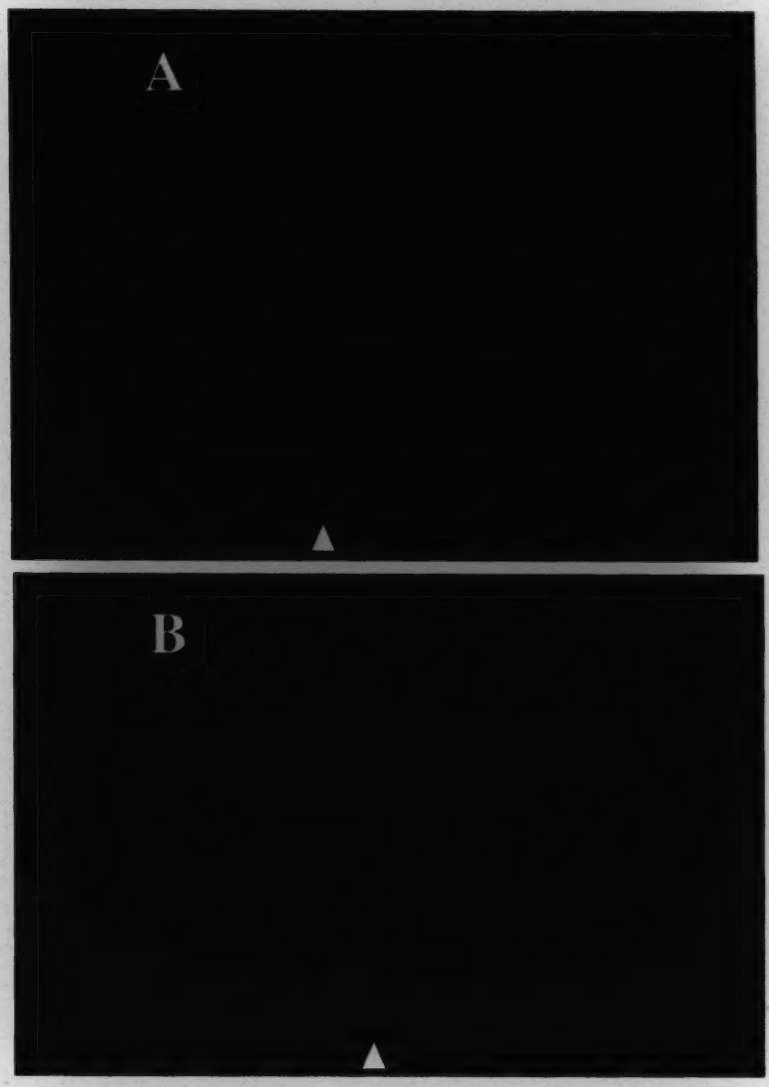

Figure 3-3: Eye discs dissected from *EGUF/+; FRT82B huc95^{DE}/ FRT82B GMR-hid3R CL3R* larvae that were stained to visualize apoptosis by acridine orange staining. Disc from a larva grown on normal media (A) or from larvae grown on caffeine-containing media (B). Apoptosis is elevated in cells anterior to the morphogenetic furrow (right of the arrowhead) in larvae grown on caffeine(B), whereas posterior to the furrow (left of the arrowhead), caffeine-independent apoptosis is due to the expression of *GMR-hid3R* (both A and B).

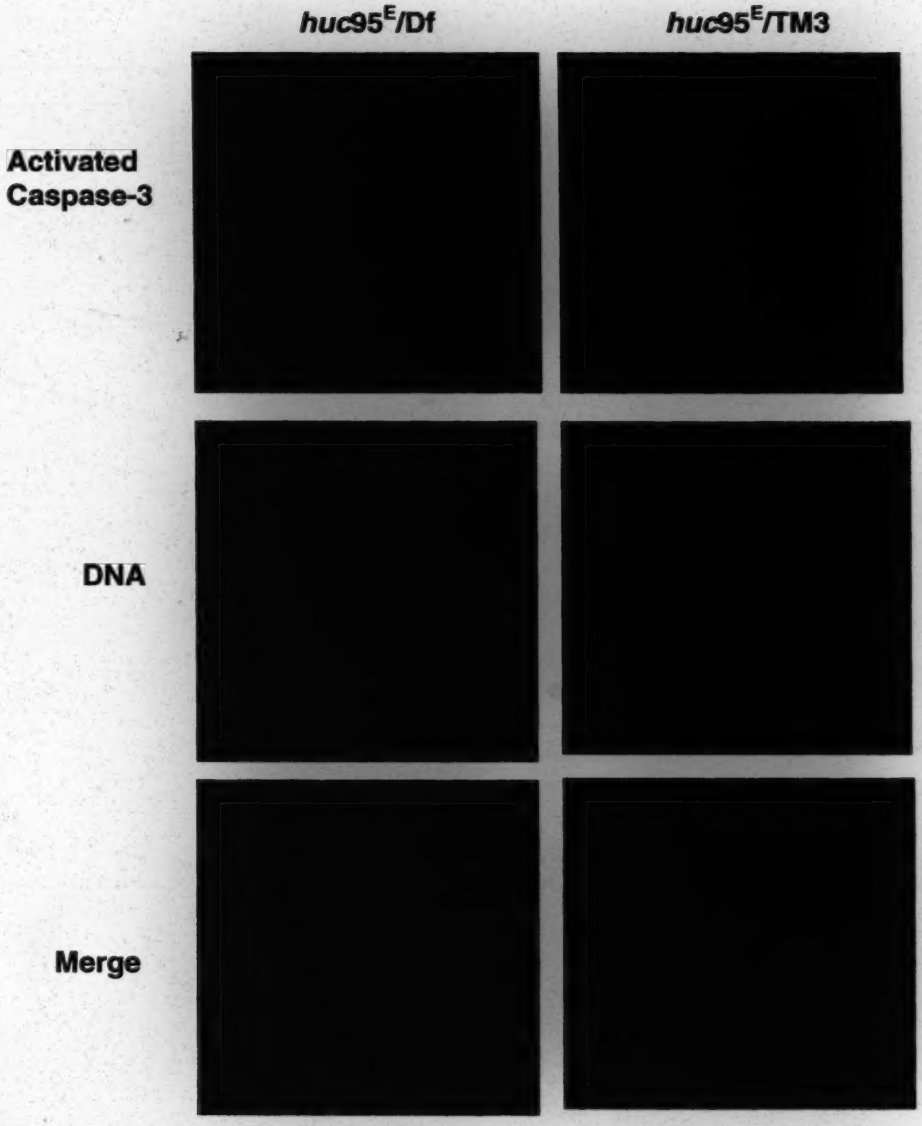

Figure 3-4: Degeneration of *huc*95^{E} hemizygous imaginal discs in the presence of caffeine. Brains from third instar larvae grown in the presence of caffeine added at day 4 AEL were stained with cleaved caspase-3 and hoescht. Hemizygotes exhibit greater caspase-3 staining at imaginal leg discs while heterozygotes show no staining. DNA stain is added to aid in the visualization of imaginal discs.

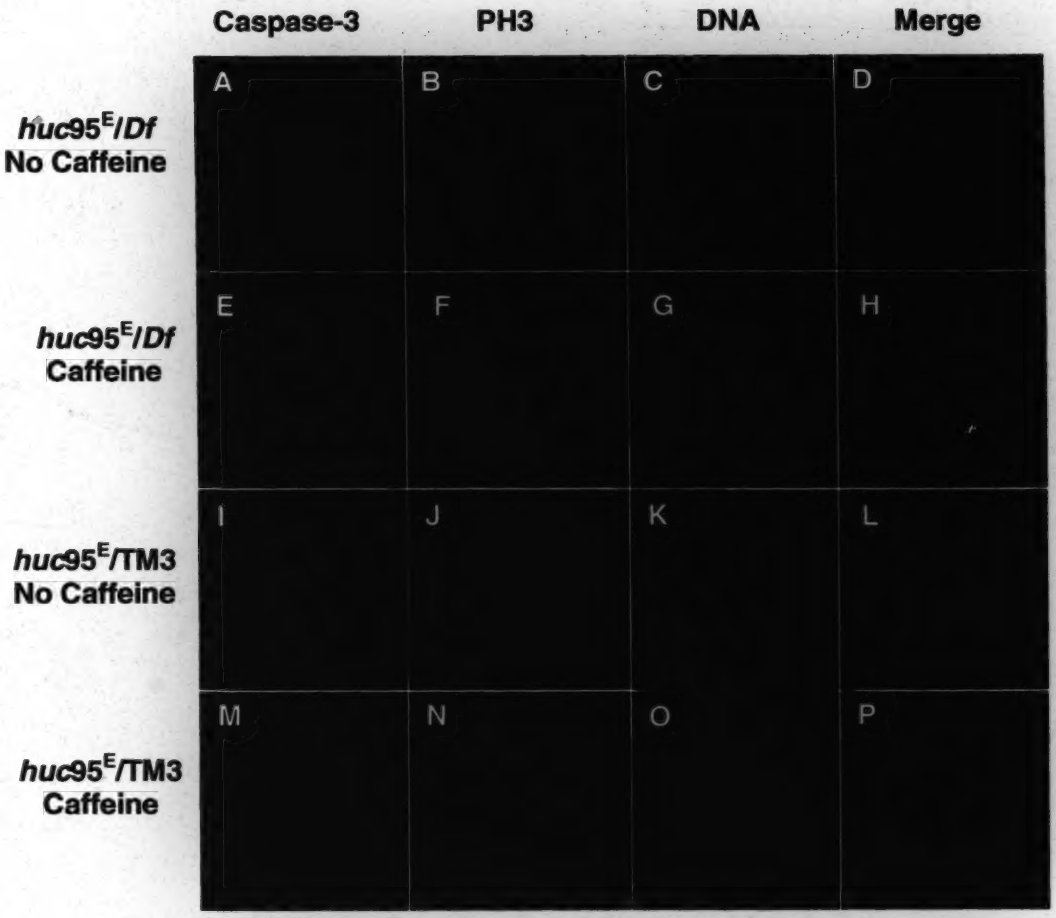

Figure 3-5: Apoptosis and cellular proliferation in eye-antennal discs from *huc*95^{E} hemizygotes in the presence and absence of caffeine. Third instar larval eye-antennal discs from *huc*95^{E} hemizygotes raised in the presence (E-F) and absence (A-D) of caffeine were stained with antibodies to caspase-3, PH-3, and hoescht (o visualize apoptosis, mitosis, and DNA respectively). Eye-antennal discs from *huc*95^{E} heterozygotes in the presence (M-P) and absence (I-L) of caffeine were also stained for a comparison.

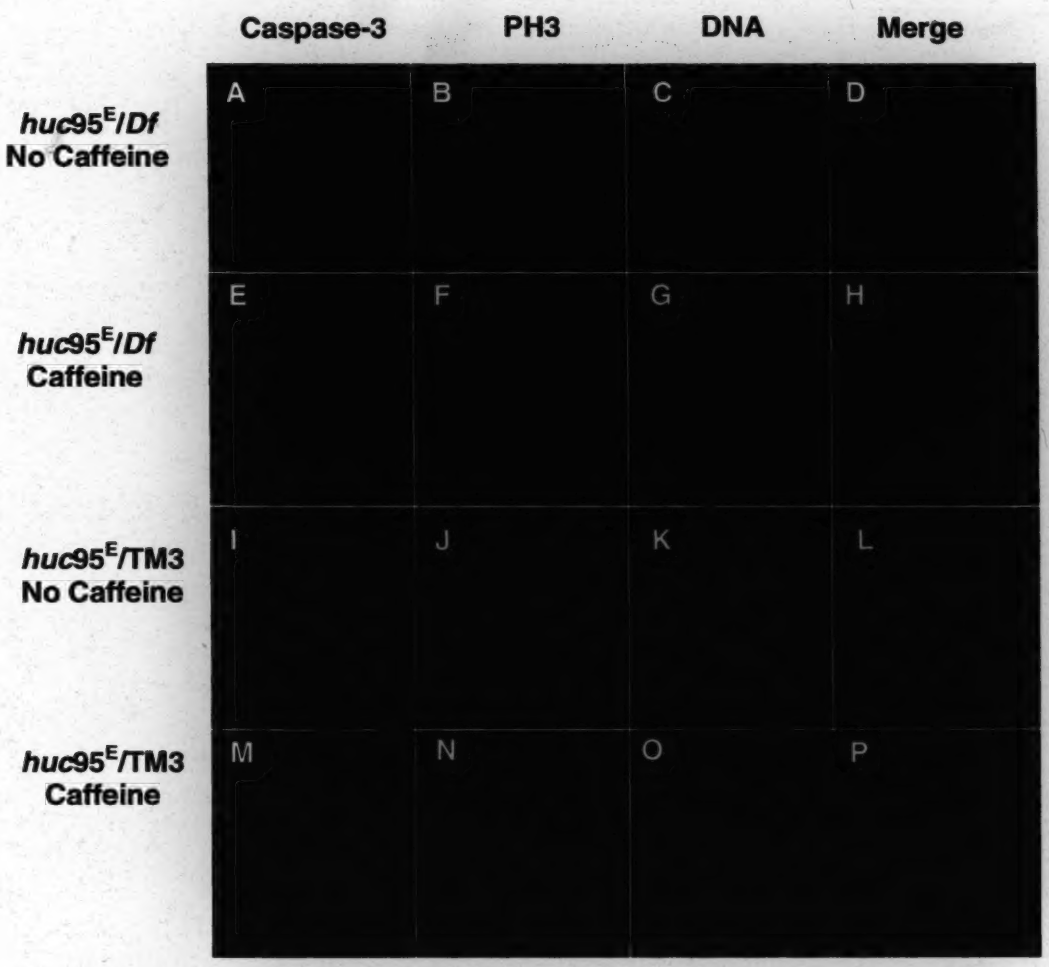

Figure 3-6: Apoptosis and cellular proliferation in wing discs from *huc*95^{E} hemizygotes in the presence and absence of caffeine. Third instar larval wing imaginal discs from *huc*95^{E} hemizygotes raised in the presence (E-F) and absence (A-D) of caffeine were stained with antibodies to caspase-3, PH-3, and hoescht (o visualize apoptosis, mitosis, and DNA respectively). Wing discs from *huc*95^{E} heterozygotes in the presence (M-P) and absence (I-L) of caffeine were also stained for a comparison.

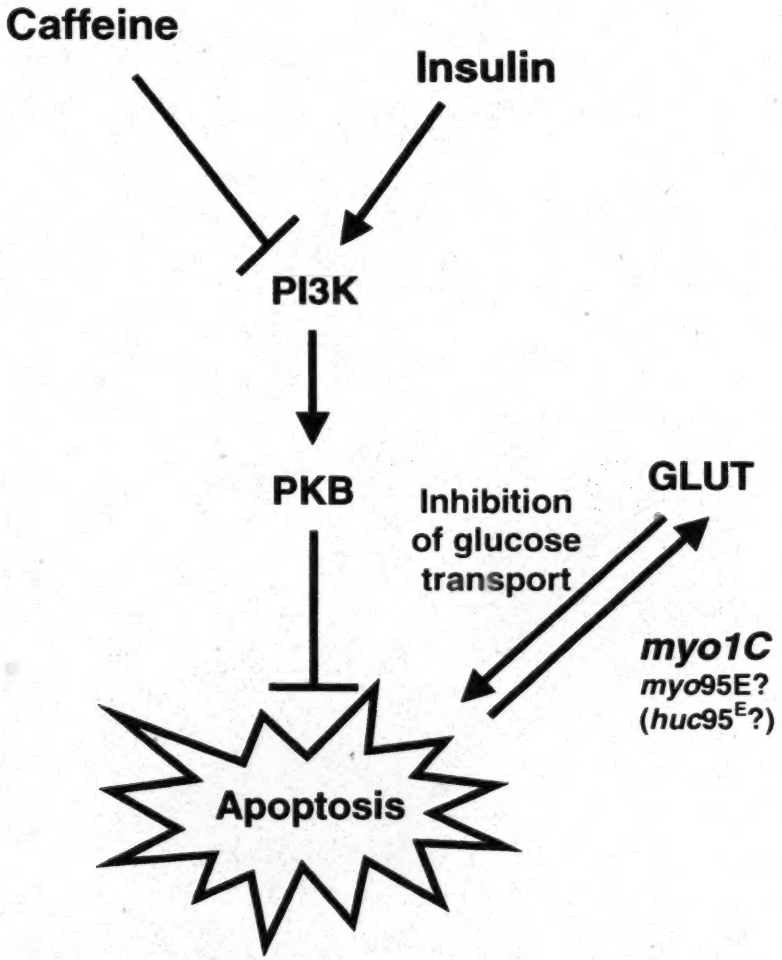

Figure 3-7: Possible model for the caffeine-induced apoptosis in *huc*95^{E} hemizygotes. Normally, insulin signalling stimulates phosphoinositide 3-kinase (PI3K), which in turn activates protein kinase B (PKB). PKB inhibits apoptosis, thereby allowing cellular proliferation and growth. Inhibition of PI3K by caffeine serves to block activation of PKB, making the cell susceptible to apoptosis. Inhibition of PI3K prevents fusion and allocation of GLUT receptors into the membrane thereby decreasing glucose transport, which can trigger apoptosis. Overexpression of Myo1C in 3T3-L1 adipocyte cells can override PI3K inhibition to allow fusion, which may also be the case with *huc*95^{E} (if it is *myo*95E).

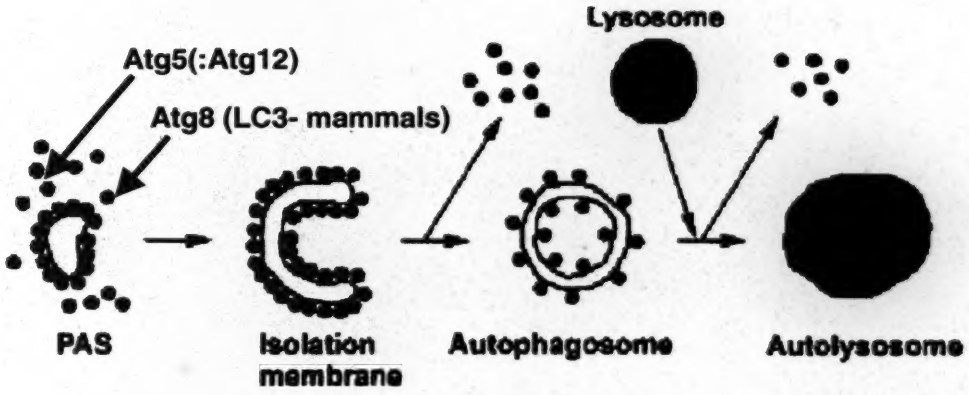

Figure 3-8: Mechanism of autophagy. Conjugates of Atg5:Atg12 and Atg8 (LC3 in mammals) is localized to the preautophagosomal structure (PAS). The PAS closes in on itself to form an autophagosome, which is coupled with the loss of Atg5 from the PAS. Fusion of the autophagosome to the lysosome forms an autolysosome, where the membrane and its contents are degraded. (Figure adapted from Rusten *et al.*, 2004)

Chapter 4: Conclusion

As of the writing of this thesis, the identity of *huc*95^{E} is still unknown. However, out of 23 initial candidates, I have managed to reduce the number to 9, which should make identification easier through molecular-based methods. Out of these candidates, *myo*95E is of particular interest in that *huc*95^{E} hemizygotes have a mutation in this gene which obliterates a splicing acceptor site at the junction of intron 8 and exon 9, which is predicted to result in a non-functional protein. Alternative splicing predictions bypassing this mutation by using typical splice sites are predicted to also result in a protein with no function as a myosin, and all of the predicted full-length transcripts utilize this splice site, suggesting that a mutation at this site would have effects on myosin function. Furthermore, RT-PCR analysis confirmed the splicing defect, suggesting that the gene is expressed as well as the splicing mutation. However, a genomic rescue construct containing the full *myo*95E gene as well as upstream and downstream regions was not able to relieve the caffeine sensitivity of the *huc*95^{E} mutants. This might be the result of inadequate expression of the construct or could mean that this gene is not a candidate for *huc*95^{E}. If not, several other interesting candidates exist within region one of which is *CG6129*. This gene is thought to encode a ciliary rootlet component with homology to the Nek2-associated protein C-Nap1, a core centrosomal protein that is responsible for holding the centrioles together during interphase. Nek2 has been implicated in formation of the mitotic spindle and phosphorylation of C-Nap1 by Nek2 at the G_2/M transition is required for centrosomal splitting by displacing C-Nap1 (Rapley *et al.*, 2005; Fry *et al.*, 1998a; Fry *et al.*, 1998b). Furthermore, another related kinase Nek11 is involved in a caffeine-sensitive checkpoint for DNA damage and genotoxic stress (Noguchi *et al.*,

2002). Since the premise of the screen was to find novel cell cycle checkpoint mutants, this gene is an interesting candidate to pursue and currently efforts to sequence this gene are under way. *CG5510* is also an interesting candidate in that it may be involved in secretion and intracellular transport. Other than this, the remaining candidate genes are *CG13605*, *CG13607*, *CG5463*, *Kal-1*, *CG6164*, and *CG13606* and continued efforts should be able to either eliminate or confirm the status of these genes as candidates for *huc*95^{E}.

huc95^{E} hemizygotes exhibit pupal lethality in the presence of caffeine and examination of hemizygous pupae reveal no adult structures. In light of this, I have demonstrated that imaginal discs within *huc*95^{E} third instar hemizygotic larvae exhibit increased apoptosis when exposed to caffeine. This suggests that the caffeine-induced pupal lethality of the *huc*95^{E} mutants is due to caffeine-induced apoptosis within adult-forming tissues, resulting in the inability to complete metamorphosis and might allude to a temporal role for *huc*95^{E} in development. The role of *huc*95^{E} in apoptosis within the imaginal discs is unclear and will have to be studied further. Interestingly, *huc*95^{E} hemizygotes are quite sensitive to caffeine as levels as low as 0.25 mM is enough to compromise their viability (as compared to heterozygous controls which can withstand concentrations of 2 mM caffeine). The role that caffeine plays in this sensitivity is also unclear and is of particular interest in that caffeine is a commonly used reagent in research as well as the most highly consumed drug in the world today.

First and foremost, the identity of *huc*95^{E} should be determined as such identification could help to elucidate the nature of the caffeine sensitivity displayed by the *huc*95^{E} mutants. *myo*95E is a promising candidate, containing a mutation that is

predicted to produce a non-functional myosin and an attractive model of how a mutation in this gene could impart caffeine sensitivity has been formulated however, without a suitable rescue to confirm this gene, *myo*95E only still remains an attractive candidate along with 8 other genes within the region. Currently, efforts are underway to both sequence the remaining genes and to isolate more *huc*95^{E} alleles through a screen for caffeine sensitive mutants. Hopefully, these efforts will serve to identify the gene responsible once and for all. Furthermore, although the original premise of the screen that had isolated *huc*95^{E} was to isolate novel cell cycle checkpoint mutants, no work has been done to test whether *huc*95^{E} has any real checkpoint function. It was determined that huc95E was not sensitive to ionizing radiation, however, this could have been due to redundant checkpoint pathways still present within the *huc*95^{E} mutant. To address this, the same experiment could be performed but this time, the larvae could be treated with caffeine a day prior to irradiation and eye-antennal or wing imaginal discs could be analyzed for mitotic events. This experiment would test the ability of caffeine to override checkpoint mechanisms (an important assumption in the design of the screen) and if *huc*95^{E} is involved with a checkpoint response, then perhaps it will be more sensitive to both caffeine treatment and ionizing radiation. Furthermore, the nature of the caffeine sensitivity should be further studied. It was previously determined that caffeine induces apoptosis within the imaginal discs of *huc*95^{E} hemizygotes however, how or why this occurs still remains a mystery. By determining what pathways are affected by caffeine in these mutants (ie. whether caffeine directly acts on an apoptotic pathway or whether apoptosis is mediated through caffeine's effects on PI3K signalling or DNA repair or checkpoint pathways) could help to elucidate the nature by which *huc*95^{E} mediates

caffeine sensitivity. It would also be interesting to determine if huc95^{E} is also sensitive to other adenosine analogues (such as purine) and whether these analogues can mediate the same effect as caffeine. Hopefully through this analysis, a better picture will emerge as to why only the imaginal discs seem to be affected and what *huc*95^{E}'s role is in development. Identification and further characterization of *huc*95^{E} may lead to newer insights into the mechanism of caffeine and its many effects as the world's most popular drug.

Section 4-2: Literature cited

Fry, A. M., T. Mayor, P. Meraldi, Y. D. Stierhof, K. Tanaka *et al.*, 1998a. C-Nap1, a novel centrosomal coiled-coil protein and candidate substrate of the cell cycle-regulated protein kinase Nek2. *J Cell Biol* 141:1563-1574.

Fry, A. M., P. Meraldi and E. A. Nigg. 1998b. A centrosomal function for the human Nek2 protein kinase, a member of the NIMA family of cell cycle regulators. *EMBO J* 17:470-481.

Noguchi, K. H. Fukazawa, Y. Murakami and Y. Uehara. 2002. Nek11, a new member of the NIMA family of kinases, involved in DNA replication and genotoxic stress responses. *J Biochem* **277**:39655-39665.

Rapley, J., J. E. Baxter, J. Blot, S. L. Whattam, M. Casenghi et al., 2005. Coordinate regulation of the mother centriole component nlp by nek2 and plk1 protein kinases. *Mol Cell Biol* **25**:1309-1324.

Appendix

Sequencing Primers: sequences in bold were also used in RT-PCR analysis

Mpk2

		RP-A2	gtgctctacacctcgcgact
LP-B1	caagagctgctatcagtcgc	RP-B2	atacggcgacacaaacgaat
LP-C1	atgctctagttgggagtccg	RP-C2	cacgggcacttcattcaaac
LP-D1	taagggtgtcgcatttgctt	RP-D2	gttgcgcaatgagctaaagg
LP-E1	ggttgggcaagtgcagatag	RP-E2	catctccgcgctgtacataa
LP-F1	tacggctgcagagtcacata	RP-F2	ccacgagattcggaacttc
LP-G1	atgcaaatcaagttggtcagg	RP-G2	cgacgagggagtttatcacc
LP-H1	ccatgcttatcccggtgataa	RP-H2	taccaaatactgcggggact
LP-I1	aacaaccccggcactatgta	RP-I2	cgagttcgttcgttttctgg
LP-J1	gtctcaccttagccacctgg	RP-J2	tcacctcttgggcaggatct
LP-K1	gatgcgtgttaggcattcat	RP-K2	gcaacgccgtgtgtttattt
LP-L1	agcccatataccgtaaaatttgg	RP-L2	gttcgtcggagaatggtagg
LP-M1	cgccggggttatcaaataag	RP-M2	caatgttcccgctatctgag
LP-N1	ggactggcaaacatgcagat		
Mpk2 Wave 7B	tagacccaaagatcctgcccaagag	Mpk2 Wave 7A	ttgcccgtagacaaatggaaggaat
Mpk2 Wave 6B	cctgagcatacgatggtgggggctt	Mpk2 Wave 6A	catctggtcggtgggctgcatcat
MpK2 Wave 5B	ggtgaatatggtcggtgcctgggaa	Mpk2 Wave 5A	gatgcagcacttgtccgacgaccac
Mpk2 Wave 4B	tcgttgacggcaatgtttgagggct	Mpk2 Wave 4A	ccatgcaaagaggacgtaccggga
Mpk2 Wave 3B	tccagcagaccgattacgttctcat	Mpk2 Wave 3A	tggatataaatcgaacggaatggga
Mpk2 Wave 2B	cctgtccgtaagctcccgatcccac	Mpk2 Wave 2A	gcatggaattatcgttcgcatggca
Mpk2 Wave 1B	tgccatgcgaacgataattccatgc	Mpk2 Wave 1A	cgcattcgtgtgtcgcttctgatcg
LP Mpk2 102	ccatttgtctacgatggtgggggctt	RP Mpk2 201	cagacctcaccaccatacgat
LP Mpk2 103	ttagctggtgaatatggttcgg	RP Mpk2 202	tcatggccgaactaattaccag
LP Mpk2 104	caagccacggagtatctggt	RP Mpk2 203	gatggacgcagatctgaacaa
LP Mpk2 105	cgaacaactgcctttgacac	RP Mpk2 204	aatcgaacggaatgggagat
LP Mpk2 106	tccacgcccaagaatatca	RP Mpk2 205	acgcatcggaatggagtaat
		RP Mpk2 206	caaattttacggtatatgggcttta

mRpS24

L1	**tcgtaaacaaggccatcaaa**	R1	tccatctctagcgaaccgtta
L2	gaccgccatagaggatgtgt	R2	**tccatctctagcgaaccgtta**

p38c

L1	agcgggtgactaaatgcaag	R1	tgccagatccggaagatta
L2	**tactcgcgcgttcgaaaaggat**	R2	ttttcgggtaccatttcgag
L3	aaggtgcgattttcatcacc	R3	**gtatgcgcacctcggctattt**
		R4	catcctcctccctctcgaat

CG6178

CG6178-TP1-LP1	gctgtgatcgtatggtggtg	CG6178-TP1-RP1	acaatgtttccgggcagtag
CG6178-TP1-LP2	aattagttcggccatgatgc	CG6178-TP1-RP2	aggctttcaagcgaacactc
CG6178-TP1-LP3	tcagatctgcgtccatcaag	CG6178-TP1-RP3	gcaacgccgtgtgtttattt
CG6178-TP1-LP4	atatccgggatctcccattc	CG6178-TP1-RP4	caaatgtagcgcattcgtgt
CG6178-TP1-LP5	gatcagaagcgacacacgaa	CG6178-TP1-RP5	cccttcctcaagcaatacc
CG6178-TP1-LP6	aaatttgagcagcaccatcc	CG6178-TP1-RP6	gctggagaacttccaacagg
CG6178-TP1-LP7	ctccccaaaggcgtgtataa	CG6178-TP1-RP7	caacggagaacgagatgaca
CG6178-TP2-LP1	gaacctggactggcaaacat	CG6178-TP2-RP1	cctgtgctggatgagcagta

CG6178-TP2-LP2	gtacggctggcatacatcct	CG6178-TP2-RP2	cgacatggaaatccatcagt
CG6178-TP2-LP3	gacacagcctgacttcacga	CG6178-TP2-RP3	agaatgcgacgcagaatctt
CG6178-TP2-LP4	gctcttcctttctgccattg	CG6178-TP2-RP4	agccaatatcgccagtatgc
CG6178-TP2-LP5	ttggttgcatactggcgata	CG6178-TP2-RP5	cacagcaggaccatcaaaga
CG6178-TP2-LP6	ttcaactgaccgagaacgaa	CG6178-TP2-RP6	agcaggttcatttgggtcag
CG6178-TP2-LP7	tgtgacatcgctgaagctct	CG6178-TP2-RP7	ggacaagttaatggcgtgg

myo95E

TP1-LP1-Myo95E	gtacggctggcatacatcct	TP1-RP1-myo95E	cctgtgctggatgagcagta
TP1-LP2-Myo95E	taaggagctgatggaggacg	TP1-RP2-myo95E	agagcttcagcgatgtcaca
TP1-LP3-Myo95E	gctcttcctttctgccattg	TP1-RP3-myo95E	cgttctcggtcagttgaaca
TP1-LP4-Myo95E	atacgaagtccacgcagacc	TP1-RP4-myo95E	tcttaagcatttcccgcaga
TP1-LP5-Myo95E	tctgcgggaaatgcttaaga	TP1-RP5-myo95E	ggtctgcgtggacttcgtat
TP1-LP6-Myo95E	tatcttgctttgtcgcagca	TP1-RP6-myo95E	caatggcagaaaggaagagc
TP1-LP7-Myo95E	cgacttggtgcacgatttac	TP1-RP7-myo95E	tcgtgaagtcaggctgtgtc
TP2-LP1-Myo95E	tgggttcatttgtgtttcca	TP2-RP1-myo95E	aagcgctgccttttatcaga
TP2-LP2-Myo95E	tctgcttttggcacaatcct	TP2-RP2-myo95E	tcgccctcataatccgtaac
TP2-LP3-myo95E	aagatgacagtctgctggcc	TP2-RP3-myo95E	atttggcattcccttcactg
TP2-LP4-myo95E	aaagcgatgacgtggatagc	TP2-RP4-myo95E	agaaggtcacagccagcatt
TP2-LP5-myo95E	tgtagcacttccaacgatgg	TP2-RP5-myo95E	tatccacgtcatcgcttttg
TP2-LP6-myo95E	ttccttgcgtgatacattcg	TP2-RP6-myo95E	ggccagcagactgtcatctt
TP2-LP7-myo95E	gttacggattatgagggcga	TP2-RP7-myo95E	aggattgtgccaaaagcaga
TP3-LP1-myo95E	gttacggattatgagggcga	TP3-RP1-myo95E	gaaaatccgtcaggcagtgt
TP3-LP2-myo95E	gtgctgggctttttggtaac	TP3-RP2-myo95E	agagcctggaaaaggaggag
TP3-LP3-myo95E	**aatgcgagaccattccaatc**	TP3-RP3-myo95E	gtaaggttctgggcgatctg
TP3-LP4-myo95E	tgttcgtgctattcgctctg	TP3-RP4-myo95E	gcaagaatacctccgcactt
TP3-LP5-myo95E	aaaattcatgcggtcctcct	TP3-RP5-myo95E	aggaggaccgcatgaatttt
TP3-LP6-myo95E	aagtgcggaggtattcttgc	TP3-RP6-myo95E	**acgacaagcagctaccaacc**
TP3-LP7-myo95E	ctcctcctttccaggctct	TP3-RP7-myo95E	cttttgcgagttcagcaatg
TP4-LP1-myo95E	ctcctcctttccaggctct	TP3-RP8-myo95E	gttaccaaaaagcccagcac
TP4-LP2-myo95E	tgtgggtcagaaagttcacg	TP4-RP1-myo95E	tggcttagcaaatggtttcc
TP4-LP3-myo95E	acagtaccgagtcccaggtg	TP4-RP2-myo95E	gcttgacgcactccttcttc
TP4-LP4-myo95E	agtctctgagccaccaatcg	TP4-RP3-myo95E	tttgtggagcgggagaatac
TP4-LP5-myo95E	gtattctcccgctccacaaa	TP4-RP4-myo95E	cgattggtggctcagagact
TP4-LP6-myo95E	gaagaaggagtgcgtcaagc	TP4-RP5-myo95E	catcgttcccgttcttgttt
		TP4-RP6-myo95E	ttaggaggctggcccattat
		TP4-RP7-myo95E	aatccgtcaggcagtgtttc
5'-myo95E-L1	actgaagcgcgaagatttgt	5'-myo95E-R1	gtgctccgtctactgcacaa
5-myo95E-L2	tcgtaaacaaggccatcaaa	5'-myo95E-R2	ccaaggaggtcacagtaccc
5'-myo95E-L3	gacaaacttgcggatgaaca	5'-myo95E-R3	ccagttcgcacatagtctgg
5'-myo95E-L4	cagaaacaattttgcgtcca	5'-myo95E-R4	gtttccggatttcgagacag
5'-myo95E-L5	agttgtcggtgggaaaatgt	5'-myo95E-R5	cgctccagtgctaccgatta
5'-myo95E-L6	agaagcaaagctgcaaaggt	5'-myo95E-R6	ccgttacgtcacgtcaatca
5'-myo95E-L7	tgaggctatcgcagatgatg	5'-myo95E-R7	agacccgccatagaggatgtg
5'-myo95E-L8	ggtgtgcttcgcaatctttc	5'-myo95E-R8	acttcgctgctgttgttttg

Df(3R)W6 Analysis

dMyt+ATG	gacggatccatggaaaagcatcatcgcctg	dMyt-12	atagggcggaacacggactct
LP-CG6178-1	gtacggctggcatacatcct	RP-CG6178-1	ttatccacgatggggtgttt
LP-mRpS24-1	tggacgcaaaattgtttctg	RP-mRpS24-1	gagcagctcctccgtgtaac
LP-CG6182-1	gtattctcccgctccacaaa	RP-CG6182-1	tggcttagcaaatggtttcc
LP-CG13607-2	tgaggcatcagtttcagacg	RP-CG13607-2	tcgtgcatgtgtgtatgtgg
LP-CG18428-1	ccgcataatcggaaaaagtg	RP-CG18428-1	ttagctatttgcgacgcttg
LP-CG13605-1	ctgggcattgtggatcttct	RP-CG13605-1	gctttggcattgggaattta
LP-CG6129-1	gcgaagattcagtccgtctc	RP-CG6129-1	ggccatttgtagcctggtaa
LP-CG5463-1	gctggtttttgcaccagatt	RP-CG5463-1	cagagcacgcaccactaaaa
LP-CG5510-1	acgacattctgtcggtttcc	RP-CG5510-1	ccggataatctcatcgtgct
LP-CG13606-1	ttggcttttgcttttgcttt	RP-CG13606-1	acatgtgtacgccatgcact
LP-CHORD-1	agaatcttgtcggcaccatc	RP-CHORD-1	actgggaaaagtccgaggtt
LP-Apc2	ctcggggactatcccatctca	RP-Apc2	gctccacctgcttctttgac
LP-Tsc1-2	tcggttaagggagcagctta	RP-Tsc1-2	tgctttccagctgtgatgtc